Detection of the Cortical Network Underlying Executive Control of Auditory Attention in Early Psychosis with Multimodal Imaging

by

Mark T. Curtis

B.A., Illinois Wesleyan University, 2016

Submitted to the Graduate Faculty of the

School of Medicine in partial fulfillment

of the requirements for the degree of

Doctor of Philosophy

University of Pittsburgh

2022

UNIVERSITY OF PITTSBURGH

SCHOOL OF MEDICINE

This dissertation was presented

by

Mark T. Curtis

It was defended on

January 20, 2022

and approved by

Howard Aizenstein, M.D., PhD., Endowed Chair in Geriatric Psychiatry, Psychiatry

Julie Fiez, Ph.D., Chair, Psychology

Cecile D. Ladouceur, Ph.D., Professor, Psychiatry

Kirk Erickson, Ph.D., Professor, Psychology

John J. Foxe, Ph.D., Chair, Neuroscience, University of Rochester Medical Center

Dissertation Director: Dean F. Salisbury, Ph.D., Professor, Psychiatry

Detection of the Cortical Network Underlying Executive Control of Auditory Attention in Early Psychosis with Multimodal Imaging

Mark T. Curtis, Ph.D.

University of Pittsburgh, 2022

Selective attention is impaired at the first episode of psychosis (FEP). EEG and MEG can measure selective attention during an auditory oddball task, as the amplitude of the event-related potential ~100ms post-stimulus (EEG-measured N100/MEG-measured M100) increases with attention. N100/M100 enhancement is reduced in FEP. This project aimed to examine functional and structural abnormalities of the selective attention network underlying this impairment at the first episode of psychosis (FEP). Understanding the brain circuit underlying impaired selective attention in the early disease course can identify potential therapeutic targets. First, state-of-the-art infrastructure, which included the Human Connectome Project's (HCP) processing pipelines and multi-modal parcellation, was implemented. Two experiments validated the use of these pipelines and parcellation and provided a novel understanding of structural deficits and structure-function relationships in early psychosis. This infrastructure was used to investigate the auditory attention network, a candidate model system susceptible to deficits in early psychosis. MEG source activity of the M100 revealed sensory and attention modulation deficits in auditory cortex regions in FEP. The cortical network underlying the attention modulation and deficits within this network in FEP was examined. A whole-brain analysis of the M100 source activity identified strong activation within several prefrontal and parietal regions, with additional strong modulatory activity within the bilateral precuneus. The next experiments examined functional connectivity between regions. It was determined that theta frequency (5-7Hz) was the frequency range for inter-regional

connectivity. Changes in connectivity patterns with attention, using precuneus functional subregions as seed regions, revealed left and right hemisphere networks that increased activity with attention. Increased theta-band connectivity within these networks was impaired in early psychosis. Further, gray matter thickness was reduced within the left hemisphere network in FEP. The novel use of the HCP pipelines and parcellation to investigate auditory attention network deficits in FEP revealed functional deficits in auditory cortex and in a distributed network, with the precuneus as a hub, and structural deficits in the left hemisphere network. This circuitopathy provides a precise target system for novel interventions, such as non-invasive brain stimulation, which could ultimately improve functional outcome if targeted early in the disorder.

Table of Contents

Preface xiv

1.0 Introduction 1

1.1 Schizophrenia and Psychotic Disorders 1

1.2 Treatment for Psychosis 3

1.3 Cognitive Deficits in Psychosis 4

1.4 Selective Attention 5

1.5 N100 in Psychosis 6

1.6 Advantages of MEG 7

1.7 Project Overview 8

2.0 Implementation of State-of-the-Art Infrastructure for Analysis 9

2.1 General Introduction 9

2.2 Parahippocampal Area 3 Gray Matter is Reduced in First-Episode Schizophrenia-Spectrum: Discovery and Replication Samples 12

2.2.1 Introduction 13

2.2.2 Methods: Discovery Sample 17

2.2.2.1 Participants 17

2.2.2.2 Data Acquisition & Processing 19

2.2.2.3 Analysis 20

2.2.3 Methods: Independent Replication Sample 20

2.2.3.1 Participants 21

2.2.3.2 Data Acquisition & Processing 22

2.2.3.3 Analysis 24

2.2.4 Methods: Correlations with Symptoms and Cognition 25

2.2.5 Results: Discovery Sample 25

2.2.5.1 Uncorrected Cortical Thickness 25

2.2.5.2 FDR-Corrected Cortical Thickness 25

2.2.6 Results: Replication Sample 27

2.2.7 Results: Exploratory Correlations with Symptoms and Cognition 29

2.2.8 Discussion 31

2.3 General Discussion 35

2.3.1 Exploring Brain Structure and Function with the HCP Parcellation 36

2.4 Pitch and Duration Mismatch Negativity Are Associated with Distinct Auditory Cortex and Inferior Frontal Cortex Volumes in the First-Episode Schizophrenia-spectrum 37

2.4.1 Introduction 37

2.4.2 Methods 40

2.4.2.1 Participants 40

2.4.2.2 Data acquisition & Processing 42

2.4.2.3 Analysis 45

2.4.3 Results 46

2.4.3.1 Mismatch Negativity 46

2.4.3.2 Gray Matter Volume Group Comparisons 47

2.4.3.3 Pitch MMN and Gray Matter Volume Correlations 47

2.4.3.4 Duration MMN and Gray Matter Volume Correlations 48

2.4.4 Discussion 51

2.5 Overall Discussion 57

3.0 Attention Modulation of Source activity in Auditory Cortex and Deficits in Early Psychosis 59

3.1 Introduction 59

3.2 Methods 62

3.2.1 Participants 62

3.2.2 Task 64

3.2.3 MEG Data Acquisition & Processing 65

3.2.4 MRI Data Acquisition & Processing 67

3.2.5 Analysis 68

3.3 Results 69

3.3.1 Sensor Level Data 69

3.3.2 Cortical Source Data 69

3.3.3 Exploratory Correlations with Clinical and Cognitive Measures 73

3.4 Discussion 74

3.5 Next Analysis: Detecting the Systems-Level Auditory Attention Network 77

4.0 The Underlying Executive Attention Network 79

4.1 M100 Modulation with Attention: Whole-Brain Analysis 79

4.1.1 Introduction 79

4.1.2 Methods 81

4.1.2.1 Analysis 81

4.1.3 Results 82

4.1.4 Brief Discussion 83

4.2 Oscillatory Dynamics of the Attention Network 85

4.2.1 Introduction 85

4.2.2 Methods 88

4.2.2.1 MEG Processing 88

4.2.2.2 Time-Frequency Analysis 88

4.2.2.3 Phase-Amplitude Coupling 88

4.2.2.4 Analysis 89

4.2.3 Results 89

4.2.3.1 Time-Frequency Analysis in Primary Auditory Cortex 89

4.2.3.2 Phase-Amplitude Coupling: Exploratory Uncorrected Statistics 90

4.2.3.3 Phase-Amplitude Coupling: Corrected Statistics 91

4.2.4 Brief Discussion 92

4.3 Attention Modulation Network Functional Connectivity 94

4.3.1 Introduction 94

4.3.2 Methods 96

4.3.2.1 Phase-Locking Value 96

4.3.2.2 Precuneus Clustering Approach 97

4.3.2.3 Analysis 99

4.3.3 Results 100

4.3.3.1 Precuneus Subregion Clustering 100

4.3.3.2 Cluster Connectivity with Attention in Healthy Individuals 102

4.3.3.3 Cluster Connectivity Differences between Groups 103

4.3.4 Discussion 105

5.0 Gray Matter Correlates of the Auditory Attention Measures 109

5.1 Introduction 109

5.2 Methods 111

5.2.1 MRI Data Acquisition and Processing. 111

5.2.2 Analysis 112

5.3 Results 114

5.3.1 Gray Matter Group Differences 114

5.3.2 Gray Matter Correlations with M100 Modulation, PAC, and PLV 117

5.4 Discussion 118

6.0 Overall Discussion 120

6.1 Summary and Significance 120

6.2 Limitations 123

6.3 Further Considerations and Future Directions 124

6.3.1 Effective Connectivity 124

6.3.2 Treatments Impacting Cortical Oscillations 125

6.3.3 White Matter Connectivity 127

6.3.4 Relevance for a Biomarker for Psychosis 128

6.3.5 Mechanistic and Animal Model Relevance 129

6.4 Conclusion 130

Bibliography 131

List of Tables

Table 1. Experiment 1: Sample 1 Demographic, Neuropsychological, and Clinical Information..... 19

Table 2. Experiment 1: Sample 2 Demographic, Neuropsychological, and Clinical Information..... 22

Table 3. Experiment 1: Sample 1 Gray Matter Thickness Reductions in FESz. 27

Table 4. Experiment 1: Sample 2 Gray Matter Thickness Reductions in FESz. 28

Table 5. Experiment 1: Exploratory Correlations with Symptoms and Cognitive Ability in FESz. 30

Table 6. Experiment 2: Demographic, Neuropsychological, and Clinical Information (previously reported in Salisbury et al., 2020). 42

Table 7. MMN and GM Correlations in FESz. 50

Table 8. Experiment 3: Demographic, Neuropsychological, and Clinical Information. 63

Table 9. M100 Cortical Source Activity. 72

Table 10. Connectivity Changes with Attention..... 105

Table 11. Gray Matter Thickness. 116

Table 12. Gray Matter Volume..... 117

List of Figures

Figure 1. Experiment 1 Gray Matter Thickness Differences. 26

Figure 2. Experiment 1 Exploratory Correlations 29

Figure 3. MMN Regions of Interest 45

Figure 4. Group Mismatch Negativity Grand Averages Information (previously reported in Salisbury et al., 2020). 47

Figure 5. Gray Matter Volume Associations with Pitch and Duration MMN in FESz 48

Figure 6. Scatterplots of Significant MMN and Gray Matter Correlations. 49

Figure 7. Auditory Attention Task. 65

Figure 8. Impaired Auditory Cortex Attention Modulation in First-episode Psychosis. 71

Figure 9. Scatterplots of the M100 Modulation Group Differences in Auditory Cortex Regions. 73

Figure 10. Whole-Brain M100 Modulation in Healthy Individuals. 83

Figure 11. Time-Frequency Analysis in Left Primary Auditory Cortex. 90

Figure 12. Exploratory Uncorrected Phase-Amplitude Coupling Analysis in Auditory Cortex and Precuneus. 91

Figure 13. Significant Phase-Amplitdue Coupling Analysis in Left Primary Auditory Cortex. 92

Figure 14. Precuneus Functional Subregions Defined by the HCP-MMP. 98

Figure 15. Cluster Analysis. 101

Figure 16. Regions with Signficant Connectivity Increases with Attention. 102

Figure 17. Left Hemisphere Network Connectivity Changes in HC and FEP. 103

Figure 18. Right Hemisphere Network Connectivity Changes in HC and FEP. 104

Figure 19. Gray Matter Thickness in the Left Hemisphere Attention Network..... 115

Preface

The work completed in this dissertation could not have been accomplished without the help and support of a community. First, I thank my dissertation advisor, Dr. Dean Salisbury for his tremendous mentorship and support throughout the years. I am grateful for his decision to take a chance on me during my third laboratory rotation in the first year of my program. Without his expertise, guidance, challenges, motivation, and feedback, I would not be in the position that I am now.

I would also like to thank the current and previous members of our laboratory. Dr. Brian Coffman has selflessly offered his time to train me on data acquisition, processing, and analysis approaches. This work would not have been possible without the effort of the research technicians over the years including Tim Murphy, Justin Leiter-McBeth, Natasha Torrence, Vanessa Fishel, Yiming Wang, Rebekah Farris, and Dylan Seebold. The countless hours we spent together at the MEG, MRI, and in the laboratory were not only essential to the project, but also critical to shaping a wonderful work environment. I am also thankful for the rest of my lab members (current and past) Dr. Alfredo Sklar, Dr. Julia Longenecker, Dr. Francisco Lopez, Dr. Sarah Haigh, and Dr. Xi Ren for their help and support along the way.

I would like to thank all the individuals who participated in the studies. This work was also made possible with the help from the faculty and staff of the WPH Psychosis Recruitment and Assessment Core, who offered tremendous support in the recruitment and clinical assessments of the participants.

I am grateful to the members of my committee. I appreciate all the time and effort that they have given to be involved in numerous in-person and virtual meetings. They have also offered tremendous professional advice and provided invaluable feedback on my projects.

I would also like to thank my family. I am thankful for my parents' dedication and time to raising me, for them setting examples of a strong work ethic, and for their encouragement of my pursuit of studying neuroscience. I am grateful for the important advice and guidance provided by my brothers. I appreciate the support and encouragement offered by my in-laws. My son provided motivation to be my best every day, and his smiles and laughter cheered me up even after the most challenging days. Finally, this could not have been accomplished without the love and support from my wife, Anelise. She has helped me celebrate during my highs and helped support me through my lows. I often leaned on her strength and encouragement. She consistently motivated me to persevere when times were challenging. She provided wonderful feedback on my presentations and offered light-hearted humor while I worked. This work could not have been accomplished without her support, and for her, I am abundantly grateful.

1.0 Introduction

1.1 Schizophrenia and Psychotic Disorders

Schizophrenia is a late neurodevelopmental disorder that is devastating for the affected individual, their families, and society as a whole. Approximately 0.3-0.7% of individuals worldwide, including 1-2 million individuals in the United States, are diagnosed with schizophrenia (Moreno-Kustner, Martin, & Pastor, 2018; NIMH; Saha, Chant, Welham, & McGrath, 2005). It is one of the leading causes of disability in the world, and those with schizophrenia have a mean life-expectancy ~14 years lower than the general population (Hjorthoj, Sturup, McGrath, & Nordentoft, 2017). Over half who develop the disorder are unable to work again for the remainder of their lives, and the total economic burden of schizophrenia in the U.S in 2013 was a staggering $155.7 billion. This total included $37 billion in healthcare costs and $117.3 billion in indirect costs (unemployment, reduced work productivity, & increased family caregiving) (Cloutier et al., 2016). Thus, it is essential to address this illness by gaining a better understanding of this disease and improving treatment methods to ameliorate its debilitating effects.

Schizophrenia is distinguished by waxing and waning episodes of psychosis, an experience in which an individual loses some contact with reality, often characterized by hallucinations (perceptions without external stimuli) or bizarre delusions (fixed false beliefs). Psychosis can be a symptom of several other mental disorders, such as bipolar disorder and major depressive disorder (American Psychiatric & American Psychiatric Association, 2013), but it is the defining feature of schizophrenia. The newest edition of the Diagnostic and Statistical Manual of Mental Disorders

(DSM-5), categorizes schizophrenia as part of a spectrum of disorders. Schizophrenia-spectrum disorders differ from one another by the number, severity, and duration of symptoms. The major symptom categories of schizophrenia-spectrum disorders include positive symptoms (e.g., hallucinations, delusions), negative symptoms (e.g., blunted affect), and disorganized behavior (American Psychiatric & American Psychiatric Association, 2013; Arciniegas, 2015). Schizophrenia-spectrum disorders are neurodevelopmental disorders that develop as a result of a combination of genetic risk factors and environmental exposures (Millan et al., 2016). The initial diagnosis is given when psychotic symptoms progress to the severity of needing medical attention, termed the first episode of psychosis (FEP). However, individuals do not always seek or receive treatment at their first psychotic episode, leading to periods of untreated psychosis, and longer durations of untreated psychosis (DUP) are associated with worse disease prognosis (Marshall et al., 2005; McGlashan, 1999). This symptom severity progression occurs relatively late in the neurodevelopmental trajectory, typically in late adolescence or early adulthood. During this early psychosis phase, the full syndrome is still emerging and there is some overlap of symptoms between schizophrenia-spectrum and affective psychosis disorders (bipolar, depression), making it difficult to discern between the disorders and requiring a follow-up diagnosis 6 months or more later. To distinguish between schizophrenia spectrum and affective disorders with psychosis, schizophrenia-spectrum disorder includes psychosis as the primary, enduring feature (with a 6-month duration of psychotic symptoms), whereas affective psychosis disorders have relatively brief periods of psychosis superimposed on longer periods of affective instability. Further, some individuals have concurrent severe mood symptoms and enduring psychosis, typically classified as schizo-affective, where the primary psychotic disorder is more debilitating and can occur with mild mood symptoms. In part due to this overlap early in the disorders, the field has increasingly

gone to a more dimensional approach, opposed to the strict categorical approach, in studying those experiencing a first episode of psychosis. The theory behind this approach is that there is a common neural system disruption that is leading to the presence of specific symptoms such as hallucinations or delusions regardless of the eventual categorical diagnosis (Morris & Cuthbert, 2012). Thus, when investigating the early course of psychotic disorders, it can be beneficial and informative to include all individuals presenting with a first episode of psychosis in conjunction with precise measures of symptoms and symptom dimensions.

1.2 Treatment for Psychosis

Despite decades of effort, effective treatments are still limited for this complex disorder. Current antipsychotic medications are effective against positive symptoms in most patients; however, around 30% of patients do not experience improved symptoms. Further, these medications do not seem to markedly improve negative symptoms or neurocognitive deficits (Kane, 2012). Non-pharmacological therapies, such as cognitive-behavioral therapy and cognitive enhancement therapy, appear to be neuroprotective and have a better impact on treating negative symptoms and neurocognitive deficits, particularly if initiated early in the disease course (Eack et al., 2010; McGorry et al., 2013; van der Gaag et al., 2012). Non-invasive brain stimulation (NIBS) therapies that target specific cortical regions and networks offer improvement in negative symptoms and cognitive ability in psychosis (Gupta, Kelley, Pelletier-Baldelli, & Mittal, 2018; Kennedy, Lee, & Frangou, 2018). Interventions initiated early in the disease improve functional outcome and reduce long-term treatment costs (Eack et al., 2010; Kane et al., 2016; Srihari, Shah,

& Keshavan, 2012). Thus, research that can aid in better interventions to reduce the burden on the individual and society by promoting better long-term functional outcomes is of great significance.

1.3 Cognitive Deficits in Psychosis

Cognitive deficits are a core feature of psychotic disorders that are present before psychosis, endure throughout the disorder, and are associated with long-term functional outcome (Caspi et al., 2003; Fett et al., 2011). In participants at clinical high-risk for transitioning to psychosis, those who converted to psychosis were significantly more cognitively impaired than non-converters (Seidman et al., 2010). Throughout the disorder, cognitive deficits are stable at 1 to 2 standard deviations below healthy controls (Hoff et al., 1999). One fundamental cognitive deficit is the impairment of selective attention, the ability to focus on one sensory stimulus in the presence of competing stimuli (B. Cornblatt, Obuchowski, Roberts, Pollack, & Erlenmeyer-Kimling, 1999; Kraepelin, 1889).

Attention has long been considered a major deficit in psychotic disorders. Emil Kraepelin (1850-1929), an influential psychiatrist who helped shape the modern understanding and study of psychiatric disorders, described what is now classified as schizophrenia as “dementia praecox”. He described the illness as a chronic psychotic illness that begins in early adulthood and is characterized by an early rapid cognitive deterioration manifested by the destruction of the cortex. Attention was one of these cognitive functions impacted in the disorder (Kraepelin, 1889). In contrast to Kraepelin, Eugen Blueler (1857-1939) defined dementia praecox as schizophrenia, or the split mind, as he believed the illness was defined by the splitting of, or in modern parlance the inability to integrate, different psychological functions. In his definition, Blueler argued dementia

was not a usual characteristic of the disorder but could better be explained by other primary and secondary symptoms. The primary symptoms of schizophrenia were the loss of association between cognitive processes, emotion, and behavior, and this fundamental process could lead to the secondary psychotic symptoms, such as hallucinations and delusions. Attention deficit was a main symptom of the disorder, according to Bleuler (Ashok, Baugh, & Yeragani, 2012; Bleuler, 1950). Thus, while Kraepelin and Blueler diverged in how they defined schizophrenia and the manifestation of symptoms, both recognized the centrality of attention deficits in the disorder. Novel treatments that ameliorate selective attention deficits early in the course of schizophrenia (and other manifestations of psychosis) would have great benefit for disease expression and course and are a critical unmet need in psychiatry.

Although attention is a broad construct that is affected by many processes and pathologies, it can be reduced or operationalized to evaluate specific neurobiological processes that are specifically impaired in specific diseases. In our studies of early psychosis, we examine the ability to focus on one sensory item among the myriad sensations in the sensory environment, known as selective attention.

1.4 Selective Attention

Selective attention is a cognitive process essential for facilitating task performance. Cross-modal attention, for example attending sounds while ignoring a movie or vice-versa, represents a type of selective attention well explored in cognitive psychology (e.g., Parasuraman, 1985). In humans, the neural underpinnings of this aspect of selective attention can be measured in the auditory system with high temporal resolution using electroencephalography (EEG) and

magnetoencephalography (MEG). EEG can record activity as early as 10ms from the vestibulocochlear nerve, with earliest auditory cortex activity recorded ~20ms after the sound. Late sensory processing of sounds is measured by the event-related negativity present ~100ms post-stimulus (N100) for EEG and its MEG counterpart (M100). When healthy individuals pay attention to a sound, N100/M100 amplitudes increase relative to ignore or divided attention conditions (Neelon, Williams, & Garell, 2006; Woldorff et al., 1993).

1.5 N100 in Psychosis

Individuals with schizophrenia have an impaired passive N100 response and an impaired ability to enhance the N100 with attention (Foxe et al., 2011; O'Donnell et al., 1994; Rosburg, Boutros, & Ford, 2008), demonstrating that the N100 is sensitive to both bottom-up sensory perceptual deficits and top-down executive modulation with attention in psychosis. These impairments are present as early as the first episode of psychosis. Individuals at their first episode of psychosis (FEP) have a reduced N100, though it was previously unclear if it was primarily a sensory or executive deficit in that the auditory tasks were active attention tasks (Foxe et al., 2011; Salisbury, Collins, & McCarley, 2010). It was recently demonstrated by comparing active and passive tasks that the attentional gain modulation of N100 is deficient in FEP (Ren, Fribance, Coffman, & Salisbury, 2021). Thus, N100 enhancement is an objective measure of selective attention deficits very early in psychosis. The dysfunction in N100 enhancement indexes a distributed cortical circuit involving the interaction of frontal executive and temporal auditory areas and presents a neurobiological system amenable for targeted intervention. However, it is unknown which auditory cortical areas contribute to this deficit in sensory gain, critical for both

understanding the cortical circuit deficits and for development of targeted interventions, whether employing pharmacologic or non-invasive brain stimulation (NIBS) techniques.

1.6 Advantages of MEG

In this project, the M100 was source-resolved to identify where cross-modal selective attention increased M100 gain, and where auditory sensory and attention-related deficits arise in FEP, which have not previously been directly investigated. While fMRI provides high spatial resolution, the measure of neural activity (neuro-vascular coupling) is indirect and less sensitive to changes at high temporal resolution (with a limit of around one second). EEG and MEG provide an advantage, as neural activity can be measured directly on the scale of milliseconds, necessary for the measurement of sensory processes such as the N100/M100, and the rapid modulation of these processes with attention. Both EEG and MEG measure neurophysiological activity from pyramidal cells in the cortex, but they measure distinct aspects of the activity. EEG measures extracellular currents of post-synaptic potentials, while MEG primarily measures the intracellular currents from pyramidal cells (Coffman & Salisbury, 2020). Compared to EEG, MEG provides an improved source solution for determining cortical generators inside the head from sensors outside the head because magnetic fields are unaffected by the skull and skin, while keeping the high temporal resolution needed to detect rapid neural activity (Coffman & Salisbury, 2020). Understanding the precise cortical areas underlying this impaired ability to modulate the N100/M100 with selective attention in the early disease course can provide insight to the etiology of the disorder and identify potential targets for therapeutic interventions and anatomic circuit locations for translation to animal models.

1.7 Project Overview

To define the circuit involved in auditory selective attention and underlying pathology in FEP, we utilized the combination of functional measures of MEG and structural measures of MRI. Relationships between brain function and structure were examined between FEP and psychiatrically-well individuals matched for age, gender, estimated premorbid intellect and parental socioeconomic status. There were major methodological hurdles that needed to be overcome for the project. The traditional approach of a whole-brain analysis is limiting statistically and is difficult to translate to animal models, and the most commonly used brain atlases rely on one modality to define regions and are thus unable to delineate regions accurately defined only by function and structure, such as belt regions in auditory cortex. The major methodological advances included the implementation of the Human Connectome Project pipelines and multimodal parcellation, which defines cortical region by structure and function. The implementation of these methods allowed for major analytic advances for the utility in understanding M100 attention modulation deficits in auditory cortex, impairments in the executive auditory attention network, and relating these functional abnormalities to underlying structural gray matter deficits in FEP. This is all described in detail in the following chapters.

2.0 Implementation of State-of-the-Art Infrastructure for Analysis

2.1 General Introduction

In order to study the precise cortical circuitry underlying the executive control of attention, methodological limitations needed to be addressed. Traditional approaches in human neuroimaging use either whole brain voxel-wise analysis or a region-of-interest approach. In a voxel-wise analysis, the brain volume is reconstructed from the MRI and divided into hundreds of thousands of volume pixels (or voxels), that contain the data of interest (gray matter intensity, fMRI BOLD response, etc.). These brain volume images can also be used to create cortical surfaces by tracing the boundaries of the different tissue types (gray, white, pial) in each hemisphere and constructing a surface mesh of intersecting triangles. The intersecting points between triangles on these surfaces are called vertices, and similar to voxels, they can represent information of interest when using surface-based vertex-wise analyses (Dale, Fischl, & Sereno, 1999). While this method allows for comparisons on the same spatial scale at which the MRI data were collected, it creates statistical limitations when performing whole-brain analyses, as one needs to correct for the thousands of comparisons. Further, there is no clear correspondence between a particular voxel/vertex in the cortex and anatomical and functional location in animal models, making translational findings difficult. The other common approach is to group voxels or vertices into regions of interest (ROIs), or parcels based on their anatomic location. By dividing the cortex into a limited number of regions, ROI analyses have greater statistical power than voxel-wise analyses. The gold-standard for ROI analyses is manual tracing of regions of interest on the structural MRI, but this technique is limited by reliance on structural information (i.e., sulcal-gyral boundaries).

Manual tracing is unable to delineate purely functional regions, such as primary sensory cortices or functional subregions that often are smaller than sulcal and gyral borders. For example, Heschl's gyrus in the auditory area of the temporal lobe can be traced manually, but the gyrus includes primary auditory cortex and portions of surrounding auditory belt regions (Sweet, Dorph-Petersen, & Lewis, 2005), which cannot be disentangled with standard structural MRI. Further, manually traced ROIs are time-consuming to create for each individual slice-by-slice and therefore less practical for whole brain analyses and larger datasets. Automated or semi-automated cortical parcellations are ideal for larger datasets and whole brain ROI analyses but are similarly restricted to defining regions based on structural information alone, which results in the division of cortex into coarse ROIs and an inability to parcellate smaller functional areas. Further, these traditional parcellations are based on one neurobiological property (e.g., sulcal-gyral boundaries, function, connectivity, etc.). It is not possible with these traditional methods to parcellate cortical areas that can only be defined by both structure and function (e.g., primary sensory areas).

To address this methodological issue, we used a multi-modal atlas recently developed by the Human Connectome Project (HCP). This HCP group collected high resolution T1-weighted (T1w) and T2-weighted (T2w) MRI images along with resting-state and task-based functional MRI in a total of 420 individuals. Relative cortical myelin content and functional connectivity information were derived for each vertex in the brain. Relative myelin content was calculated from the T1w/T2w ratio, which has been shown to be a relatively accurate estimate of relative myelin content in the cortex (Glasser 2011). The functional MRI data were used to derive canonical resting-state networks. The motivation for including these multimodal data was that each modality offers strengths and weaknesses in aligning and defining different cortical regions. For example, in general, primary sensory areas (e.g., auditory, visual, and somatosensory cortices) are more

heavily myelinated than association areas (e.g., prefrontal, parietal, and insular cortices) (Glasser 2011). Thus, while myelination information is helpful for definition of primary sensory regions, the lightly myelinated association regions are better defined by functional connectivity information (Turner 2019). This myelination and connectivity information is used to drive alignment between individuals with a registration technique called multimodal surface matching (MSM). Traditionally, alignment of cortical surfaces was limited to one modality, such as curvature, but this flexible MSM framework allows for the addition of other useful information such as resting state connectivity to help drive alignment, improving the cortical surface alignment between individuals. This improved alignment decreases variability of areal definition between individuals and increases confidence of correct correspondence of areas between individuals.

In addition to the improved alignment feature, the HCP used the structural and functional information to define regions and parcellate the cortex into 360 quasi-functional areas. To define areas within the atlas, the HCP calculated the rate-of-change in each modality at each spatial location, with the underlying assumption that locations with transitions in multiple modalities make strong candidates for region boundaries. Parcellated areas had borders that reflected significant differences by at least two multimodal features. For example, in the auditory cortex, the HCP parcellation separates primary auditory cortex (A1), medial belt (MBelt), lateral belt (LBelt), and parabelt (PBelt). Primary auditory cortex is bordered by MBelt and LBelt. A1 was defined by being more heavily myelinated than both MBelt and LBelt. In addition, A1 has significantly different functional connectivity than LBelt and significantly different connectivity with the Medial Geniculate Nucleus than MBelt. Then, compared to PBelt, LBelt is significantly more myelinated and has significantly stronger connectivity with the MGN (Glasser 2016). These comparisons were conducted by an algorithm to delineate potential area borders, followed by

examination and confirmation from two neuroanatomists. For complete details see (Glasser et al., 2016). The HCP multi-modal parcellation (HCP-MMP) provides the most precise and functionally relevant regions of interest to investigate structure and/or function in the human cortex. As these methods and the parcellation were released for public use, we implemented them for the use on the analyses in early psychosis.

To demonstrate validity for the use of these novel pipelines and parcellation, we first explored if using these cutting-edge techniques could identify very specific gray matter deficits in first-episode schizophrenia, at a specificity not previously achieved. To accomplish this, we first investigated cortical gray matter thickness differences between individuals with first episode schizophrenia and matched healthy controls (HC), using the HCP-MMP to precisely parcellate the whole-brain and define our regions of interest. The goal of this study was to demonstrate the HCP pipelines and HCP-MMP were able to identify very specific regions with gray matter loss in early psychosis and whether gray matter within these regions correlates with symptoms and cognition.

2.2 Parahippocampal Area 3 Gray Matter is Reduced in First-Episode Schizophrenia-Spectrum: Discovery and Replication Samples

The following is adapted from a published manuscript for this dissertation.

Curtis MT, Coffman BA, & Salisbury DF. Parahippocampal area three gray matter is reduced in first-episode schizophrenia spectrum: Discovery and replication samples. Hum Brain Mapp. 2021;42(3):724-736. PMID: 33219733

2.2.1 Introduction

Schizophrenia-spectrum disorder is associated with widespread reductions in cortical and subcortical gray matter. The most commonly reported cortical volume reductions in chronic schizophrenia-spectrum are in the prefrontal, parietal, temporal, and parahippocampal cortices, while subcortical volume loss is frequently detected in the amygdala, hippocampus, and thalamus (Birur, Kraguljac, Shelton, & Lahti, 2017; Cropley et al., 2017; Goldman et al., 2009; Haijma et al., 2013; Rimol et al., 2010; Shenton, Dickey, Frumin, & McCarley, 2001; T. G. van Erp et al., 2016). Widespread cortical thinning is also present in chronic schizophrenia with the most pronounced thinning observed in the frontal and temporal lobes (Rimol et al., 2010; Rimol et al., 2012; T. G. M. van Erp et al., 2018; van Haren et al., 2011). Specific regional gray matter differences emerge early in the disorder. In first-episode schizophrenia-spectrum disorder (FESz), meta-analyses report reduced volumes in the hippocampus, insula, and anterior cingulate (Ellison-Wright, Glahn, Laird, Thelen, & Bullmore, 2008; Vita, De Peri, Silenzi, & Dieci, 2006). Gray matter volume deficits are also often reported in temporal and prefrontal cortical areas at the first episode (Hirayasu, McCarley, et al., 2000; Hirayasu et al., 2001; Kasai, Shenton, Salisbury, Hirayasu, Onitsuka, et al., 2003; Keshavan et al., 1998; C. U. Lee et al., 2002), though some studies report nonsignificant changes in these areas (Cahn et al., 2002; Molina, Sanz, Sarramea, Benito, & Palomo, 2004). Frontal and temporal cortices are most consistently thinner in FESz, while thickness differences in other cortical regions (i.e., parietal, anterior cingulate, and medial temporal cortices) are less consistently reported (Narr et al., 2005; Schultz et al., 2010; Sprooten et al., 2013; van Haren et al., 2011). In the first few years of the disorder, there is widespread progressive gray matter volume decline in the bilateral frontal, parietal, cingulate, and superior temporal cortex (Asami et al., 2012; Kasai, Shenton, Salisbury, Hirayasu, Onitsuka, et al., 2003). Similarly, the

cortex experiences widespread thinning, most substantially in frontal and temporal lobes (van Haren et al., 2011). Thus, gray matter deficits are present at the first episode of schizophrenia-spectrum and there is a progressive decline throughout the disorder.

Gray matter differences are reported as early as the prodrome for psychosis. Compared to non-converters, individuals at clinical high-risk for psychosis (CHR) who later convert to psychosis have less gray matter volume in lateral and medial temporal, frontal, cingulate, and bilateral insula cortices (Mechelli et al., 2011; Pantelis et al., 2003; Takahashi, Wood, Yung, Phillips, et al., 2009). Further, CHR converters experience a progressive decrease of gray matter volumes in frontal, insular, fusiform, and parahippocampal cortices (Pantelis et al., 2003; Takahashi, Wood, Yung, Phillips, et al., 2009). It remains inconclusive if there are cortical thickness deficits in CHR who later convert to psychosis at baseline (Cannon et al., 2015; Chung et al., 2019; Tognin et al., 2014), however, those who later convert experience a progressive thinning in right frontal cortical regions (Cannon et al., 2015). While there is accumulating evidence of progressive gray matter deficits in schizophrenia-spectrum disorder that are present in the prodrome and continue throughout the disorder, the evidence is limited to relatively large cortical regions, such as entire anatomical gyri, and thus it remains unresolved which specific functional subregions are impacted early in the disorder.

As schizophrenia is associated with early course progressive gray matter loss, it is particularly important to study this population as early as possible in the disease course to capture which areas are impacted when initial pathology is emerging. While many FESz studies report on individuals within one year (or more) of their first hospitalization (DeLisi et al., 1997; Hirayasu, McCarley, et al., 2000; C. U. Lee et al., 2002), the individuals in this study were at their first clinical contact for psychosis, with less than 2 months of lifetime antipsychotic medication

exposure. This project is thus uniquely situated to investigate differences very early after the onset of full psychosis and has the marked advantage of utilizing a discovery and a replication sample for statistical control.

The uncertainty regarding which specific cortical regions are affected early in the disorder may also reflect methodological limitations. Previous studies investigating gray matter differences performed voxel-based morphometry (VBM) or region of interest (ROI) analyses, either manually-edited or automated. VBM makes comparisons at each of the thousands of voxels in the MRI brain reconstruction, resulting in inflated type-2 error due to multiple comparisons and a lack of sensitivity to small effect sizes, which may be expected in the early course of schizophrenia. By dividing the cortex into a limited number of regions, ROI analyses have greater statistical power than voxel-wise analyses. The gold-standard for gray matter ROI analyses is manual tracing of regions of interest, but this technique is limited by reliance on anatomical information and are time-consuming to create, and therefore they are less practical for whole brain analyses and larger datasets. Automated or semi-automated cortical are similarly restricted to defining regions based on structural information alone, which results in the division of cortex into large ROIs and an inability to parcellate smaller functional areas. It is not possible with these traditional methods to parcellate cortical areas that can only be defined by both structure and function (i.e., primary sensory areas). We used a multi-modal atlas developed by the Human Connectome Project (HCP), which uses structural and functional information to parcellate the cortex into 360 areas (Glasser et al., 2016). The HCP multi-modal parcellation (HCP-MMP) provides the most precise and functionally relevant regions of interest to investigate gray matter deficits in FESz (or, for that matter, any disorder).

Likely in concert with the early gray matter changes, symptoms, particularly auditory perceptual abnormalities among the attenuated positive symptoms, and cognitive deficits begin to emerge prior to full psychosis. Auditory verbal hallucinations (AVH) are a common and debilitating symptom of schizophrenia present in >70% of FESz (Salisbury, Kohler, Shenton, & McCarley, 2019). AVH likely involve a number of areas that are also engaged in language, memory, and auditory processing, such as the striatum, Broca's area, Wernicke's area, anterior cingulate, medial temporal lobe, and superior temporal gyrus (Ćurčić-Blake et al., 2017; Dierks et al., 1999; Hoffman, 1986; Jardri, Pouchet, Pins, & Thomas, 2011; Raij et al., 2009), and gray matter deficits within the superior temporal gyrus are related to hallucinations in chronic schizophrenia (Asami et al., 2012; Barta, Pearlson, Powers, Richards, & Tune, 1990; Shenton et al., 2001). Similarly, delusions and thought disorder involve the anterior cingulate and medial temporal lobe (Epstein, Stern, & Silbersweig, 1999; Lahti et al., 2006; Prasad, Rohm, & Keshavan, 2004; Shenton et al., 1992), and gray matter deficits in the STG, anterior cingulate, and medial temporal lobe are related to the severity of delusions and thought disorder in chronic schizophrenia (Asami et al., 2012; Shenton et al., 1992). Cognitive deficits are also a core feature of schizophrenia (Green & Nuechterlein, 1999; McCleery et al., 2015; Seidman et al., 2010). Gray matter in temporal and frontal lobes are related to cognitive performance, such as working memory, verbal recall, and semantic fluency in chronic schizophrenia and in first-episode psychosis (schizophrenia-spectrum and affective psychoses) (Baare et al., 1999; Nestor et al., 1993; Radua et al., 2012; Shenton et al., 2001). While it is evident that gray matter is related to symptoms and cognitive performance in chronic schizophrenia (Shenton et al., 2001; T. G. M. van Erp et al., 2018), these relationships are not commonly found or reported in the first episode schizophrenia-spectrum (Crespo-Facorro et al., 2011; Hirayasu, McCarley, et al., 2000; Hirayasu

et al., 2001; C. U. Lee et al., 2002). For this reason, we were interested in performing exploratory correlations with symptoms, with a focus on hallucinations, delusions, and thought disorder, and cognitive domains typically impaired in schizophrenia-spectrum disorder.

The aim of this study was to determine which specific brain structures show gray matter deficits very early in schizophrenia-spectrum disorder and how such gray matter deficits relate to cognition and symptoms. To examine differences early in the disease course, this study investigated 2 different first episode schizophrenia-spectrum (FESz) samples. In the discovery sample, the HCP-MMP atlas was used to estimate gray matter thickness in 180 bilateral cortical ROIs. Differences in gray matter thickness were examined between FESz and matched healthy controls (HC). To investigate whether these reductions were replicated in an independent sample of FESz, cortical regions that were thinner in FESz in the discovery sample were used as ROIs in a replication sample. High-resolution MRI scans were acquired, and gray matter differences in these ROIs were again examined between FESz and matched HC. Finally, we examined exploratory associations with symptoms measured with the Positive and Negative Syndrome Scale (PANSS) and cognitive measures from the MATRICS consensus cognitive battery (MCCB).

2.2.2 Methods: Discovery Sample

2.2.2.1 Participants

All participants were recruited from Western Psychiatric Hospital (WPH) inpatient and outpatient services. Participants included 31 FESz individuals (paranoid: n=8; undifferentiated: n=5; residual: n=1; schizoaffective: n=5; schizophreniform: n=5; psychotic disorder NOS: n=7;) within their first episode of psychosis with less than 2 months of lifetime antipsychotic medication exposure, and 31 healthy controls (HC). None of the participants had a history of concussion or

head injury with sequelae, history of alcohol or drug addiction or detox in the last five years, or neurological comorbidity. Groups were matched for age, gender, parental social economic status, and premorbid IQ, measured by the vocabulary component of the Wechsler Abbreviated Scale of Intelligence (WASI) (**Table 1**). The work described was carried out in accordance with The Code of Ethics of the World Medical Association (Declaration of Helsinki) for experiments involving humans. All participants provided informed consent and were paid for participation.

Socioeconomic status (SES) for all participants and their parents was measured with the 4-factor Hollingshead Scale. FESz participants' diagnoses were based on the Structured Clinical Interview for DSM-IV (SCID-P) (First, Spitzer, Gibbon, & Williams, 1997) and were confirmed six months after initial clinical assessment (5 were lost to follow up). Symptoms were rated using the PANSS for 25 of the 31 FESz (**Table 1**) (Kay, Fiszbein, & Opler, 1987). Cognitive ability was assessed with the MCCB (Nuechterlein et al., 2008). MCCB was collected for all participants (HC and FESz) except one FESz, who was unable to complete testing. All tests were conducted by an expert diagnostician.

Just over half of the FESz participants were medicated (17/31, 54.8%) (range=1-56 days, median=16.0 days). Gray matter thickness was not different between medicated (n=19) and unmedicated (n=14) FESz, and gray matter thickness did not correlate with chlorpromazine (CPZ) equivalent dose or duration of medication use (p values>0.1). These analyses suggest gray matter was unaffected by medication, which will not be discussed further.

Table 1. Experiment 1: Sample 1 Demographic, Neuropsychological, and Clinical Information

Descriptive and inferential statistics for healthy controls (HC) and first-episode schizophrenia spectrum (FESz).

FESz and HC groups were matched for age, gender, PSES, and WASI Vocab

	Mean±SD			
	HC (n=31)	FESz (n=31)	*p*	X^2
Sociodemographic data				
Age (years)	21.2 ± 3.1	21.5 ± 4.4	.83	
Gender (M/F)	20/11	20/11	1.0	1.0
SES	33.3 ± 13.5	27.0 ± 12.0	.06	
Parental SES	49.2 ± 12.6	44.3 ± 11.5	.11	
Neuopsychological tests				
WASI Vocab (t-score)	50.8 ± 8.1	53.7 ± 8.6	.18	
MCCB-total	48.9 ± 6.5	39.4 ± 14.0	.001*	
Symptoms				
PANSS-total		70.6 ± 11.8		
PANSS-positive		18.3 ± 4.9		
PANSS-negative		16.0 ± 4.1		
PANSS-general		36.3 ± 6.6		
Medication data				
Medicated/unmedicated		17/14		
Cpz. Equivalent dose (mg)		223 ± 147		
Duration (days)		20.3 ± 16.8		

Note: SES = socioeconomic status. WASI = Wechsler Abbreviated Scale of Intelligence Vocabulary t score. MCCB =MATRICS Consensus Cognitive Battery composite scaled t score. PANSS = Positive and Negative Syndrome Scale. Cpz Equivalent Dose= chlorpromazine equivalents.

* denotes significance ($p<.05$).

2.2.2.2 Data Acquisition & Processing

MRI data were acquired with a Siemens Tim Trio using a 32-channel phase array head coil. Sagittal T1-weighted anatomical MR images were obtained with a multi-echo 3D MPRAGE sequence [TR/TE/TI = 2530/1.74, 3.6, 5.46, 7.32/1260 ms, flip angle = 7°, field of view (FOV) = 220 x 220 mm, 1 mm isotropic voxel size, 176 slices, GRAPPA acceleration factor = 2]. FreeSurfer (stable v6.0) was used for MRI processing (Dale et al., 1999; Fischl & Dale, 2000; Fischl, Sereno,

& Dale, 1999). Briefly, processing involved registration to MNI space, intensity normalization, skull stripping, segmentation of white matter, and the generation of white and pial surfaces.

Cortical thickness was estimated for 180 bilateral ROIs using the HCP-MMP atlas (Glasser et al., 2016). Using the HCP workbench, the HCP-MMP cortical parcellation was resampled to fsaverage space. In Freesurfer, the parcellation was applied to individual data (see HCP Users FAQ (https://wiki.humanconnectome.org/display/PublicData/HCP+Users+FAQ#HCPUsersFAQ-9.HowdoImapdatabetweenFreeSurferandHCP?)). Cortical thickness was calculated as the average distance from each point of the WM surface within each ROI to the closest point on the pial surface.

2.2.2.3 Analysis

Group demographics were compared using independent samples t-test and chi-square tests where appropriate. Gray matter thickness compared between groups using independent samples t-tests. To minimize type II error, we first performed an exploratory analysis by identifying regions with significant gray matter thickness differences of at least medium effect size (Cohen's $d>0.5$). Benjamini-Hochberg False Discovery Rate (FDR) correction was applied to correct for multiple comparisons (360 comparisons).

2.2.3 Methods: Independent Replication Sample

All methods and procedures were identical to Sample 1 with the following differences.

2.2.3.1 Participants

Participants included new, independent groups of FESz and healthy controls (HC). This included 23 FESz individuals (paranoid: n=10; undifferentiated: n=9; schizophreniform: n=2; psychotic disorder NOS: n=2;) and 32 matched HC. Symptoms were rated using the PANSS for 22 of the 23 FESz. Cognitive ability was assessed with the MCCB and was collected for all participants (**Table 2**).

Table 2. Experiment 1: Sample 2 Demographic, Neuropsychological, and Clinical Information

Descriptive and inferential statistics for healthy controls (HC) and first-episode schizophrenia spectrum (FESz).

FESz and HC groups were matched for age, gender, PSES, and WASI Vocab

	Mean±SD			
	HC (n=32)	FESz (n=23)	*p*	X^2
Sociodemographic data				
Age (years)	25.4 ± 5.6	24.0 ± 5.0	.35	
Gender (M/F)	21/11	17/6	.52	.51
SES	42.0 ± 14.4	32.2 ± 16.1	.03*	
Parental SES	48.8 ± 10.0	43.4 ± 15.1	.13	
Neuopsychological tests				
WASI Vocab T-score	52.5 ± 6.8	49.2 ± 100.5	.17	
MCCB-total	47.7 ± 6.5	29.7 ± 14.4	<.001*	
Symptoms				
PANSS-total		82.8 ± 15.0		
PANSS-positive		21.5 ± 5.3		
PANSS-negative		19.4 ± 4.9		
PANSS-general		42.2 ± 8.0		
Medication data				
Medicated/unmedicated		19/4		
Cpz. Equivalent dose (mg)		253 ± 140		
Duration (days)		22.2 ± 17.6		

Note: SES = socioeconomic status. WASI = Wechsler Abbreviated Scale of Intelligence Vocabulary t score. MCCB =MATRICS Consensus Cognitive Battery composite scaled t score. PANSS = Positive and Negative Syndrome Scale. Cpz Equivalent Dose= chlorpromazine equivalents.

* denotes significance (p<.05).

2.2.3.2 Data Acquisition & Processing

High-resolution MRI data were acquired on a Siemens 3T MAGNETOM Prisma scanner using a 32-channel phase array head coil. Sagittal T1-weighted anatomical MR images were obtained with a 3D MPRAGE sequence [TR/TE/TI = 2400/2.22/1000 ms, flip angle = 7°, field of view (FOV) = 256x240 mm, 0.8 mm isotropic voxel size, 208 slices, GRAPPA acceleration factor = 2]. T2-weighted T2-SPACE images were obtained [TR=3200 ms TE=563 ms, FOV = 256x240,

0.8 mm isotropic voxel size, 208 slices]. A standard fieldmap [TR=731ms, TE= 4.92/7.38, FOV=208x180, 2.0mm voxel size, 72 slices] was collected for correcting readout distortion in the T1w and T2w images. Ten minutes of eyes-open (passive crosshair viewing) resting state BOLD fMRI data were acquired using a multiband pulse sequence [TR =800 ms, TE =37 ms, multiband factor=8, flip angle = 52°, FOV=208x208mm, voxel size = 2.0 mm3, 72 slices]. A single-band reference image with no slice acceleration was acquired at the beginning of each run to improve registrations. Finally, two spin echo EPI images (TR=8000ms, TE=66ms, flip angle=90, FOV=208x208mm, 2.0mm voxel size, 72 slices) with reversed phase encoding directions were acquired.

The publicly available HCP-pipelines (https://github.com/Washington-University/HCPpipelines) were used for MRI processing (detailed in Glasser et al., 2013). The structural images were corrected for gradient nonlinearity, readout, and bias field, followed by AC-PC alignment. Myelin maps were created by dividing the T1w image by the T2w image. Native space images were used to generate white and pial surfaces with Freesurfer software (Dale et al., 1999; Fischl & Dale, 2000; Fischl et al., 1999). Surfaces were refined using T2w data, which improves pial and white surface reconstructions, ultimately improving cortical thickness measurements (Glasser, Goyal, Preuss, Raichle, & Van Essen, 2014; Glasser et al., 2013). Thickness was calculated in FreeSurfer using the improved white and pial surfaces. Then, the individual's native-mesh surfaces were registered with a multimodal surface matching (MSM) algorithm with MSMsulc to the Conte69 folding-based template (Robinson et al., 2014; Van Essen, Glasser, Dierker, Harwell, & Coalson, 2012).

The functional resting-state data were first corrected for gradient-nonlinearity. A 6 DOF FLIRT registration of each frame to the single-band reference image was used to correct for

motion. The reverse phase spin-echo images were used to correct functional distortion. The single band reference image was registered to the T1w image with FreeSurfer's BBRegister (Greve & Fischl, 2009). All the transforms and distortion correction were applied in a single resampling step. The data were brain masked and intensity normalized to a 4D whole brain mean of 10,000. Then, a voxel to surface mapping was performed to sample the volumetric fMRI data to the individual's native surfaces, which were subsequently resampled to a standard 32k fs_LR surface. The ICA+FIX pipeline was used to remove artifactual noise (Griffanti et al., 2014; Salimi-Khorshidi et al., 2014). Finally, individual subjects were registered to a group average atlas surface using a two-stage process based on the multimodal surface matching (MSM) algorithm (Robinson et al., 2014). The first stage was driven by cortical folding patterns, and the second stage utilized cortical areal features (myelin, resting-state network maps, and topographic maps) (Glasser et al., 2016). The group average HCP-MMP was applied to individuals' MRI data and mapped to individuals' native space where thicknesses were computed.

2.2.3.3 Analysis

The 18 regions that were reduced (uncorrected) in the discovery sample were used as ROIs for the analysis in the replication sample. Differences in gray matter thickness between groups were compared using one-tailed independent samples t-tests. Benjamini-Hochberg False Discovery Rate (FDR) correction was then applied to correct for multiple comparisons (18 comparisons).

2.2.4 Methods: Correlations with Symptoms and Cognition

To investigate relationships among replicated gray matter thickness reductions, symptoms, and cognition, thickness data from each dataset were normalized using z-scores, which were calculated separately for each sample. Spearman's correlations were used to examine relationships between gray matter thickness, PANSS scores, and MCCB gender- and age-normalized t-scores. We report uncorrected exploratory correlations ($p<0.05$).

2.2.5 Results: Discovery Sample

2.2.5.1 Uncorrected Cortical Thickness

Eighteen cortical regions were thinner in FESz compared to HC with at least medium effect size ($p<.05$, Cohen's $d>0.5$). Thinner gray matter in FESz was identified bilaterally in the parahippocampal gyrus (PHA2, PHA3), subgenual anterior cingulate cortex (area 25), and prostriate cortex (ProS). In the left hemisphere, FESz had thinner gray matter in the rostral premotor area (6r), left frontal operculum (FOP1), temporal pole (TGv), cingulate motor cortex (24dd), and anterior ventral insula (AVI). In the right hemisphere, FESz had thinner gray matter in the right Brodmann area 9 in prefrontal cortex (9a, 9m), parahippocampal area 1 (PHA1), posterior operculum (OP2-3), and ventral visual complex (VVC) (**Table 3, Figure 1**).

2.2.5.2 FDR-Corrected Cortical Thickness

After using FDR to correct for multiple comparisons, two regions remained significantly reduced relative to HC. The left parahippocampal area 3 (PHA3) was significantly thinner ($p<0.001$, $q<0.05$), as was the right PHA3 ($p<0.001$, $q<0.05$) (**Table 3, Figure 1**).

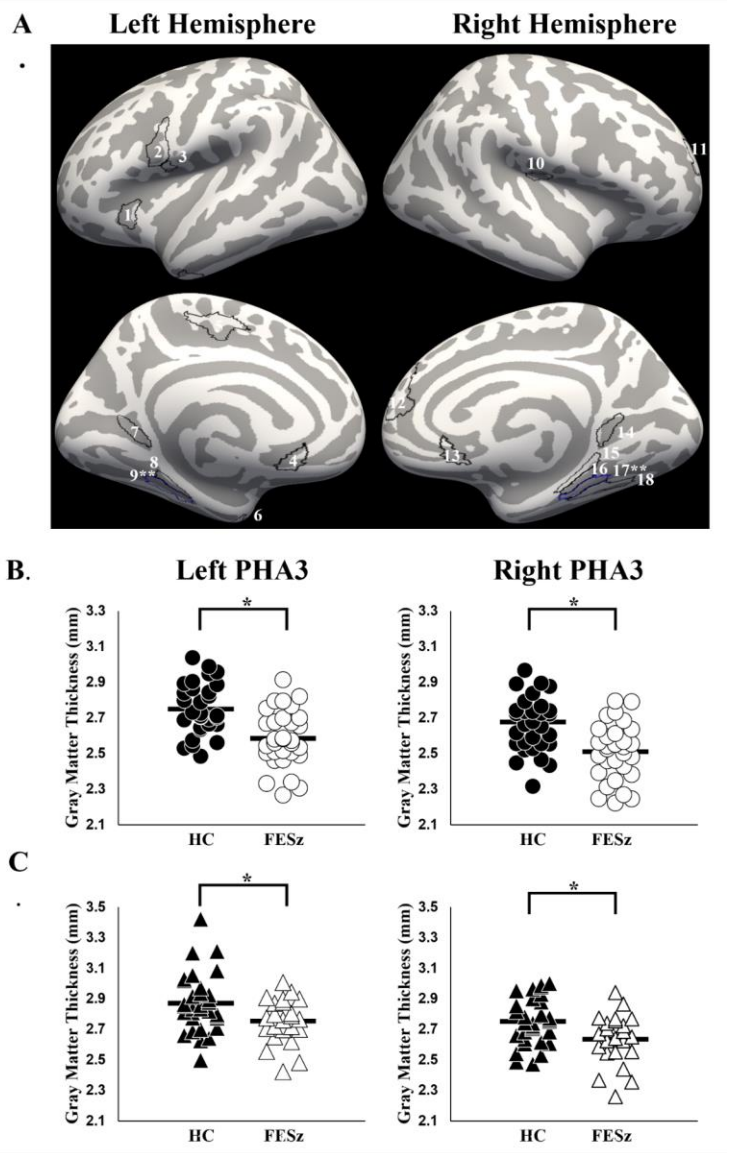

Figure 1. Experiment 1 Gray Matter Thickness Differences.

A. Outlines of the areas that were thinner in FESz with a moderate effect size (Cohen's d ≥0.5) in the discovery sample. Bilateral PHA3 is outlined in blue. Refer to Table 3 for region names associated with the numerical indices. B. After FDR correction for multiple comparisons (q<0.05), the left and right parahippocampal area 3 (PHA3) were significantly thinner in FESz. C. After FDR correction in the replication sample, left and right PHA3 were significantly thinner in FESz. ** denotes q<.05. * denotes p<.05.

Table 3. Experiment 1: Sample 1 Gray Matter Thickness Reductions in FESz.

Gray matter thickness in mm (mean±SD) differences between HC and FESz with at least moderate effect sizes (Cohen's d ≥0.5).

Brain Area	Mean±SD HC (n=31)	FESz (n=31)	*t*	*p*	Cohen's *d*
Left Hemisphere					
1. AVI	2.86 ± 0.16	2.77 ± 0.19	2.06	0.044	0.51
2. 6r	2.83 ± 0.15	2.72 ± 0.17	2.66	0.010	0.69
3. FOP1	3.06 ± 0.18	2.95 ± 0.23	2.02	0.048	0.53
4. Area 25	3.10 ± 0.32	2.95 ± 0.22	2.07	0.043	0.55
5. 24dd	2.77 ± 0.15	2.69 ± 0.17	2.07	0.042	0.50
6. TGv	3.48 ± 0.19	3.37 ± 0.19	2.48	0.016	0.58
7. ProS	2.25 ± 0.27	2.12 ± 0.19	2.02	0.047	0.56
8. PHA2	2.51 ± 0.17	2.38 ± 0.19	2.85	0.006	0.78
9. PHA3	2.75 ± 0.14	2.59 ± 0.16	4.33	<0.001*	1.06
Right Hemisphere					
10. OP2-3	2.63 ± 0.13	2.54 ± 0.16	2.55	0.013	0.62
11. 9a	2.64 ± 0.19	2.53 ± 0.24	2.10	0.040	0.51
12. 9m	2.85 ± 0.14	2.77 ± 0.17	2.04	0.046	0.51
13. Area 25	3.16 ± 0.35	2.98 ± 0.30	2.23	0.029	0.55
14. ProS	2.42 ± 0.27	2.27 ± 0.23	2.30	0.025	0.60
15. PHA1	3.02 ± 0.24	2.88 ± 0.29	2.10	0.040	0.53
16. PHA2	2.46 ± 0.21	2.33 ± 0.17	2.90	0.005	0.68
17. PHA3	2.68 ± 0.17	2.51 ± 0.16	4.01	<0.001*	1.03
18. VVC	2.90 ± 0.15	2.80 ± 0.20	2.25	0.028	0.57

Abbreviations : AVI, anterior ventral insula; 6r, rostral premotor area 6; FOP1, frontal opercular area 1; Area 25, subgeneal area 25; 24dd, dorsal midcingulate cortex area 24d; TGv, temporal gyrus ventral; ProS, prostriate area; PHA2, parahippocampal area 2; PHA3, parahippocampal area 3; OP2-3, posterior opercular area 2-3; 9a, dorsolateral prefrontal area 9 anterior; 9m, dorsolateral prefrontal area 9 medial; PHA1, parahippocampal area 1; VVC, ventral visual complex

2.2.6 Results: Replication Sample

After FDR correction for multiple comparisons (q=.05), four regions remained significantly thinner in FESz. The left and right PHA2 and the left and right PHA3 were significantly thinner in FESz (p's<0.01, q<0.05) (**Table 4**).

Table 4. Experiment 1: Sample 2 Gray Matter Thickness Reductions in FESz.

Gray matter thickness in mm (mean±SD) differences between HC and FESz from the ROIs that were reduced sample 1. One-tailed hypotheses (HC>FESz) were used.

	Mean±SD				
Brain Area	HC (n=32)	FESz (n=23)	*t*	*p*	Cohen's *d*
Left Hemisphere					
1. AVI	3.04 ± 0.21	2.96 ± 0.17	1.57	0.062	0.42
2. 6r	2.80 ± 0.13	2.80 ± 0.16	-0.20	0.423	0.04
3. FOP1	2.98 ± 0.19	2.98 ± 0.24	-0.06	0.475	0.02
4. Area 25	3.21 ± 0.26	3.12 ± 0.22	1.41	0.082	0.37
5. 24dd	2.86 ± 0.17	2.77 ± 0.16	2.00	0.025	0.55
6. TGv	3.29 ± 0.16	3.23 ± 0.27	0.98	0.166	0.27
7. ProS	2.20 ± 0.20	2.16 ± 0.25	0.70	0.243	0.18
8. PHA2	2.54 ± 0.25	2.31 ± 0.22	3.44	<0.001*	0.98
9. PHA3	2.87 ± 0.19	2.75 ± 0.15	2.48	0.008*	0.70
Right Hemisphere					
10. OP2-3	2.66 ± 0.19	2.69 ± 0.19	-0.67	0.252	0.16
11. 9a	2.61 ± 0.17	2.61 ± 0.23	0.03	0.489	0.00
12. 9m	3.04 ± 0.19	3.09 ± 0.19	-0.96	0.170	0.26
13. Area 25	3.24 ± 0.22	3.16 ± 0.35	0.98	0.166	0.27
14. ProS	2.35 ± 0.26	2.24 ± 0.25	1.44	0.078	0.43
15. PHA1	2.86 ± 0.31	2.80 ± 0.28	0.79	0.216	0.20
16. PHA2	2.38 ± 0.21	2.20 ± 0.18	3.39	<0.001*	0.92
17. PHA3	2.75 ± 0.15	2.63 ± 0.16	2.75	0.004*	0.77
18. VVC	3.00 ± 0.16	2.96 ± 0.15	0.95	0.173	0.26

Abbreviations : AVI, anterior ventral insula; 6r, rostral premotor area 6; FOP1, frontal opercular area 1; Area 25, subgeneal area 25; 24dd, dorsal midcingulate cortex area 24d; TGv, temporal gyrus ventral; ProS, prostriate area; PHA2, parahippocampal area 2; PHA3, parahippocampal area 3; OP2-3, posterior opercular area 2-3; 9a, dorsolateral prefrontal area 9 anterior; 9m, dorsolateral prefrontal area 9 medial; PHA1, parahippocampal area 1; VVC, ventral visual complex

* denotes comparisons that survived FDR correction (*q*=.05)

2.2.7 Results: Exploratory Correlations with Symptoms and Cognition

In FESz, left PHA3 was significantly positively associated with hallucinatory behavior (p<.05). In FESz, right PHA3 was significantly positively related to processing speed, working memory, and verbal learning (p<.05). There were no other significant correlations with any other PANSS or MCCB scores in FESz or HC (p's>0.05) (**Table 5, Figure 2**).

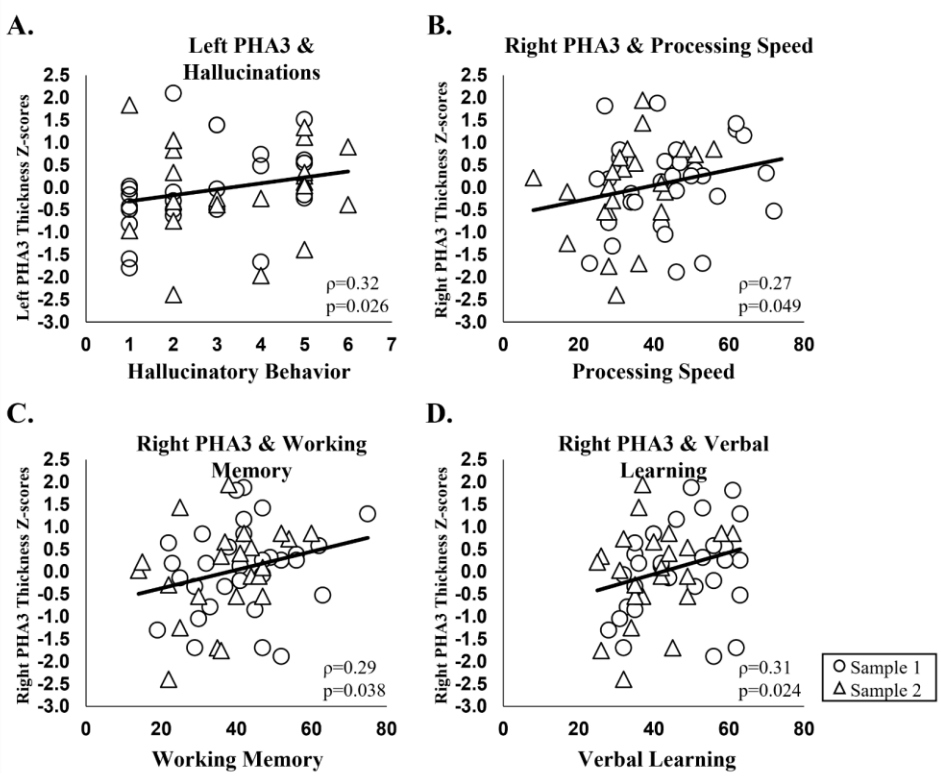

Figure 2. Experiment 1 Exploratory Correlations.

A. Thinner left PHA3 was related to lower hallucinatory behavior scores in FESz. B. Thinner right PHA3 was related to deficits in processing speed, working memory (C.), and verbal learning (D.) Spearman's correlations were used. p<.05.

Table 5. Experiment 1: Exploratory Correlations with Symptoms and Cognitive Ability in FESz.

Relationships between PHA3 gray matter and both PANSS and MCCB gender- and age-normalized t-scores.

Brain Area	ρ	*p*
Left PHA3		
PANSS		
Total	0.11	0.451
Positive	0.13	0.379
Delusions (P1)	0.23	0.127
Hallucinations (P3)	0.32	0.026*
Unusual Thought Content (G9)	0.22	0.146
Negative	0.01	0.968
General	0.09	0.529
MCCB		
MCCB Composite	0.07	0.620
Speed of Processing	0.09	0.545
Attention/Vigilance	0.03	0.821
Working Memory	0.09	0.631
Verbal Learning	0.11	0.429
Visual Learning	-0.01	0.920
Reasoning and Problem Solving	0.08	0.579
Social Cognition	-0.05	0.725
Right PHA3		
PANSS		
Total	-0.10	0.486
Positive	-0.01	0.976
Delusions (P1)	-0.03	0.828
Hallucinations (P3)	0.22	0.132
Unusual Thought Content (G9)	0.05	0.731
Negative	-0.12	0.431
General	-0.08	0.603
MCCB		
Composite	0.26	0.061
Speed of Processing	0.27	0.049*
Attention/Vigilance	0.17	0.232
Working Memory	0.28	0.038*
Verbal Learning	0.31	0.024*
Visual Learning	0.05	0.752
Reasoning and Problem Solving	0.13	0.357
Social Cognition	0.03	0.820

* denotes significance ($p<.05$)

2.2.8 Discussion

This study was the first to utilize the HCP-MMP atlas to investigate cortical gray matter thickness abnormalities in FESz. The HCP-MMP improves upon traditional, strictly anatomical parcellations as it divides cortex into functionally relevant ROIs. Using this more precise parcellation in a discovery sample, we were able to identify several specific cortical areas that were thinner in FESz. A specific subregion of the parahippocampal gyrus (PHA3) was robustly thinner bilaterally in FESz, surviving conservative correction for multiple comparisons. This finding was replicated in the independent replication sample, as the regions to survive correction for multiple comparisons were bilateral parahippocampal area 2 (PHA2) and PHA3. While many previous studies of first-episode patients report on individuals within the first year following first hospitalization (DeLisi et al., 1997; Hirayasu, McCarley, et al., 2000; C. U. Lee et al., 2002), the individuals in this study were within their first-episode of psychosis, but their symptoms had not necessarily progressed to the severity of needing hospitalization, and participants had less than 2 months of lifetime antipsychotic medication exposure. This allowed us to probe gray matter deficits very early in the disorder. Thus, the findings indicate these specific parahippocampal subregions are particularly impacted very early in the disease course and thus may play a critical role in the etiology of schizophrenia-spectrum disorder.

Parahippocampal gray matter has previously been shown to be reduced in chronic and first-episode schizophrenia and in individuals at high risk for psychosis (Borgwardt et al., 2007; Jung et al., 2011; Mechelli et al., 2011; Meisenzahl et al., 2008; Shenton et al., 2001; Tognin et al., 2014; T. G. M. van Erp et al., 2018; van Haren et al., 2011). However, parahippocampal gyrus gray matter deficits are not consistently observed in schizophrenia-spectrum disorder or to the extent observed in this study (Sprooten et al., 2013; T. G. M. van Erp et al., 2018). The large multi-

site ENIGMA metanalysis reported a small effect size for the parahippocampal gyrus reduction in schizophrenia (T. G. M. van Erp et al., 2018). The current study had several differences that likely contributed to the ability to detect a much larger effect size in the parahippocampal areas. An advantage was the ability to maintain precision without the need to average across heterogenous samples with varying scan quality. In addition, we had the advantage of high-resolution MRI scans, particularly in the replication sample, and improved surface reconstructions with the HCP pipelines improving cortical thickness measurements. Finally, the novel use of the HCP-MMP divides the parahippocampal gyrus into three functional subregions, instead of averaging across a large area that includes all parahippocampal subregions and additional cortex. Thus, it allows a more precise detection of thickness within each specific subregion.

The current study did not find thickness differences in other temporal or frontal regions that are commonly reported in FESz (Narr et al., 2005; Schultz et al., 2010; Sprooten et al., 2013; van Haren et al., 2011). This may in part be explained by methodological differences. Previous studies have either used structural based regions of interest or all cortical vertices, while this study used new regions parcellated by both structure and function. Further, the participants were very early in the disease course and may not show significant gray matter deficits in other subregions until later. Future longitudinal analyses can investigate this directly.

As less gray matter in schizophrenia is likely due to neuropil loss, rather than neuronal loss (Selemon & Goldman-Rakic, 1999), parahippocampal cortex may undergo an abnormal dendro-toxicity that manifests as thinner gray matter. Early imaging studies have revealed hippocampal reductions in FESz (Hirayasu, Shenton, Salisbury, & McCarley, 2000), and medial temporal lobe regions undergo significant neuroanatomical changes as high-risk patients transition to psychosis (Wood et al., 2008). In fact, hippocampal damage has long been suspected as one etiology of

schizophrenia (Lipska, Jaskiw, & Weinberger, 1993; Lipska & Weinberger, 2002). Post-natal ventral hippocampal lesions in rats have been associated with EEG-derived oscillatory auditory abnormalities similar to those observed in schizophrenia (Vohs et al., 2010; Vohs et al., 2009). As the parahippocampal gyrus has bidirectional connections with hippocampus and other limbic structures and provides a major hub of bidirectional communication between polymodal cortical areas, including auditory association cortex, it likely serves a key role in cortical-subcortical communication in service of contextual memory (Aminoff, Kveraga, & Bar, 2013). The current data provide strong support for parahippocampal gyrus as a key early anatomical site of pathology proximal to the emergence of psychosis.

PHA3 is a subregion of the parahippocampal gyrus, primarily within the collateral sulcus (Baker, Burks, Briggs, Milton, et al., 2018). It has functional connections to inferior frontal, temporal, and parietal areas and is involved in spatial and contextual information processing (Baker, Burks, Briggs, Milton, et al., 2018). In this study, exploratory analyses suggest right PHA3 thickness may be associated with processing speed, working memory, and verbal learning. This would be consistent with known cognitive functions of the parahippocampal cortex (i.e., spatial memory and verbal fluency) (Frith, Friston, Liddle, & Frackowiak, 1991; Squire, Stark, & Clark, 2004). While the left medial temporal lobe is commonly associated with verbal memory and the right medial temporal lobe with spatial memory, right medial temporal lobe structures appear to have a role in verbal tasks, specifically verbal retrieval (Persson & Soderlund, 2015). In individuals with schizophrenia, right medial temporal lobe structures appear to be related to both verbal and working memory performance (Antoniades et al., 2018; Ehrlich et al., 2012; Hurlemann et al., 2008). Further, patients with lower verbal memory ability have less bilateral parahippocampal thickness (Guimond, Chakravarty, Bergeron-Gagnon, Patel, & Lepage, 2016). Our data support

that right PHA3 in particular may be related to some cognitive deficits in early schizophrenia, though this should be interpreted with caution, as the correlations were exploratory in nature and need replication.

In the context of schizophrenia, the parahippocampal gyrus is associated with positive symptoms, such as thought disorder, delusions, and hallucinations (Prasad et al., 2004; Shenton et al., 1993). In this study, we did not find significant associations between PHA3 thickness and delusions or thought disorder, but instead, we found a potential relationship with hallucinations. The parahippocampal gyrus has a role in hallucinations as it appears to deactivate before auditory verbal hallucinations and activate during hallucinations (Diederen et al., 2010; Escartí et al., 2010; van Lutterveld et al., 2014). While this study suggests that left PHA3 thickness may be positively related to hallucinations, the nature of this relationship is not entirely clear. We speculate that within the context of overall reduced PHA3 in FESz, the more intact PHA3 contributes dysfunctional activity to the language circuit (e.g., imprecise information content and dysfunctional information transfer), contributing to hallucinations. Future studies will be able to support or refute our initial speculation regarding this somewhat paradoxical and exploratory finding.

This study was not without limitations. The sample size is relatively small compared to larger multisite studies; thus, replication of these findings is needed in larger samples. This newer HCP parcellation is restricted to cortex, yet many subcortical volume deficits (e.g., hippocampus) have been implicated in schizophrenia, which we were unable to identify here. Future studies can use traditional volumetric approaches to examine subcortical area deficits in FESz. In addition, although this study suggests that this area of parahippocampal cortex is particularly impacted in early schizophrenia, it is unclear if this area is specific to schizophrenia or if it is common to other

disorders of psychosis. Finally, it is unclear if this difference is related to the transition to psychosis. This study was a cross-sectional design, and future studies investigating clinical high-risk patients can use this HCP-MMP to investigate the longitudinal trajectories of these deficits.

In summary, using the HCP multi-modal parcellation we identified robust gray matter deficits in specific subregions of the parahippocampal gyrus in early schizophrenia. These deficits may be related to hallucinations and cognitive deficits, though future work is needed to replicate these relationships and explore possible mechanisms. This study provides insight to the initial pathology near the onset of schizophrenia and suggests the parahippocampal area 3 may be a specific subregion particularly critical to the emergence of psychosis.

2.3 General Discussion

These results would likely not have been detected with previous analytic strategies, demonstrating the HCP pipelines and HCP parcellation are able to delineate functional subregions with high sensitivity and detect subtle gray matter deficits within these areas. The most commonly used parcellations include the parahippocampal subregion with other regions. The Desikan-Killiany atlas labels this PHA3 area as a small part of the fusiform area, as the fusiform includes several other HCP areas. In the Destrieux atlas, this PHA3 region lies within the lingual sulcus parcel (s_oc-temp_med_and_Lingual), again along with several other HCP areas. If one were to use these parcels instead of the HCP parcels, it is likely the significant effect would not be found, as the inclusion of these additional areas in the average across the ROI would diminish the effect of the subregion. It also has interpretation implications, as one would not consider it part of the parahippocampal region, but instead either the fusiform or lingual region. This experiment also

demonstrated that in very early psychosis, gray matter within sulcal-gyral boundary defined ROIs relates to symptoms and cognitive performance. For example, left PHA3 gray matter was significantly positively associated with hallucinatory behavior, and right PHA3 gray matter was significantly positively related to processing speed, working memory, and verbal learning.

2.3.1 Exploring Brain Structure and Function with the HCP Parcellation

In early psychosis, gray matter is also related to brain neurophysiological function measured with EEG (Salisbury, Kuroki, Kasai, Shenton, & McCarley, 2007; Salisbury, Shafer, Murphy, Haigh, & Coffman, 2020). Of particular interest is the mismatch negativity, which is an event-related potential measured as a heightened response to a rare stimulus in the presence of frequent stimuli. While the MMN is reduced in chronic schizophrenia patients (Umbricht & Krljes, 2005), it is not reliably reduced in early psychosis (Haigh, Coffman, & Salisbury, 2017; T. K. Murphy, Haigh, Coffman, & Salisbury, 2020). Nevertheless, some individuals have a reduced MMN in early psychosis and the amplitude of the MMN is related to gray matter volume in Heschl's gyrus in auditory cortex, a known neural generator of the MMN, such that those with a diminished MMN also have reduced Heschl's gyrus gray matter (Salisbury et al., 2020).

However, again the region of interest previously studied was limited to an area defined strictly by sulcal-gyral boundaries, Heschl's gyrus, which contains the functional area of A1, along with parts of the surrounding functional belt regions. It is possible that certain subregions contribute more to this relationship than others. It is also possible that parcellation into functional subregions do not contribute any new meaningful information on the relationship with scalp-recorded neurophysiology because the signal may be related to a larger region of cortex, such as the entirety of Heschl's gyrus. Thus, the question remains whether the HCP pipelines and HCP

parcellation, which can delineate the functional subregions of Heschl's gyrus, provide improvement in detecting patterns of how gray matter within these regions relate to neurophysiology.

In the next experiment, we aimed to determine whether the quasi-functional parcels identified by the HCP parcellation provided the same associations between scalp-recorded MMN and auditory sensory cortex parcel GM volumes as measurement of HG, as well as explore associations with inferior frontal gyrus volumes, a known auditory executive center involved in the generation of MMN.

2.4 Pitch and Duration Mismatch Negativity Are Associated with Distinct Auditory Cortex and Inferior Frontal Cortex Volumes in the First-Episode Schizophrenia-spectrum

The following is adapted from published manuscript for this dissertation.

Curtis MT, Coffman BA, Salisbury DF. Pitch and Duration Mismatch Negativity are Associated with Distinct Auditory Cortex and Inferior Frontal Cortex Volumes in the First-Episode Schizophrenia Spectrum. Schizophr Bull Open. 2021 Feb 23;2(1): PMID: 33738454

2.4.1 Introduction

The mismatch negativity (MMN) is an event-related potential (ERP) typically measured with electroencephalography (EEG) that has been extensively studied in schizophrenia (Erickson, Ruffle, & Gold, 2016; Light & Naatanen, 2013). MMN is a response elicited by changes in stimuli and is commonly studied in the auditory domain where frequent standard tones are presented along

with infrequent tones that differ in some feature (pitch, duration, loudness, etc.). The MMN is calculated as the difference between the ERP waveform to the standard tones and the ERP waveform to the deviant tones. MMN to both pitch and duration deviant tones is robustly and reliably reduced in chronic schizophrenia (Umbricht & Krljes, 2005). MMN is much less reduced at first psychosis (Erickson et al., 2016; Salisbury et al., 2017; Salisbury, Shenton, Griggs, Bonner-Jackson, & McCarley, 2002). A Metanalysis suggests that MMN to duration deviants may be slightly reduced at first episode, while MMN to pitch deviants is not consistently reduced at first-episode (Haigh et al., 2017). When the MMN is followed longitudinally in first-hospitalized schizophrenia patients, their MMN amplitude decreases within the first two years of the disorder (Salisbury et al., 2007). Therefore, while MMN may not be reduced at first episode, it progressively declines during the early disease course.

Schizophrenia is associated with gray matter deficits that are present early in the disorder and progressively decline in the first few years of the disease course (Haijma et al., 2013; Shenton et al., 2001). Areas that are particularly impacted early are the frontal and temporal lobes (Cropley et al., 2017; Kasai, Shenton, Salisbury, Hirayasu, Lee, et al., 2003; Kasai, Shenton, Salisbury, Hirayasu, Onitsuka, et al., 2003; Keshavan et al., 1998). Gray matter volumes are related to MMN in chronic schizophrenia (Rasser et al., 2011), and during the early course of schizophrenia, the longitudinal decline of pitch MMN is associated with a decline in left Heschl's gyrus gray matter (Salisbury et al., 2007). A recent study found that both pMMN and dMMN are associated with left hemisphere Heschl's gyrus gray matter in individuals with schizophrenia within two months of their first clinical contact for psychosis (Salisbury et al., 2020). This suggests that very early in the disorder, the MMNs to pitch and duration deviants are associated with pathological deficits in left auditory cortex. However, Heschl's gyrus is a strictly anatomical region that contains primary

auditory cortex and portions of the medial and lateral belt regions (Sweet et al., 2005), while excluding other important auditory areas, such as parabelt. Thus, it is unable to differentiate between the specific auditory areas' gray matter contributions to the MMN decline in early schizophrenia.

Pitch MMN and dMMN have slightly different neural generators (Alho, 1995; Paavilainen, Alho, Reinikainen, Sams, & Naatanen, 1991). Animal depth recordings, human intracranial recordings, and localization of human-scalp-recorded EEG and MEG MMN demonstrate that the primary generator for MMN is within primary and secondary auditory cortex (Alho, 1995; Csepe, 1995; Hari et al., 1984; Hari, Rif, Tiihonen, & Sams, 1992; Javitt, Steinschneider, Schroeder, Vaughan, & Arezzo, 1994; Kasai et al., 1999; Kropotov et al., 1995; Naatanen & Alho, 1995; Rosburg et al., 2005). However, MMN generated by pitch/frequency deviants have a more anterior auditory source compared to the MMN generated by duration deviants (Frodl-Bauch, Kathmann, Moller, & Hegerl, 1997; Giard et al., 1995; Levanen, Ahonen, Hari, McEvoy, & Sams, 1996; Rosburg, 2003). Similarly, functional MRI reveals that BOLD activity increases to pitch MMN in a more anterior location in auditory cortex, while activity from dMMN is located more posterior and in secondary auditory cortex (Molholm, Martinez, Ritter, Javitt, & Foxe, 2005). Further, the generation of the MMN also involves a source in bilateral inferior frontal cortex, with a stronger contribution from the right hemisphere (Giard, Perrin, Pernier, & Bouchet, 1990; Park et al., 2002; Rinne, Alho, Ilmoniemi, Virtanen, & Naatanen, 2000). This source is difficult to detect with MEG, indicating its source may be oriented radial to the surface of the scalp, such as on a sulcal wall (Rinne et al., 2000). Dynamic causal modeling suggests this inferior frontal source is hierarchically organized with auditory cortex in generating the MMN (Garrido et al., 2008; Garrido, Kilner, Kiebel, & Friston, 2009; Lieder, Stephan, Daunizeau, Garrido, & Friston, 2013). Therefore, pitch

and duration MMN are likely generated in slightly different auditory areas with additional contributions from an inferior frontal source.

The current study is a critical improvement on the previous MMN-HG study (Salisbury et al., 2020) with a new, advanced analysis technique that differentiates gray matter volumes within A1 and surrounding belt regions. We overcame the previous sulcal-gyral limitation by applying the quasi-functional Human Connectome Project Multimodal Parcellation (HCP-MMP) atlas. This parcellation defined cortical regions by both functional and structural information, resulting in a delineation of primary auditory cortex (A1) and surrounding auditory belt regions (Glasser et al., 2016). Due to our previous studies demonstrating that both pMMN and dMMN were associated with gray matter volume in left Heschl's gyrus in FESz, we used the HCP-MMP atlas to more precisely parcellate Heschl's gyrus and surrounding auditory cortex into functionally meaningful regions. We assessed correlations between gray matter volume and pMMN/dMMN within these regions to investigate if the pathological association between these biological measures would follow the same anterior-posterior pattern seen in putative auditory generators of pMMN/dMMN. In addition, this study extends the regions of interest to include the inferior frontal cortex to investigate if pMMN and dMMN are also associated with gray matter in the frontal source location of the MMN in FESz.

2.4.2 Methods

2.4.2.1 Participants

This study included the same participants as in the sample reported in Salisbury and colleagues (2020) and as a subset of participants in Murphy and colleagues (2020), 27 FESz individuals (paranoid: n=9; undifferentiated: n=3; residual: n=2; schizoaffective: n=5;

schizophreniform: n=2; psychotic disorder NOS: n=6) and 27 healthy controls (T. K. Murphy et al., 2020; Salisbury et al., 2020). All FESz participated within their first episode of psychosis and had less than 2 months of lifetime antipsychotic medication exposure. Ten FESz were unmedicated. All participants had normal hearing as assessed by audiometry. None of the participants had a history of concussion or head injury with sequelae, history of alcohol or drug addiction, detox in the last five years, or neurological comorbidity. Groups were matched for age, gender, parental social economic status, and premorbid IQ, measured by the Wechsler Abbreviated Scale of Intelligence (WASI) (**Table 6**). The work described was carried out in accordance with The Code of Ethics of the World Medical Association (Declaration of Helsinki) for experiments involving humans. All participants provided informed consent and were paid for participation. All procedures were approved by the University of Pittsburgh IRB.

Socioeconomic status (SES) for all participants and their parents was measured with the 4-factor Hollingshead Scale. FESz participants' diagnoses were based on the Structured Clinical Interview for DSM-IV (SCID-P) and were confirmed six months after initial clinical assessment. Symptoms were rated using the Positive and Negative Syndrome Scale (PANSS) (Kay et al., 1987) (**Table 6**). Neuropsychological functioning was assessed with the MATRICS Consensus Cognitive Battery (Nuechterlein et al., 2008). All tests were conducted by an expert diagnostician.

Table 6. Experiment 2: Demographic, Neuropsychological, and Clinical Information (previously reported in Salisbury et al., 2020).

FESz and HC groups were matched for age, gender, PSES, and WASI IQ.

	Mean±SD				
	HC	FESz	t/X^2	*p*	Cohen's *d*
Sociodemographic data					
Age (years)	21.1 ± 3.0	22.6 ± 5.1	1.36	0.18	0.36
Gender (M/F)	18/9	19/8	0.09	0.77	
SES	33.7 ± 13.6	31.9 ± 13.2	-0.51	0.61	0.13
Parental SES	47.5 ± 13.5	43.1 ± 12.6	-1.21	0.23	0.34
Neuropsychological tests					
WASI	108.0 ± 10.7	110.4 ± 14.5	0.71	0.48	0.19
MCCB-total	47.2 ± 8.2	42.5 ± 13.3	-1.54	0.13	0.43
Symptoms					
PANSS Total		75.2 ± 14.8			
PANSS Positive		20.0 ± 5.6			
PANSS Negative		16.9 ± 4.9			
PANSS General		38.3 ± 7.5			
PANSS TD		11.2 ± 3.1			
SAPS Global		5.9 ± 2.9			
SANS Global		9.7 ± 3.1			
Illness Duration		73.3 ± 120.4			
DUP (days)		192.2 ± 201.1			
Medication data					
Medication		228.8 ± 147.9			

Note: SES = socioeconomic status. WASI = Wechsler Abbreviated Scale of Intelligence. MATRICS = composite scaled t score. PANSS = Positive and Negative Syndrome Scale. TD = PANSS Thought Disorder factor. SAPS = Scale for the Assessment of Positive Symptoms. SANS = Scale for the Assessment of Negative Symptoms. DUP = duration of untreated psychosis. Medication = chlorpromazine equivalents.

2.4.2.2 Data acquisition & Processing

The acquisition and processing methods have previously been described in detail (Salisbury et al., 2020). The procedures are briefly described here.

EEG was recorded from a custom 72 channel Active2 high impedance system (BioSemi). The EEG amplifier bandpass was DC to 104 Hz (24dB/octave rolloff) digitized at 512 Hz, referenced to a common mode sense site near PO1. Auditory stimuli were presented while EEG

was recorded, and participants watched a silent video. Stimuli comprised of 1,280 standard tones (80%, 1kHz, 50ms duration), 160 pitch deviants (10%, 1.2kHz, 50ms duration), and 160 duration deviants (10%, 1 kHz, 100ms). Due to time constraints, 6 FESz and 7 HC participants were only presented a total of 800 tones, including 640 standards (80%), 80 pitch deviants (10%) and 80 duration deviants (10%). Using BESA (BESA GmbH), EEG data were filtered between 0.5 (to remove DC drifts) and 20Hz (to remove muscle and other high frequency artifact), bad channels interpolated, and eye/cardiac artifact removed with independent component analysis. In BrainVision Analyzer2 (brain Products GmbH), data were re-referenced to the nosetip. Epochs of 350ms (including 50ms pre-stimulus baseline) were extracted for deviant tones and standard tones preceding a deviant. Epochs were baseline corrected and a rejection criterion of ±50 μV was applied. Epochs were then averaged for the standard tones, pitch deviants, and duration deviants. The standard average was subtracted from the pitch average to generate the pMMN. To generate the dMMN, the standard average was subtracted from the duration average. MMN was measured by automatic peak detection at Fz for each individual (pMMN range: 90-145 msec, dMMN range: 140-200 msec, verified visually and adjusted if necessary) and averaged over a 100ms time window (peak ±50 ms). The Fz site was used to quantify the MMNs, where they are typically the largest and to replicate the procedure used in Salisbury and colleagues (2007) (Salisbury et al., 2007).

MRI data were acquired using a Siemens Tim Trio on a 32-channel phase array head coil. Sagittal T1-weighted anatomical MR images were obtained with a multi-echo 3D MPRAGE sequence. For quality assurance, the MRI scans were visually inspected for scanner artifacts, motion, and gross neuroanatomical abnormalities. FreeSurfer (stable v6.0) was used for MRI processing (Dale et al., 1999; Fischl & Dale, 2000; Fischl et al., 1999). Briefly, processing involved

registration to MNI space, intensity normalization, skull stripping, segmentation of white matter, and the generation of white and pial surfaces. Cortical surfaces were examined to ensure accurate delineation of white matter and pial surfaces. Using the HCP workbench, the HCP-MMP was resampled to fsaverage space. In Freesurfer, the parcellation was applied to individual data (see HCP Users FAQ (https://wiki.humanconnectome.org/display/PublicData/HCP+Users+FAQ#HCPUsersFAQ-9.HowdoImapdatabetweenFreeSurferandHCP?)). Freesurfer was used to calculate gray matter volume in 32 ROIs using the HCP-MMP atlas (Glasser et al., 2016). The regions of interest included the following 8 ROIs in bilateral AC: A1, medial belt (MBelt), lateral belt (LBelt), parabelt (PBelt), A4, A5, Area 52, and area TA2. In the inferior frontal cortex, the following 8 bilateral areas were used as ROIs: Brodmann area 44, Brodmann area 45, lateral subdivision of area 47 (47L), anterior inferior frontal junction (IFJa), posterior inferior frontal junction (IFJp), anterior inferior frontal sulcus (IFSa), posterior inferior frontal sulcus (IFSp), and area posterior 47r (**Figure 3**).

A. Left Hemisphere

Regions of Interest	
Auditory Cortex	**Inferior Frontal Cortex**
1. Left A1	9. Left Area p47r
2. Left Medial Belt	10. Left Area 47L
3. Left Lateral Belt	11. Left IFSa
4. Left Parabelt	12. Left Area 45
5. Left A4	13. Left IFSp
6. Left A5	14. Left Area 44
7. Left Area 52	15. Left IFJa
8. Left TA2	16. Left IFJp

B. Right Hemisphere

Regions of Interest	
Auditory Cortex	**Inferior Frontal Cortex**
17. Right A1	25. Right Area p47r
18. Right Medial Belt	26. Right Left Area 47L
19. Right Lateral Belt	27. Right IFSa
20. Right Parabelt	28. Right Area 45
21. Right A4	29. Right IFSp
22. Right A5	30. Right Area 44
23. Right Area 52	31. Right IFJa
24. Right TA2	32. Right IFJp

Figure 3. MMN Regions of Interest.

The regions of interest in auditory cortex and inferior frontal cortex defined from the HCP-MMP atlas with Heschl's gyrus in red. Volumes were estimated from each region.

2.4.2.3 Analysis

Group demographics were compared using independent samples t-test and chi-square tests where appropriate. Gray matter volume group comparisons were made using analysis of covariance (ANCOVA) with intracranial content (ICC), gender, and age as covariates. The statistical conclusions reported remained the same when we used ANCOVA on the relative volumes ((absolute volume/ICC) x 100) with gender and age as covariates.

Absolute volumes were used for correlations, and correlations were assessed with Spearman's rho. Benjamini-Hochberg False Discovery Rate (FDR) correction was applied to correct for multiple comparisons for the group comparisons and correlations (q=0.05). Note that MMN is a negative brainwave, and thus a larger MMN has a more negative amplitude. Therefore, a negative correlation indicates that smaller GM volume is associated with a smaller absolute MMN amplitude.

2.4.3 Results

2.4.3.1 Mismatch Negativity

As reported previously in Salisbury and colleagues (2020) (Salisbury et al., 2020), peak pMMN latency did not differ between FESz (113.1±13.8 ms) and HC (117.8±14.5 ms, $t_{(52)}$=1.22, p=.23). Similarly, peak dMMN latency did not differ between groups (FESz: 174.3±14.7 ms; HC: 173.9±20.1 ms, $t_{(52)}$=0.08, p=.94). Pitch MMN amplitude was significantly reduced in this sample of FESz (2.0 µV±1.4 µV) compared to HC (3.1±1.7 µV, $t_{(52)}$=2.50, p=.016). Duration MMN amplitude did not differ between groups (FESz: 1.8 ±1.5 µV; HC: 2.1±1.6 µV, $t_{(52)}$=0.77, p=0.44) (**Figure 4**).

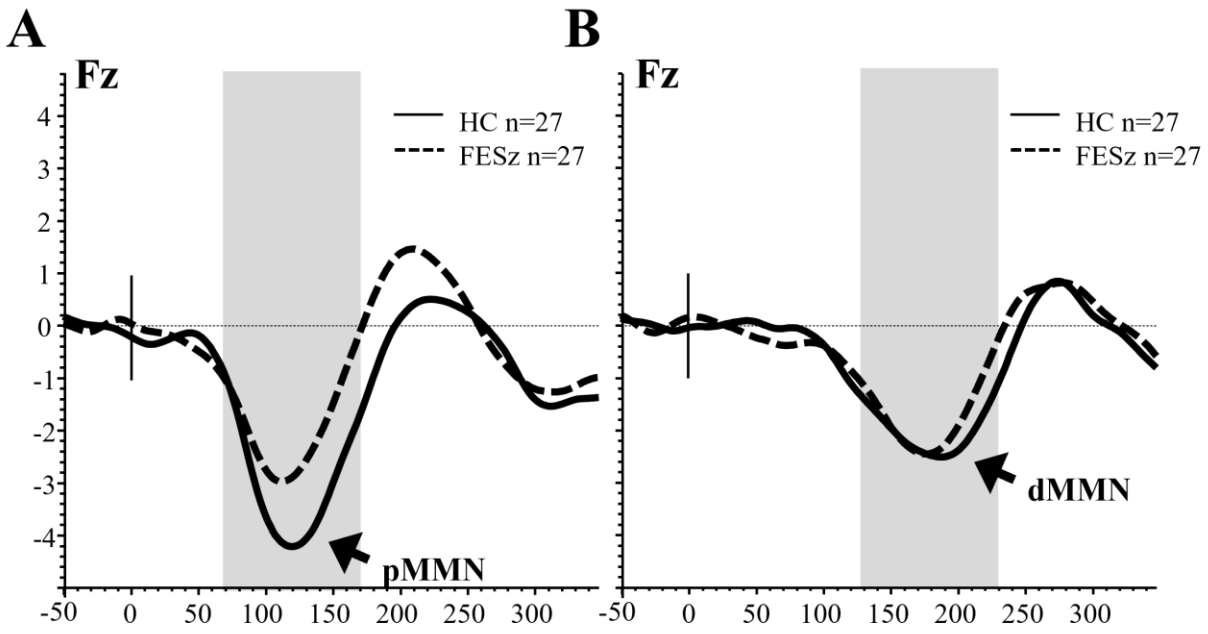

Figure 4. Group Mismatch Negativity Grand Averages Information (previously reported in Salisbury et al., 2020).

A. Mismatch negativity subtraction waveforms for pitch deviants in HC and FESz. B. Mismatch negativity subtraction waveforms for duration deviants in HC and FESz. The averaged time window is highlighted.

2.4.3.2 Gray Matter Volume Group Comparisons

Groups did not have significantly different intracranial content (FESz: 1619±198 cm^3; HC: 1649 ±178 cm^3; $t_{(52)}$=0.58, p=0.56). There were no regions of interest in which gray matter volume significantly differed between groups (p's>0.05).

2.4.3.3 Pitch MMN and Gray Matter Volume Correlations

All correlations for FESz are shown in **Table 7**. In FESz, after FDR correction of q=.05, pMMN remained significantly associated with left MBelt and left 47L (**Figures 5 & 6**). There were no significant correlations in HC (q=.05).

2.4.3.4 Duration MMN and Gray Matter Volume Correlations

All correlations for FESz are shown in **Table 7**. In FESz, after FDR correction (q=.05), dMMN significantly correlated with left MBelt, left LBelt, left PBelt, left TA2, right A5, left 47L, right area 44, and right 47L in FESz (**Figures 5 & 6**). There were no significant correlations in HC (q=.05).

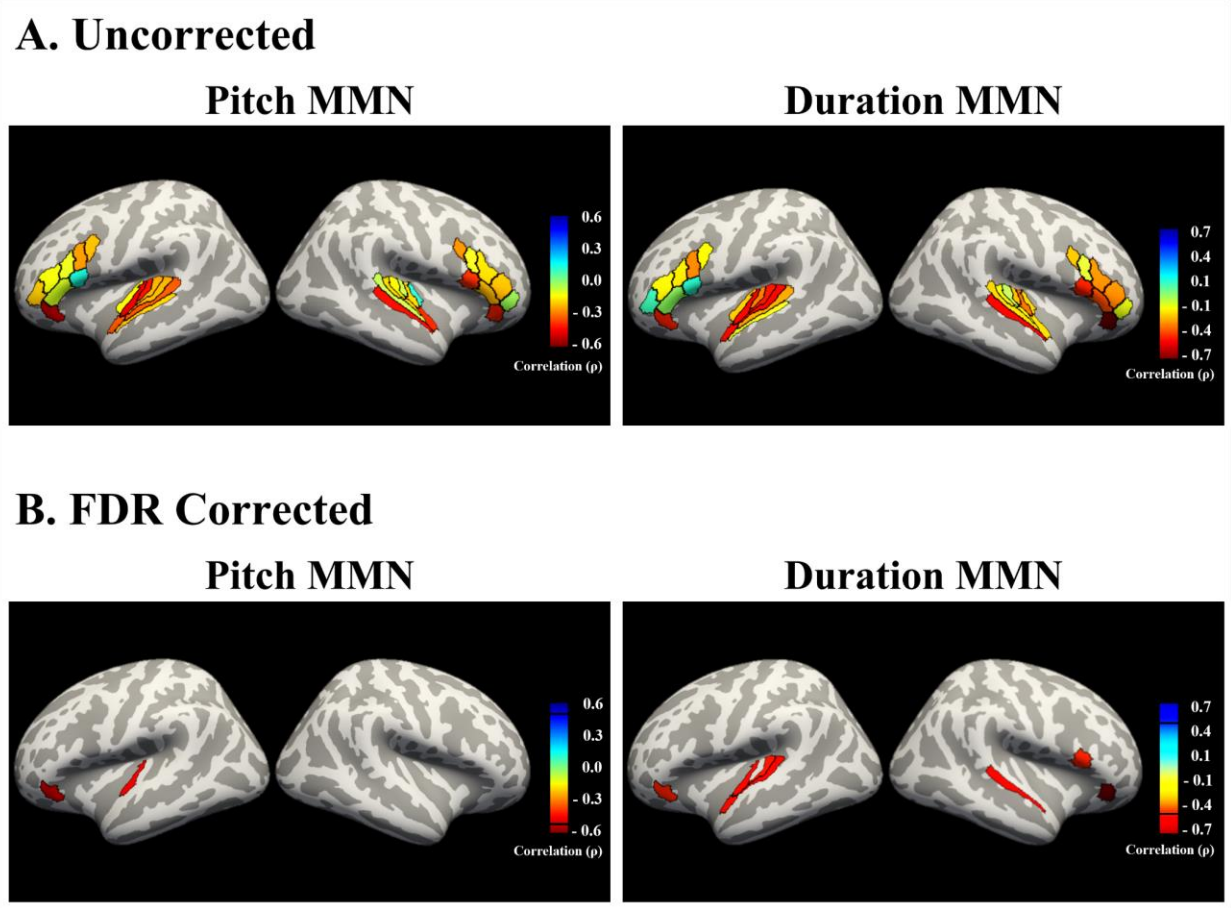

Figure 5. Gray Matter Volume Associations with Pitch and Duration MMN in FESz.

A. The correlation strengths of auditory and inferior cortex gray matter volumes with pitch and duration MMN in First-Episode Schizophrenia. B. Regions that survived FDR correction for multiple comparisons (q<0.05). In FESz, pitch MMN remained significantly associated with left MBelt and left 47L. In FESz, duration MMN significantly correlated with left MBelt, left LBelt, left PBelt, left TA2, left 47L, right A5, right area 44, and right 47L.

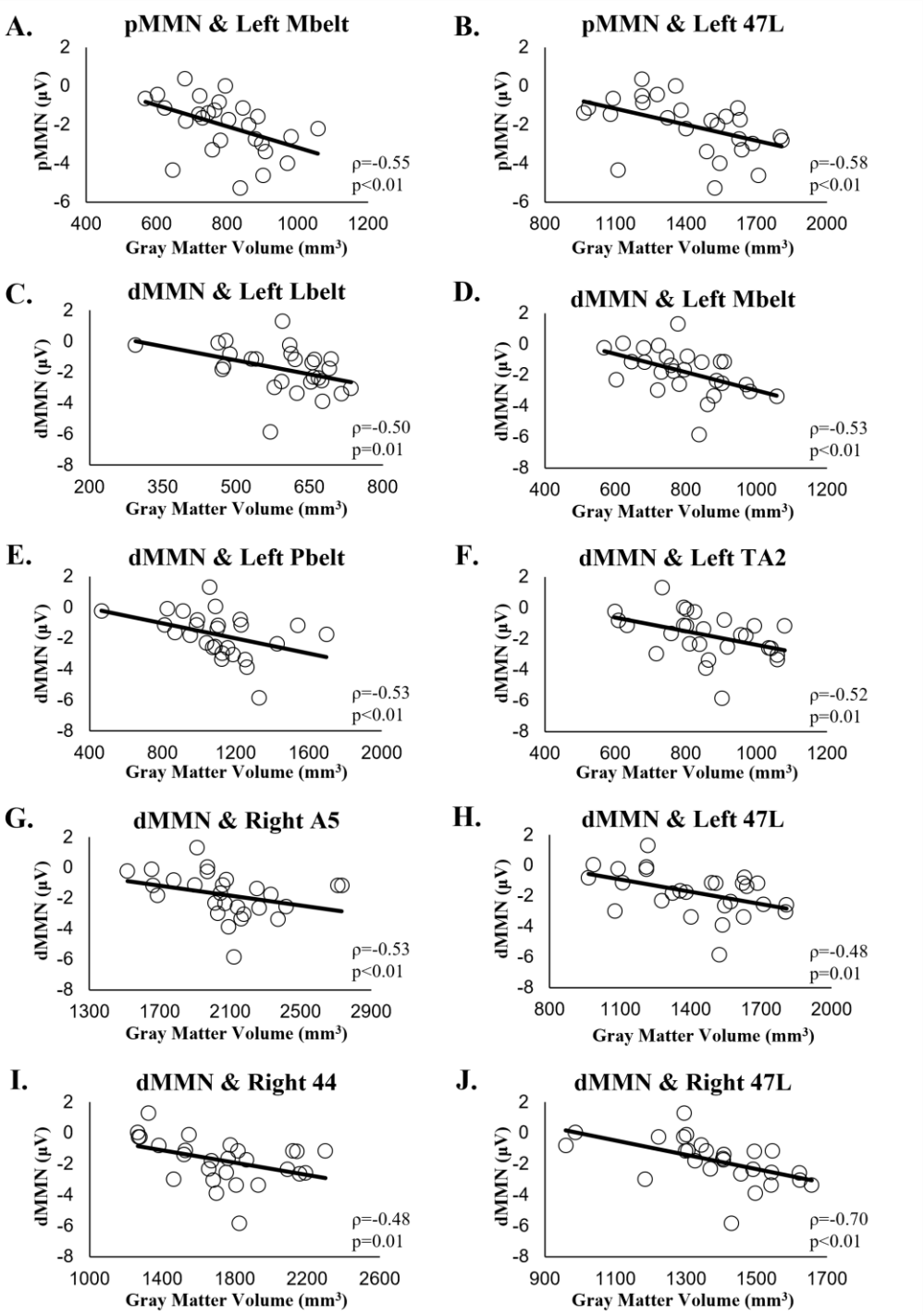

Figure 6. Scatterplots of Significant MMN and Gray Matter Correlations.

In FESz, pitch MMN was significantly (q<0.05) associated with gray matter in left MBelt (A) and left 47L (B). Duration MMN was significantly (q<0.05) associated with gray matter in left MBelt (C), left LBelt (D), left PBelt (E), left TA2 (F), right A5 (G), left 47L (H), right area 44 (I), and right 47L (J).

Table 7. MMN and GM Correlations in FESz.

Correlation strengths (Spearman's rho) for the relationships between pitch and duration MMN and regions of interest in auditory and inferior frontal cortex.

	Pitch MMN		Duration MMN	
Brain Region	ρ	p	ρ	p
Auditory Cortex				
L_A1	**-0.48**	**0.01**	**-0.38**	**0.05**
L_LBelt	-0.30	0.13	**-0.50**	**0.01**[a]
L_MBelt	**-0.55**	**<0.01**[a]	**-0.53**	**<0.01**[a]
L_PBelt	-0.30	0.13	**-0.53**	**<0.01**[a]
L_A4	**-0.40**	**0.04**	-0.34	0.08
L_A5	-0.27	0.17	-0.14	0.49
L_52	-0.16	0.42	-0.29	0.14
L_TA2	**-0.39**	**0.05**	**-0.52**	**0.01**[a]
R_A1	-0.07	0.72	-0.32	0.10
R_LBelt	-0.17	0.40	0.05	0.81
R_MBelt	-0.26	0.19	**-0.40**	**0.04**
R_PBelt	-0.26	0.19	-0.17	0.39
R_A4	-0.06	0.78	-0.27	0.17
R_A5	**-0.49**	**0.01**	**-0.53**	**<0.01**[a]
R_52	0.10	0.61	-0.28	0.15
R_TA2	**-0.45**	**0.02**	-0.26	0.19
Inferior Frontal				
L_44	0.12	0.54	0.11	0.57
L_45	-0.11	0.58	-0.03	0.89
L_47I	**-0.58**	**<0.01**[a]	**-0.48**	**0.01**[a]
L_IFJa	-0.33	0.09	-0.36	0.06
L_IFJp	-0.29	0.14	-0.19	0.33
L_IFSa	-0.15	0.45	-0.19	0.34
L_IFSp	-0.12	0.54	-0.23	0.26
L_p47r	-0.25	0.21	0.08	0.68
R_44	**-0.43**	**0.03**	**-0.48**	**0.01**[a]
R_45	-0.26	0.19	**-0.41**	**0.03**
R_47I	**-0.45**	**0.02**	**-0.70**	**<0.01**[a]
R_IFJa	-0.12	0.55	-0.10	0.61
R_IFJp	-0.35	0.07	-0.31	0.12
R_IFSa	-0.28	0.16	-0.36	0.06
R_IFSp	-0.25	0.21	-0.37	0.06
R_p47r	-0.04	0.84	-0.14	0.50

Bold denotes uncorrected $p<0.05$.

[a] denotes survives FDR correction ($q<0.05$).

2.4.4 Discussion

With the novel use of the specific and functionally relevant HCP-MMP atlas, this study provides a notably distinct and more precise understanding of the underlying pathology associated with impaired MMN in FESz. The previous analysis on this dataset was restricted to a strictly anatomically defined region, Heschl's gyrus, which contains portions of primary auditory cortex and auditory belt areas (Salisbury et al., 2020). The method utilized in this study provided an exquisite functional parcellation of cortex, allowing for the study of relationships with temporal and frontal MMN generators with high specificity to functional areas. The novel use of the HCP-MMP atlas combined with the extension to investigate the inferior frontal MMN generator, provided a new understanding of the relationships between MMN and gray matter, revealing both overlapping and distinct associations for pMMN and dMMN in FESz. After correction for multiple comparisons, both pMMN and dMMN were associated with gray matter volume of left MBelt and left 47L. Duration MMN was uniquely related to volume in left LBelt, left PBelt, left TA2, right A5, right area 44, and right 47L. The significant correlations were all in the negative direction and only within the FESz group, suggesting that less gray matter was associated with a smaller MMN in FESz. In light of the evidence of progressive gray matter decline in the early course of schizophrenia that begins as early as the prodrome (Cannon et al., 2015; Chung et al., 2019; Cropley et al., 2017; Haijma et al., 2013; Shenton et al., 2001), it suggests that within a subset of FESz there is enough underlying gray matter loss in these regions to impair functioning, represented by a reduced pMMN or dMMN. These findings provide important insights into the relationship of MMN and gray matter within MMN generators in the very early course of schizophrenia.

The shared and unique auditory cortex subregions associated with pMMN and dMMN in FESz align with previous reports regarding the underlying neural generators of the MMN. EEG and MEG source localization and dynamic causal modelling suggest MMN generators in the supratemporal plane (Heschl's gyrus and STG) and inferior frontal cortex (Garrido et al., 2008; Naatanen & Alho, 1995; Rinne et al., 2000). Both pMMN and dMMN were related to gray matter within each of these generators: left Heschl's gyrus (MBelt) and left inferior frontal cortex (47L). Further, pitch MMN has a more anterior auditory cortex generator, while the dMMN has a generator more posterior in secondary auditory cortex (Frodl-Bauch et al., 1997; Giard et al., 1995; Levanen et al., 1996; Molholm et al., 2005; Rosburg, 2003). In FESz, pitch MMN was associated with gray matter volume in MBelt, while dMMN was associated with MBelt with the addition of other secondary auditory cortex parcels, some slightly more posterior (LBelt and PBelt). The additional posterior parcels related to dMMN may provide evidence that (similar to the neural generator) dMMN is associated with underlying pathology in more posterior secondary auditory areas.

The strong correlations of MMN and gray matter early in schizophrenia is consistent with the progressive gray matter loss in the disorder (Haijma et al., 2013; Shenton et al., 2001). Gray matter loss in schizophrenia is due to a reduction in cortical neuropil (Selemon & Goldman-Rakic, 1999), and in auditory cortex specifically, there is a reduction in layer III pyramidal soma size and a decreased number and density of dendritic spines (Lewis & Sweet, 2009; Parker & Sweet, 2017; Sweet et al., 2004; Sweet, Henteleff, Zhang, Sampson, & Lewis, 2009). It is hypothesized that the consequence of these reductions is reduced synaptic connectivity, and thus reduced MMN (Lewis & Sweet, 2009; Salisbury et al., 2007; Todd, Harms, Schall, & Michie, 2013). Because there were no volume group differences and these associations were only present in the FESz individuals, it

suggests that within the HC there is enough neuropil to support healthy functioning and the production of a healthy MMN to deviant stimuli. In FESz, some individuals have experienced more gray matter loss in certain auditory and inferior frontal cortex regions beyond healthy limits, which is associated with either a deficient pMMN and/or dMMN response.

The regions that were strongly related to MMN are functionally important for auditory and attention processing. In the auditory cortex, the medial belt, located on the medial surface of Heschl's gyrus, is a relatively early auditory processing stage with local connectivity to surrounding auditory areas (Baker, Burks, Briggs, Conner, Glenn, Robbins, et al., 2018; Kusmierek & Rauschecker, 2009). The lateral belt, located on the lateral surface of Heschl's gyrus, is also a relatively early auditory processing stage with connections to local auditory areas and inferior frontal gyrus (Baker, Burks, Briggs, Conner, Glenn, Robbins, et al., 2018). The parabelt resides between Heschl's gyrus and the inferior portion of the supramarginal gyrus. Compared to the medial and lateral belts, the parabelt is considered higher in the regional auditory hierarchy. It has connectivity with local auditory areas and with motor, premotor, and inferior frontal cortices. The parabelt integrates across different frequency bands and is involved in more complex behaviors such as figure-ground segregation (Schneider et al., 2018). Area TA2, residing in the anterior portion of the superior temporal gyrus, is important for auditory stimuli perception. Left TA2 is more involved in temporal patterns of speech, while right TA2 appears to be more involved with tone of speech (Baker, Burks, Briggs, Conner, Glenn, Robbins, et al., 2018; Burton, Firszt, Holden, Agato, & Uchanski, 2012). This supports our finding that left TA2 gray matter was significantly related to duration MMN in FESz. Right A5, located on the superior lateral surface of the posterior superior temporal gyrus, has connectivity with inferior frontal gyrus and other local temporal lobe regions. Right A5 may be important for tone-matching performance in

schizophrenia, as schizophrenia patients with tone matching deficits have decreased connectivity between the medial geniculate nucleus and A5 (Donde et al., 2019). In the inferior frontal cortex, area 47L is functionally connected to several cortical regions including dorsolateral frontal, medial frontal, premotor, parietal, and temporal cortex. In the left hemisphere, commonly referred to as part of Broca's area, it is important for language production and semantic processing (Ardila, Bernal, & Rosselli, 2016; Baker, Burks, Briggs, Conner, Glenn, Morgan, et al., 2018). In the right hemisphere, it is important for response inhibition and attention (Baker, Burks, Briggs, Conner, Glenn, Morgan, et al., 2018; Hartwigsen, Neef, Camilleri, Margulies, & Eickhoff, 2019; Lai, van Dam, Conant, Binder, & Desai, 2015; Neef et al., 2016). Finally, area 44, located in posterior inferior frontal gyrus, also has connectivity with a number of frontal, parietal, and temporal cortical regions and is involved in response inhibition and attention processing (Baker, Burks, Briggs, Conner, Glenn, Morgan, et al., 2018; Hartwigsen et al., 2019; Lai et al., 2015; Neef et al., 2016). While we have identified gray matter within these regions to be related to MMN in FESz, it is unclear if they should be considered individually or as part of larger networks. For example, the auditory regions are part of an auditory somatosensory network, and resting fMRI activity within this entire network is related to responses to frequency and duration deviant tones (M. Lee et al., 2017). In addition, the inferior frontal regions are commonly included in the attention network, and resting fMRI activity within this network is related to responses to duration deviant tones (M. Lee et al., 2017). The areas 47L and 44 may be part of this attention network, which may be particularly relevant to the automatic attention switching process of MMN (Giard et al., 1990; Rinne et al., 2000). Future work can be done to further dissociate between the regional and network level contributions to MMN deficits in FESz.

There are some caveats to consider. This study may have been underpowered to detect some significant relationships, as it included a modest sample size and many regions of interest. Due to the many comparisons, a conservative FDR correction was used, and as a result, several parcels with moderate effect sizes did not survive FDR correction. In particular, the correlation between dMMN and right MBelt did not survive FDR correction. In the previous analysis of this data, dMMN was associated at a trend level with right Heschl's gyrus (Salisbury et al., 2020). The current analysis with the HCP-MMP atlas suggests that the association between dMMN and right HG is likely reflected primarily in right MBelt. Future studies are needed to investigate these other relationships and investigate directly whether dMMN is associated with right MBelt volume. In addition, a subset of individuals had 800 tones for their MMNs, and although 800 trials did not previously change MMN statistics (T. K. Murphy et al., 2020), it is possible the individuals with fewer trials had poorer signal to noise. While this study focused on the known cortical generators of the MMN, deviance detection deficits in schizophrenia may be present in subcortical structures (Gaebler et al., 2020). While beyond the scope of this study, future analyses examining relationships between deviance detection and volumes may extend the analysis to subcortical structures. Further, the analysis was correlational, and therefore, we cannot conclude that gray matter loss directly causes MMN deficits. Finally, the current study was limited to MMN measured with EEG, making source localization difficult. Future analyses with both EEG and MEG combined with high resolution MRI will resolve MMN activity to the cortical surface and investigate how it relates to gray matter within these structures.

This study was also limited to data at one time-point in the very early course of psychosis. It will be important for future analyses to investigate these relationships longitudinally during the first year of psychosis to better understand the nature of these relationships between MMN and

gray matter. It has been proposed that pMMN and dMMN may be indicators of different processes in schizophrenia. Pitch MMN appears to be more related to the degeneration experienced over the course of schizophrenia (Haigh et al., 2017; Salisbury et al., 2007; Umbricht & Krljes, 2005), while dMMN may be more closely associated with the conversion to schizophrenia (Haigh et al., 2017; Michie, 2001; Michie, Innes-Brown, Todd, & Jablensky, 2002; Naatanen & Kahkonen, 2009; Todd et al., 2013). Our previous study suggested that pMMN and dMMN may track Heschl's gyrus neuropil, but this improved, precise analysis suggests that pMMN and dMMN may indicate neuropil loss in slightly different areas, and thus may be related to different underlying processes associated with schizophrenia. Alternatively, there could be a common underlying dendrotoxic process associated with schizophrenia, but the differences may be attributed to a difference in specialization of the affected cortical areas. For example, duration deviant detection may be more sensitive to neuropil loss in areas important for precise timing mechanisms such as right prefrontal cortex (Gooch, Wiener, Hamilton, & Coslett, 2011; Harrington, Haaland, & Knight, 1998; Merchant, Harrington, & Meck, 2013; Rao et al., 1997). Nonetheless, the results suggest that pitch and duration MMN may be tools to identify distinct subgroups of individuals with neuropil loss in slightly different areas, potentially improving specificity for treatments, such as non-invasive brain stimulation. In addition, identifying that deficits are in both sensory and higher-order cognitive areas can inform individualized cognitive enhancement therapy, which can be neuroprotective in early schizophrenia (Eack et al., 2010). Future longitudinal and clinical studies in the early course of schizophrenia can investigate this speculation further.

To summarize, pMMN and dMMN are impaired in some individuals that are early in the disease course of schizophrenia. Pitch and duration MMN have slightly different neural generators in auditory cortex with the addition of an inferior frontal generator. With the novel, precise

parcellation of these regions into functionally meaningful parcels, it appears that pathological associations between MMN and gray matter volume align with these generators. Both pMMN and dMMN were associated with gray matter in the more anterior medial belt, while only dMMN was also associated with gray matter in more secondary auditory areas and right inferior frontal cortex. As the early course of schizophrenia is associated with loss of neuropil, MMN may serve as biomarker of underlying pathological deficits, with pMMN and dMMN reflecting gray matter in both similar and slightly different cortical areas.

2.5 Overall Discussion

These studies provide the foundation for future work in understanding brain structure, brain function, and how these relate to each other in early psychosis. The previous two experiments validated the use of the HCP pipelines and HCP parcellation in the service of determining structural deficits and structure-function relationships in early psychosis. The novel use of the HCP parcellation allowed for an automatic definition of cortical regions across the whole brain with precision not previously possible. This automaticity and specificity for the delineation of quasi-functional regions offers a crucial solution to the previous analysis limitations. It defines cortex into 360 relevant regions of interest, cutting down on thousands of comparisons with a voxel-wise approach. Importantly, these regions are both structurally and functionally defined, offering vast improvement from manual tracing or previous parcellation atlases. In these two experiments, we validated the utility of the HCP-MMP in detection of gray matter deficits and structure-function relationships. In the first experiment, a deficit was found in FESz in a functional subregion of the parahippocampal area. In the context of overall thinner gray matter in this region, gray matter

thickness was related to hallucination severity and cognitive performance in FESz. In the second experiment, auditory cortex and inferior frontal cortex was automatically and precisely parcellated into the functional subregions and relationships between gray matter in those regions and scalp-recorded MMN activity were investigated. The novel use of the HCP pipelines and HCP parcellation provided new evidence on how gray matter in these quasi-functional areas relate to brain function measured by the mismatch negativity in early psychosis. This expands the utility for detecting structure-function relationships, as many quasi-functional areas can be accurately detected automatically. In addition, the specificity of the areas provides an important link for translational models, particularly in auditory cortex where parcels have clear correspondence between the human A1 (and belt) and animal A1 (and belt) regions (Sweet et al., 2005). Thus, this knowledge can be more readily moved into animal model systems.

We next use this state-of-the-art infrastructure to investigate a candidate model system that is impaired in early psychosis, the auditory attention network. Selective attention deficits are present before the emergence of psychosis and endure throughout the entire course of psychosis. Interventions initiated very early in the disease can improve functional outcome, and therefore studying impairments present early in the disease is essential for understanding the primary disease pathology and creating effective targeted therapies with improved outcomes. The study of this attention system will lead to a better understanding of the etiology of the disorder and ultimately better treatment, particularly if analysis of this distributed neural system identified areas that could be targeted with next-generation non-invasive brain stimulation to improve distributed functioning early in disease course.

3.0 Attention Modulation of Source activity in Auditory Cortex and Deficits in Early Psychosis

3.1 Introduction

As previously introduced, dysfunction of selective attention is a cognitive deficit that is present before psychosis, endures throughout the disorder, and is associated with long-term functional outcome (Caspi et al., 2003; B. A. Cornblatt et al., 2003; Fett et al., 2011; Kraepelin, 1889). When healthy individuals pay attention to a sound, the amplitude of the scalp-recorded response ~100ms after the tone (N100/M100) increases relative to ignore or divided attention conditions (Neelon et al., 2006; Woldorff et al., 1993). Individuals with schizophrenia have an impaired N100 response without attention to the stimulus, and they also have an impaired ability to enhance the N100 amplitude with attention (Foxe et al., 2011; O'Donnell et al., 1994; Rosburg et al., 2008). Since the ability to enhance the sensory N100/M100 is an executive function, likely involving a frontal executive network, these studies suggest that the N100 is sensitive to both bottom-up sensory perceptual deficits and top-down executive modulation with attention in psychosis. These impairments are present as early as the first episode of psychosis. Individuals at their first episode of psychosis (FEP) have a reduced sensory N100 and are unable to modulate the response with attention (Foxe et al., 2011; Ren et al., 2021; Salisbury et al., 2010). Thus, N100/M100 enhancement is an objective measure of selective attention deficits very early in psychosis. Healthy attention modulation involves an executive network in which frontal regions enhance activity in sensory areas (Petersen & Posner, 2012). Thus, the dysfunction in N100 enhancement involves the interaction of frontal executive and temporal auditory areas and presents

a neurobiological system amenable for study and potential targeted intervention. However, it is unknown which auditory cortical areas contribute to this deficit in sensory gain, critical for both understanding the local cortical circuit deficits and for development of targeted interventions.

The general cortical network underlying selective attention involves the prefrontal cortex, through connections with posterior parietal cortex, modulating activity in sensory cortices (Petersen & Posner, 2012; Tobyne, Osher, Michalka, & Somers, 2017). In monkey visual cortex, attention enhances neuronal responses in striate (V1), pre-striate (V2), and extra-striate cortex (V4) (Luck, Chelazzi, Hillyard, & Desimone, 1997; McAdams & Reid, 2005; Spitzer, Desimone, & Moran, 1988). In the auditory domain, work in ferrets suggests prefrontal cortex modulates activity in auditory cortex at multiple hierarchical levels, with primary auditory cortex and surrounding auditory belt areas playing an important role in auditory selective attention (Elgueda et al., 2019; Fritz, Shamma, Elhilali, & Klein, 2003). Similar enhancement with attention in auditory cortex is seen in humans, with multimodal imaging demonstrating that selective attention increases activity in both primary and non-primary auditory cortex (Ahveninen et al., 2006; Petkov et al., 2004). Despite this evidence, human research has been limited in determining cortical areas differentially involved in specific processes by being restricted to identifying only relatively large, anatomically defined regions of interest in auditory cortex (e.g., Heschl's gyrus), with a lack of specificity between primary and other non-primary auditory cortex areas that is necessary for animal models (e.g., primary auditory cortex versus auditory belt areas). The Human Connectome Project's Multimodal parcellation (HCP-MMP) delineates primary auditory cortex (A1) and auditory belt areas in humans that cannot be defined by previous in vivo methods. Importantly, it also has clear correspondence to human post-mortem and monkey tracing studies (Glasser et al., 2016; Sweet et al., 2005), and thus can identify valid functionally distributed systems.

We source-resolved the M100 to identify where cross-modal selective attention increased M100 gain, and where auditory sensory and attention-related deficits arise in FEP. While fMRI provides high spatial resolution, the measure of neural activity is indirect and less sensitive to changes at high temporal resolution. EEG and MEG provide an advantage over previous studies examining attention modulation, as neural activity can be measured directly on the scale of milliseconds, necessary for the measurement of rapid sensory processes such as the N100/M100, and the modulation of these processes with attention. MEG provides an improved solution for determining cortical sources inside the head from the sensors outside the head because magnetic fields are unaffected by the skull and skin. Understanding the precise cortical areas underlying this impaired ability to modulate the N100/M100 with selective attention in the early disease course can provide important insight into the etiology of the disorder, identify targets for therapies, and determine anatomic circuit locations for translation to animal models.

In this study, we recorded MEG data during a cross-modal auditory attention task in 27 individuals within two months of their first clinical contact for their first episode of psychosis (FEP) and 31 matched healthy controls (HC). High-resolution MRI data was also collected to create individual head models for source localization of the auditory M100 and its enhancement by attention. The novel utilization of the HCP-MMP to precisely parcellate auditory cortex provided the ability to determine the specific auditory cortex areas involved in M100 attention modulation and which areas underlie auditory sensory and attention deficits in FEP.

3.2 Methods

3.2.1 Participants

All participants were recruited from Western Psychiatric Hospital (WPH) inpatient and outpatient services. Participants included 27 FEP individuals within their first episode of psychosis with less than 2 months of lifetime antipsychotic medication exposure, and 31 healthy controls (HC). No participant had a history of concussion or head injury with sequelae, history of alcohol or drug addiction or detox in the last five years, or neurological comorbidity. Groups were matched for age, gender, parental social economic status, and premorbid IQ, measured by the vocabulary component of the Wechsler Abbreviated Scale of Intelligence (WASI) (**Table 8**). All participants had healthy hearing confirmed with audiometry. All participants provided informed consent and were paid for participation. The work described was carried out in accordance with The Code of Ethics of the World Medical Association (Declaration of Helsinki) for experiments involving humans.

Socioeconomic status (SES) for all participants and their parents was measured with the 4-factor Hollingshead Scale. FEP participants' diagnoses were based on the Structured Clinical Interview for DSM-IV (SCID-P) (First et al., 1997). Provisional research diagnoses were initially at baseline, and then confirmed 5-7 months later. Symptoms were rated using the PANSS (**Table 8**) (Kay et al., 1987). Current cognitive ability was assessed with the MCCB (Nuechterlein et al., 2008) for all participants (HC and FEP). MCCB items were designed to capture the state-dependent effect of psychosis on cognition, whereas WASI vocabulary provides a more stable estimate of premorbid intellect. All tests were conducted by an expert clinical diagnostician.

Of the 27 FEP participants, 22 received diagnoses on the schizophrenia spectrum (FESz). Seventeen received diagnoses of Schizophrenia (paranoid: n=7; undifferentiated: n=10), 1 of schizoaffective disorder (bipolar subtype), 2 of schizophreniform (definite), and 2 of psychotic disorder NOS. Five individuals received diagnoses of affective disorders: 4 of Bipolar I disorder and 1 Major depressive disorder. While many of the FEP participants were medicated (21/27, 78%), CPZ equivalent dose did not correlate with source values from either condition or region (p values>0.1), and medication will not be addressed further.

Table 8. Experiment 3: Demographic, Neuropsychological, and Clinical Information.

FEP and HC groups were matched for age, gender, PSES, and WASI Vocab T-Score (Mean ± SD).

	Mean±SD				
	HC	FEP	t/X^2	p	Cohen's d
Sociodemographic data					
Age (years)	24.9 ± 5.7	23.4 ± 4.5	1.36	0.18	0.36
Gender (M/F)	22/9	17/10	0.09	0.77	
SES	41.8 ± 13.1	29.8 ± 13.9	-0.51	0.61	0.13
Parental SES	48.5 ± 10.9	43.3 ± 13.4	-1.21	0.23	0.34
Neuropsychological tests					
WASI Vocab T-Score	52.7 ± 6.2	49.2 ± 9.6	0.71	0.48	0.19
MCCB-total	50.7 ± 7.2	30.8 ± 14.6	-1.54	0.13	0.43
Symptoms					
PANSS Total		76.7 ± 19.8			
PANSS Positive		20.0 ± 6.5			
PANSS Negative		17.9 ± 6.0			
PANSS General		38.9 ± 9.8			
SAPS Global		6.2 ± 3.7			
SANS Global		10.1 ± 4.1			
Medication data					
Medication		202.5 ± 187.4			

Note: SES = socioeconomic status. WASI = Wechsler Abbreviated Scale of Intelligence. MATRICS = composite scaled t score. PANSS = Positive and Negative Syndrome Scale. SAPS = Scale for the Assessment of Positive Symptoms. SANS = Scale for the Assessment of Negative Symptoms. Medication = chlorpromazine equivalents.

3.2.2 Task

A classic oddball task with a frequent tone and a rare tone was presented in two conditions to each participant. Stimuli consisted of a standard tone (1kHz, 50 ms duration, 10 ms rise/fall) and a deviant tone (1.2 kHz, 50 ms duration, 10 ms rise/fall) presented with a stimulus onset asynchrony of 1050-1550 ms. A total of 400 tones were presented, including 340 standard tones (85%) and 60 deviant tones (15%). In one condition, participants were asked to ignore the tones and attend to a silent video. In the second condition, participants were asked to pay attention to the tones and press a button to every deviant tone (**Figure 7**). Blocks were counterbalanced. Only M100 responses to standard tones (not deviant oddballs) were analyzed to maximize the signal-to-noise-ratio for detecting M100 enhancement.

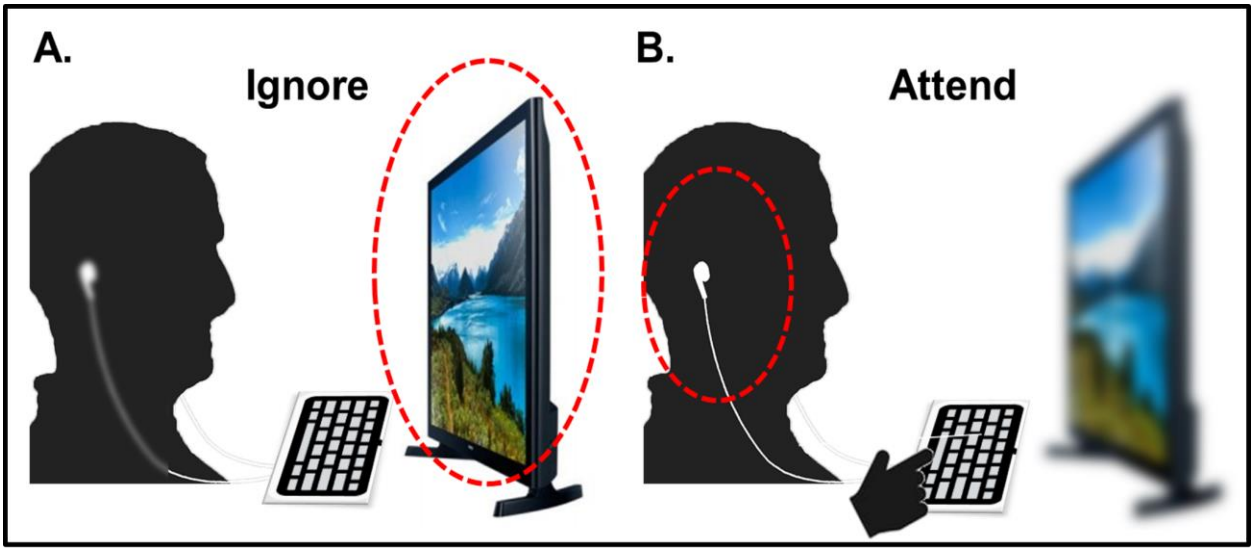

Figure 7. Auditory Attention Task.

A. In the ignore condition, individuals ignored the tones and attended to a silent film. B. In the attend condition, individuals ignored the silent film and attended to the tones and pressed a button when the tone changed in pitch.

3.2.3 MEG Data Acquisition & Processing

MEG data were recorded in a magnetically shielded room with a 306-channel whole-head system (Elekta Neuromag), consisting of 128 triplets (1 magnetometer and 2 planar gradiometers). Data were recorded using a sampling rate of 1000 Hz (online bandpass filter = 0.1–330 Hz). Eye blinks and movements were recorded with bipolar leads placed above and below the left eye (VEOG) and lateral to the outer canthi of both eyes (HEOG). Cardiac activity was recorded with bipolar ECG leads. A 3D-digitizer (ISOTRAK; Polhemus, Inc., Colchester, VT) was used to continuously record the location of 4 head position indicator coils placed on the scalp of each participant relative to their nasion and preauricular points. Neuromag MaxFilter software (http://imaging.mrc-cbu.cam.ac.uk/meg/Maxfilter_V2.2) was used to correct for head motion during the scan. Temporal signal space separation (TSSS) was used to remove electromagnetic

noise originating from outside the MEG helmet (Uusitalo & Ilmoniemi, 1997). The EEGLAB Toolbox (Delorme & Makeig, 2004) in MATLAB was used to remove channels and segments of data with excessive noise via visual inspection. A high-pass filter (0.5 Hz; 12 dB/oct) was applied to the data, and an adaptive mixture independent component analysis was performed to remove eye-blink and ECG components.

Offline processing of the MEG was performed with Brainstorm (Tadel, Baillet, Mosher, Pantazis, & Leahy, 2011), which is documented and freely available for download online under the GNU general public license (http://neuroimage.usc.edu/brainstorm). A low-pass (20Hz) filter was applied to the data to remove muscle and other high-frequency artifacts. Trials were then segmented from 100ms before to 1000ms after stimulus onset. The average baseline voltage was subtracted, and trials that exceeded were ± 5pT were rejected. The remaining trials were averaged.

MEG sensor data was registered to each participant's structural MRI. Possible sources were constrained to the individual's cortical surface and unique brain geometry. The forward solution was modeled as overlapping spheres, and a noise covariance matrix was calculated from the baseline window of all trials. Cortical source activity was estimated using minimum norm estimation (MNE) with each vertex in the surface modeled by a perpendicular dipole. To allow for possible slight head movement errors, a dipole constraint of 0.4 was used, which allowed some source variance to be ascribed to the 2 magnetic moments orthogonal to the perpendicular moment, and depth weighting applied. Current density values were normalized with the use of dynamic statistical parametric maps based on the variance in the prestimulus baseline. Auditory cortex regions of interest were bilateral A1, LBelt, and PBelt, defined by the HCP-MMP. Activity within these ROIs was measured over the 80- to 140-ms post-stimulus time window corresponding with the M100 enhancement (**Figure 8A**).

3.2.4 MRI Data Acquisition & Processing

High resolution MRI data were acquired on a Siemens 3T MAGNETOM Prisma scanner using a 32-channel phase array head coil. Sagittal T1-weighted anatomical MR images were obtained with a 3D MPRAGE sequence [TR/TE/TI = 2400/2.22/1000 ms, flip angle = 7°, field of view (FOV) = 256x240 mm, 0.8 mm isotropic voxel size, 208 slices, GRAPPA acceleration factor = 2]. T2-weighted T2-SPACE images were obtained [TR=3200 ms TE=563 ms, FOV = 256x240, 0.8 mm isotropic voxel size, 208 slices]. A standard fieldmap [TR=731ms, TE= 4.92/7.38, FOV=208x180, 2.0mm voxel size, 72 slices] was collected for correcting readout distortion in the T1w and T2w images. Ten minutes of eyes-open (passive crosshair viewing) resting state BOLD fMRI data were acquired using a multiband pulse sequence [TR =800 ms, TE =37 ms, multiband factor=8, flip angle = 52°, FOV=208x208mm, voxel size = 2.0 mm3, 72 slices]. A single-band reference image with no slice acceleration was acquired at the beginning of each run to improve registrations. Finally, two spin echo EPI images (TR=8000ms, TE=66ms, flip angle=90, FOV=208x208mm, 2.0mm voxel size, 72 slices) with reversed phase encoding directions were acquired.

The publicly available HCP-pipelines (https://github.com/Washington-University/HCPpipelines) were used for MRI processing (detailed in Glasser et al., 2013). Briefly, the structural images were corrected for gradient nonlinearity, readout, and bias field, followed by AC-PC alignment. Myelin maps were created by dividing the T1w image by the T2w image. Native space images were used to generate white and pial surfaces with Freesurfer and were refined using T2w data. Then, the individual's native-mesh surfaces were registered with a multimodal surface matching (MSM) algorithm with MSMsulc to the Conte69 folding-based template (Robinson et al., 2014; Van Essen et al., 2012).

The functional resting-state data were first corrected for gradient-nonlinearity. A 6 DOF FLIRT registration of each frame to the single-band reference image was used to correct for motion. The reverse phase spin-echo images were used to correct functional distortion. The single band reference image was registered to the T1w image with FreeSurfer's BBRegister (Greve & Fischl, 2009). All the transforms and distortion correction were applied in a single resampling step. The data were brain masked and intensity normalized to a 4D whole brain mean of 10,000. Then, a voxel to surface mapping was performed to sample the volumetric fMRI data to the individual's native surfaces, which were subsequently resampled to a standard 32k fs_LR surface. The ICA+FIX pipeline was used to remove artifactual noise (Griffanti et al., 2014; Salimi-Khorshidi et al., 2014). Finally, individuals were registered to a group average atlas surface using a two-stage process based on the multimodal surface matching (MSM) algorithm (Robinson et al., 2014). The group average HCP-MMP was applied to individuals' MRI data and mapped to individuals' cortical surface in native space. These individual cortical surfaces with the HCP-MMP were imported to Brainstorm for the ROI source analysis.

3.2.5 Analysis

Group demographics were compared using independent samples t-test and chi-square tests where appropriate. MEG sensor data were used to visualize the event-related fields and were not compared with statistical analysis. Source activity was compared using repeated measures ANOVA with one between-subjects factor (group: FEP or control) and three within-subject factors (attention: attend or ignore, hemisphere: left or right, and region: A1, LBelt, PBelt). Simple effects were examined using follow-up one-way between-subjects ANOVA or repeated-measures ANOVA, as appropriate. An exploratory analysis was performed to investigate potential M100

modulation differences between FEP who later received a diagnosis on the schizophrenia spectrum and FEP who later received a diagnosis of an affective disorder (Bipolar and Major Depression). Exploratory correlations of attention modulated source activity (attend-ignore) with symptom scores (PANSS Total, PANSS Positive, & PANSS Negative), cognitive measures (MCCB Composite t-score, WASI Vocab), and social functioning (Global Functioning: Role, Global Functioning: Social) were assessed with Spearman's correlations. Results were considered significant at $p < 0.05$.

3.3 Results

3.3.1 Sensor Level Data

MEG sensor level data were segmented and averaged to produce the event-related field. Average magnetometer sensor waveforms for HC and FEP are shown in **Figure 8A**, with M100 time-window (80-140ms) indicated by the shaded bar.

3.3.2 Cortical Source Data

High-resolution structural and functional MRI scans were obtained from all participants and processed with the HCP processing protocols. This allows for the most accurate registration of the HCP cortical parcellation, with heretofore unavailable identification of functional cortical areas. Delineation of A1, lateral belt (LBelt), and parabelt (PBelt) are shown in **Figure 8B**.

MEG sensor data was registered to individual high-resolution MRIs, and cortical activity was calculated using minimum norm estimation and normalized to the noise covariance with dynamic statistical parametric maps (dSPM). The source activity averaged across the ROIs are shown in **Figure 8C** and means and SD are reported in **Table 9**. Overall, FEP exhibited significantly reduced activity compared with HC over the 80- to 140-ms time window ($F_{(1,56)}$ = −7.41, p=0.009), indicating a broad sensory deficit. Of primary importance, there was a significant interaction between group and attention ($F_{(1,56)}$=4.10, p=0.048), where HC enhanced source activity with attention (p=0.002), but FEP did not (p=0.379). Attention modulation differed between hemispheres ($F_{(1,56)}$=4.41, p=0.040), as the left hemisphere showed more M100 attention modulation (p=0.001) than the right. This did not differ between FEP and HC (p's>0.05). There were no significant interactions with region (p's>0.05), suggesting relatively widespread deficits across several early auditory cortex regions.

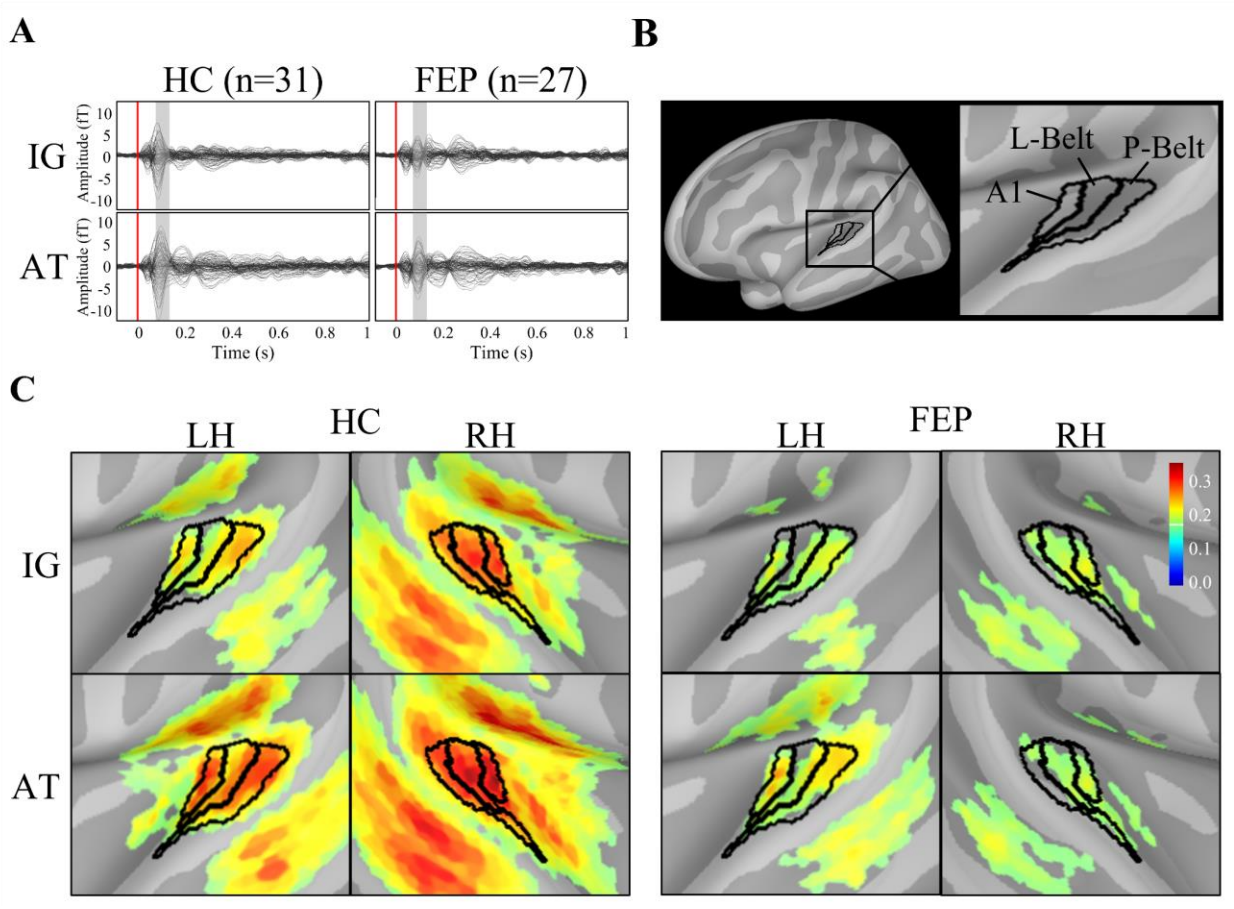

Figure 8. Impaired Auditory Cortex Attention Modulation in First-episode Psychosis.

A. The M100 modulation time window (80-140ms) is highlighted in the butterfly plot of magnetometer sensors. B. The auditory cortex regions of interest defined by the HCP-MMP included bilateral primary auditory cortex (A1), lateral belt (LBelt), and parabelt (PBelt) (only left hemisphere shown for reference). C. Cortical source activity (dSPM) averaged over 80-140ms. Within A1, LBelt, and PBelt, FEP have overall less activity and are impaired in the ability to enhance activity with attention.

Table 9. M100 Cortical Source Activity.

Averaged dSPM source values (Mean ± SD) across the 80-140ms time window within each auditory cortex ROI.

	HC		FEP	
	Attend	Ignore	Attend	Ignore
Left Hemisphere				
Left A1	0.27 ± 0.17	0.21 ± 0.13	0.20 ± 0.11	0.19 ± 0.08
Left LBelt	0.24 ± 0.16	0.20 ± 0.13	0.19 ± 0.10	0.17 ± 0.08
Left PBelt	0.25 ± 0.15	0.21 ± 0.13	0.21 ± 0.11	0.19 ± 0.09
Right Hemisphere	0.30 ± 0.17	0.28 ± 0.14	0.18 ± 0.11	0.19 ± 0.08
Right A1	0.30 ± 0.15	0.27 ± 0.14	0.18 ± 0.09	0.19 ± 0.08
Right LBelt	0.27 ± 0.15	0.24 ± 0.12	0.16 ± 0.08	0.16 ± 0.07
Right PBelt	0.27 ± 0.17	0.21 ± 0.13	0.20± 0.11	0.19 ± 0.08

The exploratory analysis of differences between individuals with a diagnosis of schizophrenia spectrum and those with a diagnosis of an affective disorder (Bipolar and Major Depression), revealed no significant differences between groups (*p*'s>0.1) (**Figure 9**).

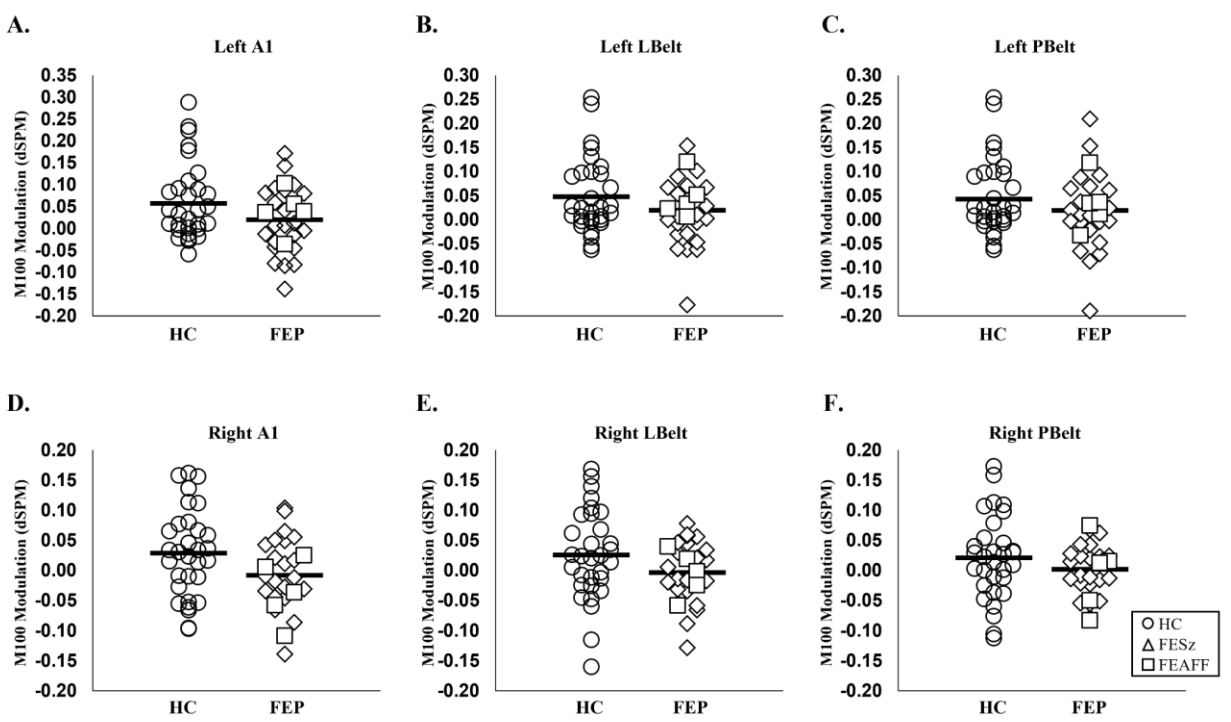

Figure 9. Scatterplots of the M100 Modulation Group Differences in Auditory Cortex Regions.

Compared to healthy individuals, FEP experienced general deficits in the ability to modulate the M100 with attention across all regions of interest (A-F). FEP with a schizophrenia spectrum diagnosis (FESz) are identified separately from those with an affective disorder diagnosis (FEAFF). There were no significant differences between FESz and FEAFF.

3.3.3 Exploratory Correlations with Clinical and Cognitive Measures

There were no significant correlations with differential source activity in FEP (p's>0.05). In HC, only left A1 modulation was negatively associated with WASI Vocab scores (ρ=-0.36, p=0.045).

3.4 Discussion

This is the first demonstration that increases in sensory M100 gain localize to A1 and auditory belt parcels, and FEP experience both sensory and attentional gain modulation deficits in these auditory cortex parcels. Similar to previous reports (Ahveninen et al., 2006; Petkov et al., 2004), M100 enhancement with attention localized to auditory cortex. Previous MEG studies source localizing the M100 have localized activity to Heschl's gyrus, planum temporale and superior temporal gyrus (Ahveninen et al., 2006; Woldorff et al., 1993). This aligns with evidence from other imaging modalities. Functional MRI activation increases in both primary and nonprimary auditory cortex during auditory attention tasks (Grady et al., 1997; Jancke, Mirzazade, & Shah, 1999; Rinne et al., 2007). Similarly PET studies have demonstrated regional cerebral blood flow increases in auditory cortex with attention (Alho et al., 2003; Zatorre, Mondor, & Evans, 1999). However, here we improved the specificity of defining this auditory attention enhancement by localizing it to A1 and auditory belt parcels. These parcels have clear correspondence between the human A1 (and belt) and animal A1 (and belt) regions (Sweet et al., 2005). Thus, this knowledge can be more readily moved into model systems, such as the monkey or ferret to further elucidate underlying auditory attention mechanisms within these regions. The ferret has become a valuable animal model for understanding the neurobiology of the auditory system, particularly understanding the neural basis for selective attention at multiple hierarchical levels in auditory cortex (Elgueda et al., 2019). This study provides an important translational step between human and animal models.

Individuals at their first episode of psychosis experienced sensory and attention impairments in these auditory regions. Individuals with a schizophrenia spectrum diagnosis and those with an affective disorder diagnosis did not significantly differ, as both groups were

impaired. These results suggest that the M100 impairment is more tightly linked to psychosis in general, supporting the value in utilizing a dimensional approach focusing on certain symptoms, opposed to categorical diagnoses, particularly in the context of very early psychosis. It was previously found that FEP have an impaired sensory EEG-recorded N100 in addition to an impaired ability to modulate the N100 amplitude with attention (Ren et al., 2021). However, the cortical regions underlying this deficit remained unknown. Here, we showed that FEP had reduced sensory activity in both primary and nonprimary auditory cortex bilaterally. Further, FEP were deficient in enhancing cortical activity with attention across these regions as well, suggesting that they have relatively widespread sensory and attention modulation deficits in auditory cortex, encompassing primary and nonprimary auditory cortex. The specificity of localizing this functional deficit in primary and auditory belt regions may provide insight to the emergence of psychosis, as specific temporal lobe abnormalities (e.g., Heschl's gyrus gray matter reduction) are present very early in the disorder (Curtis, Coffman, & Salisbury, 2021b; Kasai, Shenton, Salisbury, Hirayasu, Onitsuka, et al., 2003) and show progressive pathology with disease duration (Salisbury et al., 2007). Understanding how the underlying progressive pathology relates to decline in functional abilities such as auditory attention modulation can provide a better understanding of this interplay at the emergence of psychosis. Future longitudinal analyses in combination with structural gray matter/white matter information can address this directly. Further, this study provides specific target areas for therapies to modulate activity using non-invasive brain stimulation, such as transcranial direct stimulation (tDCS) or repetitive transcranial magnetic stimulation (rTMS). Interventions initiated early in the disease improve functional outcome and reduce long-term treatment costs (Eack et al., 2010; Kane et al., 2016; Srihari, Shah, & Keshavan,

2012). These early interventions would improve from a more precise understanding of the specific cortical regions to engage during treatment.

As a follow-up to previous work on the N100 attention modulation in FEP and informed by previous source localization of the M100, this work was limited to a specific hypothesis-driven analysis of auditory cortex activity within the time window of the M100 attention modulation. While there is a distinct deficit within these auditory regions, it is unclear if this impairment is restricted to auditory cortex or is due to an inability of long-range cortical communication from frontal cortex to modulate activity within auditory cortex. Previously, the N100 enhancement was related to functions that involve the frontal executive network (e.g., cognition, negative symptoms, and social functioning) (Ren et al., 2021). The general executive attention network includes the prefrontal cortex, posterior parietal cortex, and sensory areas (Hopfinger, Buonocore, & Mangun, 2000; Petersen & Posner, 2012; Tobyne et al., 2017). While fMRI provides ample evidence for a general auditory attention network, the dynamics underlying modulation of the N100/M100 with attention are unknown. Attention is related to increased gamma band synchrony in sensory areas, and this appears to be coordinated from PFC (Gregoriou, Gotts, & Desimone, 2012; Gregoriou, Gotts, Zhou, & Desimone, 2009). The long-range synchrony is likely mediated by a low carrier frequency (theta/alpha), as sensory gamma oscillations become organized by alpha modulations in the PFC (Spaak, Bonnefond, Maier, Leopold, & Jensen, 2012). In the auditory cortex, it may likely be mediated by theta band oscillations, as phase amplitude coupling in the auditory cortex is primarily observed between the theta and gamma band, though it is possible other frequencies may be involved as delta and alpha band coupling in auditory cortex has also been shown (Doesburg, Green, McDonald, & Ward, 2012; Gomez-Ramirez et al., 2011; Lizarazu, Lallier, & Molinaro, 2019; N. Murphy, Ramakrishnan, Walker, Polizzotto, & Cho, 2020). There has been

little study of oscillatory mechanisms associated with attentional impairments in psychosis, with one MEG study showing decreased alpha desynchrony in schizophrenia in the context of an oddball task (Koh et al., 2011) and others showing intact phase-amplitude coupling in schizophrenia during auditory steady state stimulation (Kirihara, Rissling, Swerdlow, Braff, & Light, 2012; N. Murphy et al., 2020). Future work should extend this investigation to understand functional connectivity with auditory-executive frontal cortex that may mediate this attentional modulation deficit.

The current study is the first to provide crucial insight into the specific cortical areas involved in auditory attentional gain modulation in HC and into the sensory and early attention deficits in FEP. The novel use of the HCP-MMP revealed the precise cortical areas underlying attention modulation and impairments in FEP, providing an understanding critical for translational study and for potential early interventions. The M100 sensory reduction and failure to modulate with selective attention may indicate local and systems-level pathophysiology proximal to disease onset that may be critical for etiology.

3.5 Next Analysis: Detecting the Systems-Level Auditory Attention Network

Having determined that M100 enhancement with attention is disrupted in FEP and that the use of the HCP parcellation scheme identifies discrete loci for M100 enhancement that appear to have spatial resolution on par with the source-localization precision of MNE, the next step towards identifying the distributed auditory-attention circuitry was to determine what coordinated activity within auditory cortex underlies the M100 enhancement. Knowing that M100 enhancement necessarily depends on attentional-control gain modulation signals from auditory executive control

areas and that local sensory increases are tied to increased power in the gamma-band, our next steps were to identify what frequency in auditory cortex was coupled to gamma frequency with attention, and then to determine what distributed areas were coupled to auditory cortex in that carrier frequency.

4.0 The Underlying Executive Attention Network

4.1 M100 Modulation with Attention: Whole-Brain Analysis

4.1.1 Introduction

The executive control of attention generally involves a cortical network that includes the prefrontal cortex, posterior parietal cortex, and the relevant sensory cortices. When attention is drawn to or deployed to a specific sensory stimulus, frontal regions are thought to send signals through the posterior parietal cortex to enhance responses in the sensory cortex (Fiebelkorn & Kastner, 2020). In nonhuman primates, attention alters neural signals within sensory regions and other areas of the network, such as changing spike rates and receptive field properties (Reynolds & Heeger, 2009). Electrical recordings between regions during attention also suggest that frontal and parietal regions lead and synchronize activity in sensory regions (Fiebelkorn & Kastner, 2020; Gregoriou et al., 2009; Saalmann, Pigarev, & Vidyasagar, 2007). In the human visual system, during an attention paradigm that includes a cue, followed by a delay prior to the presentation of the stimulus, fronto-parietal regions increase fMRI BOLD activation during delay periods, while visual cortex enhances the response to the stimulus (Kastner, Pinsk, De Weerd, Desimone, & Ungerleider, 1999). These data suggest frontal and parietal cortices lead and likely direct the modulation of sensory processing.

Within this general attention network framework, several network models have been introduced. Functional MRI has identified two canonical networks that are generally related to attention: the dorsal attention network and ventral attention network. The dorsal network includes

bilateral intraparietal sulcus and frontal eye fields and is involved in orienting attention in space. The ventral network includes temporoparietal junction and ventral frontal cortex and is involved when stimuli occur unexpectedly (Petersen & Posner, 2012; Vossel, Geng, & Fink, 2014). These two networks are generally grouped as orienting attention networks. In terms of executive control of attention specifically, a dual-network model of top-down attention has been proposed in which there is a fronto-parietal system that is more involved in adaptive control and a cingulo-opercular system more involved in stable set-maintenance (Petersen & Posner, 2012). The fronto-parietal system includes the dorsolateral prefrontal cortex, dorsal frontal cortex, inferior frontal lobule, intraparietal sulcus, medial cingulate cortex, and precuneus. This model suggests this system actively maintains task-relevant information and controls adjustments. The cingulo-opercular system, including the anterior prefrontal cortex, frontal operculum, anterior cingulate cortex, and thalamus, may be more involved in sustained activity associated with attention (Dosenbach, Fair, Cohen, Schlaggar, & Petersen, 2008). However, this is unclear as the role of the anterior cingulate is complicated as some suggest its role is in conflict detection and response adjustment rather than selective attention (Walsh, Buonocore, Carter, & Mangun, 2011).

The distinct frontal and parietal areas involved in attention modulation appear to be modality-biased as well. The visual attention system engages the superior precentral sulcus and inferior precentral sulcus along with the intraparietal sulcus and visual cortex. The auditory-biased network involves the transverse gyrus, precentral gyrus, caudal inferior frontal cortex, superior temporal sulcus and gyrus, and auditory cortex (Michalka, Kong, Rosen, Shinn-Cunningham, & Somers, 2015; Tobyne et al., 2017). Thus, these models agree that executive control of attention involves frontal regions communicating with parietal (Medial or lateral) and enhancing activity in sensory cortices.

However, it is unclear which precise areas are involved in the auditory attention network. We have an operationalized, measurable phenomena which is impacted by attention and is deficient in early psychosis, the M100 modulation with attention. Thus, we use this as our model system output to identify which areas may be involved in auditory attention. As we previously identified the increase in activity in sensory cortices via source resolved M100 activity increasing in A1, LBelt, and PBelt with attention, we were interested in disentangling the underlying neural network. The logic was to first identify areas outside of auditory cortex that showed greater activity simultaneously with the auditory M100 enhancement. Thus, we performed a whole brain analysis of broadband source activity during the time window of the M100.

4.1.2 Methods

The methods were the same as the previous experiment in Chapter 3 with the following differences.

4.1.2.1 Analysis

In the same sample of 31 healthy controls, cortical source activity was estimated using minimum norm estimation with a dipole constraint of 0.4 and depth weighting applied. Current density values were normalized with the use of dynamic statistical parametric maps based on the variance in the pre-stimulus baseline. This was calculated for each vertex of cortex for the attend condition and the ignore condition. In Brainstorm, all individual source maps were registered to the MNI/ICBM152 brain template based on the Freesurfer surface-based registration approach (Tadel et al., 2011). Once source activity from each individual was in the same brain space, a whole brain vertex-wise analysis was performed.

Statistical t-tests were calculated for differences between conditions for each vertex. A non-parametric permutation test was used for statistical significance. A permutation test calculates the t-statistic for each vertex for the between condition test. Then, the data are randomly shuffled between groups and the t-statistic is calculated again for each vertex, and the largest t-statistic is saved. This is repeated thousands of times to generate a null probability distribution, against which the original observed statistic is compared. It is significant if the p-value is smaller than .05 of the permutated null distribution. The Benjamini-Hochberg False Discovery Rate (FDR) correction implemented in the brainstorm software was used to correct for multiple comparisons (FDR <0.05).

4.1.3 Results

The whole-brain permutation test revealed a significant increase in activity with attention during the M100 in several cortical regions. During the attend condition, there was a significant increase in the bilateral dorsolateral prefrontal cortex (8C, 46, p9-46v), inferior frontal cortex (IFJa, IFSp), lateral parietal cortex (left PF, left PFt, right PFop, right PFm), precuneus, and auditory cortex (A1, MBelt) (**Figure 10**).

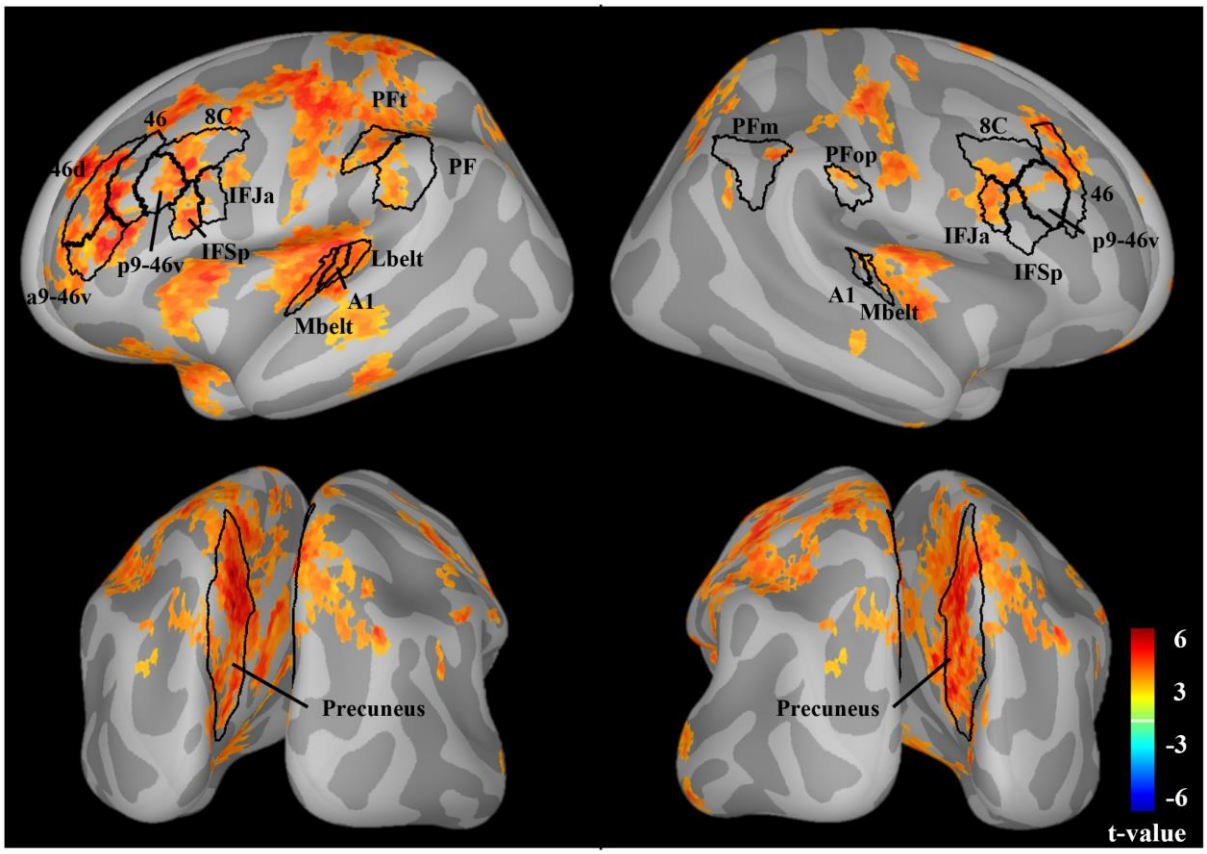

Figure 10. Whole-Brain M100 Modulation in Healthy Individuals.

There were significant increases in source-resolved MEG activity with attention compared to ignore in healthy individuals (FDR<0.05). Outlined in black are regions aligning with the general hypothesized network including prefrontal, posterior parietal, precuneus, and auditory cortices.

4.1.4 Brief Discussion

The whole brain analysis of broadband source activity during the M100 time-window revealed increased activity in several bilateral cortical areas. The dorsolateral prefrontal cortex, inferior frontal cortex, lateral parietal cortex, precuneus, and auditory cortex had increased activity with attention in healthy individuals. Thus, these regions may be involved in the healthy attention modulation of the M100. These parcels correspond to areas comprising part of the canonical

executive attention networks determined by functional MRI (Petersen & Posner, 2012; Tobyne et al., 2017). Particularly striking was the strong involvement of the bilateral precuneus. There is a central role for the precuneus in a variety of highly integrated tasks including attention (Cavanna & Trimble, 2006). The precuneus is thought to comprise a functional core component of the default mode network (DMN), a network with reliable patterns of connectivity at rest and is implicated in regulating attentional states. The precuneus, specifically, is thought to change connectivity during cognitive tasks, including those requiring attention, indicating the role of the precuneus in not only the DMN but also cognition more broadly under varied processing states (Utevsky, Smith, & Huettel, 2014). One of these processing states is auditory attention (Degerman, Rinne, Salmi, Salonen, & Alho, 2006; Krumbholz, Nobis, Weatheritt, & Fink, 2009; Utevsky et al., 2014). Thus, the precuneus is considered a hub region in executive control of attention.

While this analysis provides evidence for activity increases in other cortical areas with attention during the M100 time-window, it does not determine any direct role for these areas in auditory attention M100 enhancement. Hence, it is important to examine the network and network dynamics by investigating functional connectivity between identified regions and auditory cortex parcels. In MEG, this is done in the spectral domain, as long-range connectivity is measured by coherence between the phase of oscillatory signals that comprise the broadband source activity. To investigate the network dynamics, we performed a time-frequency analysis in primary auditory cortex and investigated coupling between an executive carrier low-frequency phase and high-frequency local sensory gamma amplitude across the entire trial. This identified the carrier frequency coming from cortical executive areas, for which we then probed functional connectivity between regions within this executive carrier frequency band.

4.2 Oscillatory Dynamics of the Attention Network

4.2.1 Introduction

The deployment of attention increases neuronal responses in primary sensory cortices (Hocherman, Benson, Goldstein, Heffner, & Hienz, 1976; Spitzer et al., 1988). In humans, attention increases the gain of the sensory response, and we have previously demonstrated this with M100 source activity increasing with attention. In concert with increased neural activity, oscillatory activity is involved in this attention modulation. In the visual system attention modulation is associated with increased gamma band synchrony in sensory areas (Gregoriou et al., 2012; Gruber, Muller, Keil, & Elbert, 1999; Shibata et al., 1999; Tallon-Baudry, Bertrand, Henaff, Isnard, & Fischer, 2005). Oscillatory changes occur in other executive control network areas as well. The gamma phase in sensory areas is led by gamma synchrony in prefrontal cortex, indicating that PFC coordinates this response, likely through alpha frequency signals (Gregoriou et al., 2009). In nonhuman primates, attention increased gamma coherence in the supraganular layers (Layers I-III) of visual sensory cortex, while also decreasing theta/alpha coherence in deep layers. As deep layers are a major source of corticocortical feedback connections, it suggests input may be coming from other cortical areas (Buffalo, Fries, Landman, Buschman, & Desimone, 2011). This is likely due to input from executive control regions.

Attention is also related to the coupling between low frequency phase and high frequency power, referred to as phase-amplitude coupling. Within nonhuman primate primary visual cortex, alpha phase in deeper layers couples to gamma amplitude in superficial layers (Spaak 2012). Thus, it appears that oscillatory theta/alpha band activity in deeper layers of sensory areas (likely driven

by fronto-parietal regions) is modulated with attention and in turn impacts the local microcircuit, leading to changes in neuronal excitability and ultimately neuronal activity.

In humans, activity measured from the cortical surface demonstrates that attention increases alpha-gamma coupling in sensory areas, and in general, gamma power bursts are phase locked to traveling alpha waves across cortex (Bahramisharif et al., 2013; Voytek et al., 2010). Alpha activity is likely related to different functions related to attentional processes. Local alpha activity is related to the suppression of distracting stimuli in both visual attention tasks and intersensory attention tasks involving auditory and visual stimuli (Foxe, Simpson, & Ahlfors, 1998; Foxe & Snyder, 2011; Fu et al., 2001; Worden, Foxe, Wang, & Simpson, 2000). While local alpha activity seems to reflect inhibitory processing, alpha synchrony between cortical regions likely reflects increased communication between regions. EEG recorded during an attention task demonstrated that alpha-band phase synchrony was increased between task-relevant regions (Doesburg, Green, McDonald, & Ward, 2009). This aligns with converging evidence that implicates theta or alpha rhythmicity in attention modulation where the alpha phase plays a mechanistic role in influencing local neuronal activity and communication between regions (Klimesch, Sauseng, & Hanslmayr, 2007; Palva & Palva, 2007, 2011).

Cognitive deficits in schizophrenia are associated with cortical oscillatory impairments. For example, increased cognitive control is related to increased gamma-band activity in prefrontal areas, however, this increase is absent in schizophrenia (Cho, Konecky, & Carter, 2006; Gonzalez-Burgos, Cho, & Lewis, 2015). This is likely due to the GABAergic interneuron class of parvalbumin (PV) neurons. PV neurons show strongest coupling to gamma oscillations (Klausberger & Somogyi, 2008; Tukker, Fuentealba, Hartwich, Somogyi, & Klausberger, 2007), and PV neurons synchronize pyramidal cell firing via inhibition. In schizophrenia, while the

number or density of PV cells remains unchanged, the functionality of PV neurons contributes to cortical pathology in schizophrenia (Gonzalez-Burgos et al., 2015).

In human auditory cortex, PAC most commonly occurs between theta phase (4-7Hz) and gamma amplitude (30-50 Hz) (Cho et al., 2015; Doesburg et al., 2012; Hirano et al., 2018). Using EEG during auditory steady state response paradigms, in which external stimuli elicit a steady state response in cortex at the stimulating frequency, gamma amplitude has consistently coupled with theta phase (Cho et al., 2015; N. Murphy et al., 2020). In MEG during a verb-generation task, task-dependent synchronization of gamma oscillations was modulated by theta phase (Doesburg et al., 2012). Coupling between gamma amplitude and theta phase has also been observed in frontal and parietal areas during cognitively demanding tasks (Tseng et al., 2019). There have been relatively few PAC coupling studies done in schizophrenia and fewer in early psychosis. In the existing studies, there have been mixed results. In an auditory steady state response paradigm, PAC appears to be relatively intact in schizophrenia (Hirano et al., 2018; Kirihara et al., 2012; N. Murphy et al., 2020). This suggests that there may be preservation of the underlying mechanisms supporting PAC. Here, we investigate differences in frequency power during the attend condition to tone pips in primary auditory cortex, followed by an investigation of changes in phase-amplitude coupling with attention in auditory cortex regions and a precuneus region of interest (precuneus visual area (PCV)) that showed significant enhancement with attention during the M100 time-window (described earlier in this Chapter). Identifying PAC changes in sensory areas and the precuneus, will give insight into which frequency may be the low-frequency carrier from executive regions.

4.2.2 Methods

The methods were the same as the previous experiment (Chapter 4.1) with the following differences.

4.2.2.1 MEG Processing

The processing steps were the same as before, but because of the interest in oscillatory activity, the low-pass (20Hz) filter was not applied to the data.

4.2.2.2 Time-Frequency Analysis

In the Brainstorm program, the time-frequency decomposition of broadband MEG source data from each trial was calculated with Morlet wavelets for the frequency range 4-100 Hz. The calculation was done as 40 bins logarithmically spaced between 4-100Hz. The other default parameters were used (central frequency was 1Hz and a 3s full width at half maximum (FWHM)). Trials were baseline corrected with event-related perturbation from a 100ms pre-stimulus baseline period. Trials were then averaged for each individual.

4.2.2.3 Phase-Amplitude Coupling

The calculation of phase-amplitude coupling was done with the method described in Ozkurt & Schnitzler (2011). First, all trials (0-1000ms post-stimulus) were concatenated, and Morlet wavelets were used for low frequency (4-13 Hz) phase and high frequency amplitude (30-100Hz). PAC was calculated at each vertex of the ROI, followed by averaging of PAC values within the ROI. This was done in auditory ROIs comprising bilateral A1, LBelt, and PBelt and in

a precuneus ROI that demonstrated significant modulation with attention from the previous analysis, bilateral precuneus visual areas (PCV).

4.2.2.4 Analysis

All individuals were included in the between-task comparison. Within each ROI, a cluster-based permutation test (5000 permutations) was used to calculate significant differences between conditions in the time-frequency power analysis. Similarly, permutation testing was used for the phase-amplitude coupling analysis and for comparisons in the between-group comparison. An uncorrected exploratory analysis of all regions of interest was performed to gain an understanding if all regions had correspondence in which low-frequency phase was most involved in coupling. Statistics are reported for the highest instance of PAC within each region.

4.2.3 Results

4.2.3.1 Time-Frequency Analysis in Primary Auditory Cortex

In all participants, after correction for multiple comparisons, there was a significant increase in theta (5-7 Hz) power in left A1 during the attend condition compared to ignore from 0-330 ms ($p<0.05$) (**Figure 11**). There were no significant differences between groups. In right A1, there were no significant differences with attention and no differences between groups.

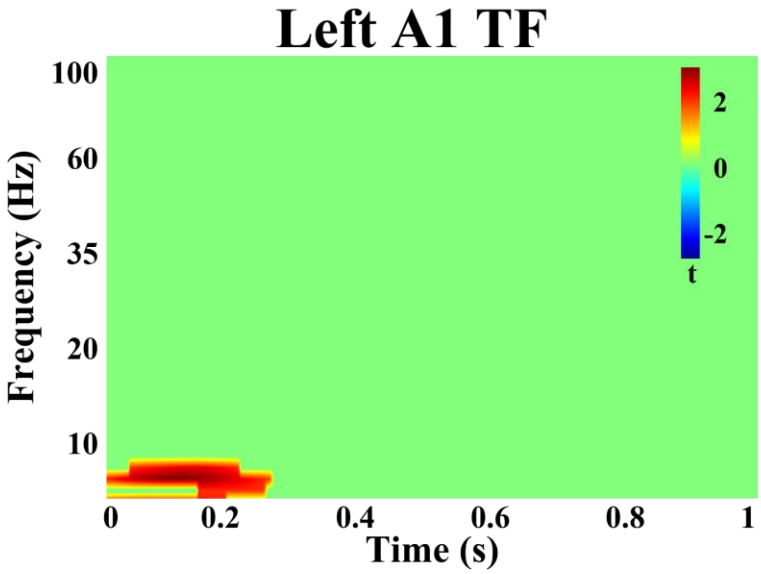

Figure 11. Time-Frequency Analysis in Left Primary Auditory Cortex.

There was a significant increase in theta frequency power with attention in left auditory cortex during from 0-330ms in all individuals.

4.2.3.2 Phase-Amplitude Coupling: Exploratory Uncorrected Statistics

In all participants, most auditory cortex regions showed maximal increase in coupling with attention between gamma amplitude and the theta frequency phase. The following were the highest instance of increase in phase amplitude coupling with attention within the region. In left A1, theta phase (5-7Hz) coupled with gamma amplitude (35-40Hz) (t_{56}=3.60, p<0.001). In the left LBelt, theta phase of 6Hz coupled with gamma amplitude at 35Hz (t_{56}=2.81, p=0.003). The left PBelt theta phase at 5Hz coupled with 36 Hz gamma amplitude (t_{56}=2.54, p=0.010). In the right A1, 7Hz theta phase coupled with gamma amplitude at 40 Hz (t_{56}=2.73, p=0.003). Right LBelt alpha phase at 9Hz coupled with 41Hz gamma amplitude (t_{56}=3.55, p=0.008). Right PBelt theta phase at 5Hz coupled with 34Hz gamma amplitude (t_{56}=2.75, p=0.006).

Similar to the auditory cortex, in the precuneus, there was an increase in coupling between theta phase and gamma amplitude. Left PCV theta phase of 5 Hz coupled with gamma amplitude at 45 Hz (t_{56}=2.70, p=.009). Right PCV theta phase at 5Hz coupled with gamma amplitude at 43Hz (t_{56}=3.06, p=0.004) (**Figure 12**).

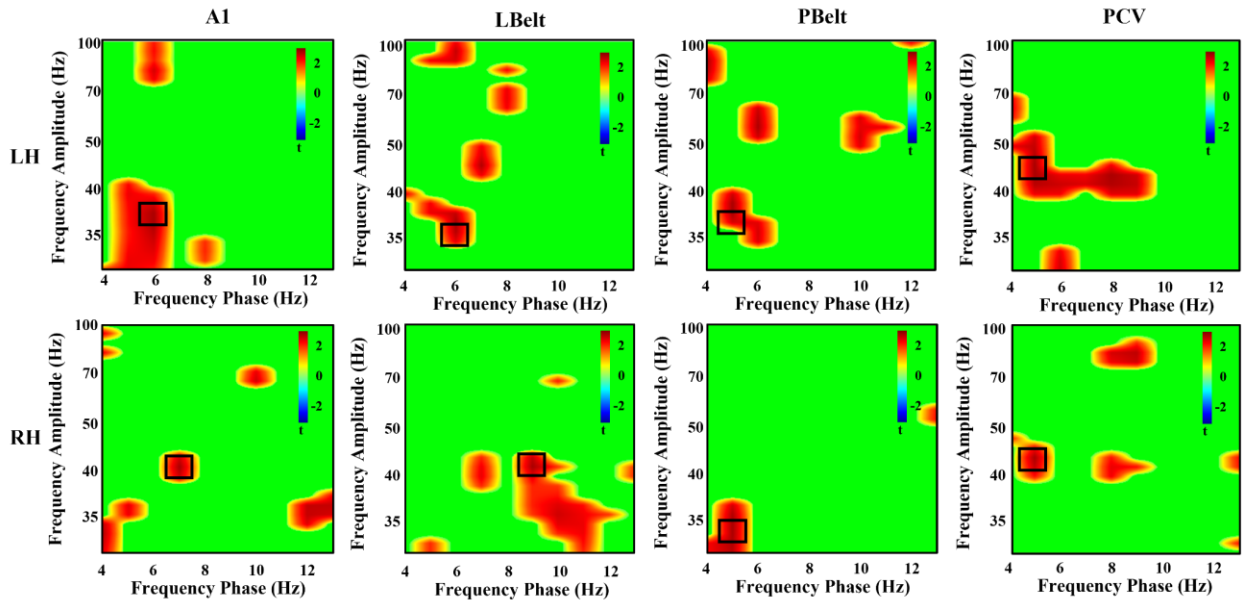

Figure 12. Exploratory Uncorrected Phase-Amplitude Coupling Analysis in Auditory Cortex and Precuneus. There were uncorrected significant increases in coupling between low-frequency phase and gamma power. All, except right LBelt, areas showed the greatest coupling increase with attention between theta phase and gamma power. Right LBelt showed the greatest coupling increase with attention between alpha phase and gamma power. Peak coupling within each area is outlined in black.

4.2.3.3 Phase-Amplitude Coupling: Corrected Statistics

After correction for multiple comparisons, in all participants, there was a significant increase in PAC with attention in left A1 between the theta phase (5-7 Hz) and gamma amplitude (35-40 Hz) (p<0.05) (**Figure 13**). There were no significant differences between groups.

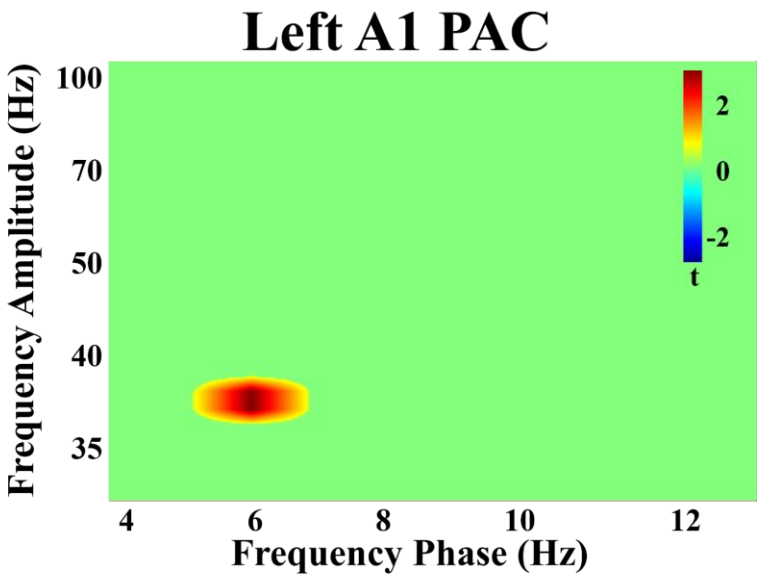

Figure 13. Significant Phase-Amplitdue Coupling Analysis in Left Primary Auditory Cortex.

There was a significnt increase in coupling with attention between theta frequency phase and gamma frequency amplitude in left auditory cortex in all individuals.

4.2.4 Brief Discussion

This study investigated whether auditory attention increases spectral power in primary auditory cortex and if attention increases coupling between low-frequency phase and high-frequency gamma amplitude in auditory cortex regions and the precuneus. In all individuals, theta power was increased with attention in left A1. This increase occurred during the time-window of the M100, and the N100/M100 has been shown to have greatest power in the theta frequency band (Lakatos, Schroeder, Leitman, & Javitt, 2013). In addition, the exploratory analysis in all regions demonstrated that every area, with the exception of right LBelt, experienced increased coupling between gamma amplitude and theta-band phase. The right LBelt experienced maximal coupling between gamma amplitude and alpha phase. Further, in all individuals, there was a significant

increase in coupling of gamma amplitude and theta phase in left A1 with attention. This provides substantial evidence that the low-frequency carrier frequency that modulates sensory regions with attention in this task is the theta frequency band. This is in agreement with previous studies that have explored PAC in auditory cortex with EEG and MEG in humans and non-human primates, where in the auditory domain local gamma activity couples with theta-band phase (Cho et al., 2015; Doesburg et al., 2012; Lakatos et al., 2005; N. Murphy et al., 2020; Tseng et al., 2019).

There were no significant differences in PAC between groups, adding to the evidence that the mechanisms underlying PAC are relatively intact in individuals with psychosis. Recent EEG and MEG analyses of individuals with schizophrenia in early and chronic stages of the disorder found intact PAC in patients at both stages of the disorder (Hirano et al., 2018; N. Murphy et al., 2020). Theta oscillations appear to be generated by somatostatin and multipolar bursting GABA interneurons (Blatow et al., 2003; Womelsdorf, Valiante, Sahin, Miller, & Tiesinga, 2014). It has been proposed that impaired interneuron interaction with pyramidal cells may be impaired in schizophrenia (Javitt & Sweet, 2015). However, it appears that while some deficits like MMN may be ascribed to local inhibition-excitation deficits, the local circuit interactions that lead to infragranular theta phase and superficial gamma amplitude coupling appear to be intact in early psychosis. Further study is necessary to understand the neural mechanisms underlying PAC and how this mechanism may remain intact in psychosis.

As it appears that PAC is intact within the auditory cortex and precuneus in early psychosis, it becomes likely that the mechanism underlying attention modulation deficits in early psychosis is experienced at the network level, perhaps as a reduction in the incoming executive-control signal. In this study, the theta frequency band was identified as the likely frequency that is underlying communication from executive control regions with attention. The next investigation

focuses on attention modulation of oscillatory network connectivity in the theta frequency and potential functional connectivity deficits in FEP.

4.3 Attention Modulation Network Functional Connectivity

4.3.1 Introduction

As previously introduced, the executive control of attention generally involves a cortical network that includes the prefrontal cortex, posterior parietal cortex, and the relevant sensory cortices. The previous analysis identified that auditory attention is related to increases in local gamma amplitude coupling with the theta frequency. In animal work, interactions between distant cortical regions occur mostly in the lower frequency (4-12 Hz) band and are dependent on the behavioral significance of the stimuli (von Stein, Chiang, & Konig, 2000). Further, these interactions occur between infragranular layers of parietal regions and supragranular layers of primary sensory cortex, matching a layer specificity indicating top-down interaction, further supporting low frequency interaction from high-order areas driving connectivity with attention (von Stein, Chiang, & Konig, 2000). In humans, low frequency signals coordinate long-range communication. In MEG resting-state connectivity analyses, networks are more spatially specific in low-frequencies (Brookes et al., 2011; de Pasquale et al., 2010). Thus, as low-frequency neuronal signal appears to be input from other cortical layers, it is likely this theta frequency is the carrier frequency from other executive areas in the service of attention.

Communication between distant areas is likely through coherence in the neural signals (Fries, 2005; Singer & Gray, 1995). In this framework, neuronal oscillations are viewed as

synchronized changes in excitability, with rhythmic sequences of excitation and inhibition. For example, if neuronal groups have relative increased excitability during the peak of an oscillation, then stimuli time-locked to the peak may be processed faster or more efficiently than other stimuli (Lakatos et al., 2005; Womelsdorf & Fries, 2007). As explained with phase-amplitude coupling, low-frequency rhythms can modulate local neuronal activity. Theta rhythms specifically can modulate firing rate and spike timing of single neurons and the gamma power of local field potentials (extracellular potential of a population of neurons). This rhythmic excitability happens both within cortical and between cortical areas. Thus, functional connectivity in MEG data has been measured with the relationship between the phase of the oscillatory signal (Jervis, Nichols, Johnson, Allen, & Hudson, 1983; Tallon-Baudry, Bertrand, Delpuech, & Permier, 1997).

These oscillatory signals between cortical regions change in the service of cognitive functions, such as attention. In the visual system, attention modulates the oscillatory connectivity in the alpha frequency band between visual, parietal, and frontal regions (Lobier, Palva, & Palva, 2018; Marzetti et al., 2019). When comparing attention between auditory and visual attention, theta connectivity changes were strongest when both stimuli were being monitored, indicating a role for theta oscillations in audio-visual integration and cognitive control (Cavanagh & Frank, 2014; Keller, Payne, & Sekuler, 2017). Further, theta synchronization measured with MEG was increased between cortical regions during auditory attention (Doesburg et al., 2012). Thus low-frequency oscillations between cortical regions are modulated with attention, with the theta frequency, seemingly important for auditory-related attention.

In this study, we investigated connectivity between cortical regions in source resolved MEG data. Many of the aforementioned studies investigating oscillation connectivity utilized EEG, but source-resolved MEG data provide a distinct advantage due to magnetic signals being

unaffected by the skull and scalp. In MEG data, synchrony of oscillations between regions can be measured with the relationship between the phase of the oscillatory signal (Jervis et al., 1983; Tallon-Baudry et al., 1997). Specifically, the phase locking value (PLV) measures the phase synchrony between two oscillatory signals over time. An advantage of this technique is that it provides temporal relationship independent of the signal amplitude (Lachaux, Rodriguez, Martinerie, & Varela, 1999).

The PLV technique was utilized here to measure connectivity between cortical regions in the theta band. Due to its role in attention and the previously demonstrated increase with attention, we used the functional subregions of the precuneus, defined by the HCP-MMP, as seed regions and calculated connectivity with the other HCP-MMP parcels in healthy individuals. Then, the functional subregions were clustered based on their connectivity profiles. Once clustered, it was determined with which areas the clusters had significant increases in theta-phase connectivity. Finally, it was investigated if these network regions also increased connectivity with attention in FEP.

4.3.2 Methods

The methods were the same as the previous experiment (Chapter 4.2) with the following differences.

4.3.2.1 Phase-Locking Value

Phase locking value (PLV) was used to assess functional connectivity in the present study (Lachaux et al., 1999; Mormann, Lehnertz, David, & E. Elger, 2000). PLV examines the instantaneous phase synchronization between two signals without the confounded of signal

amplitude. Given the previous results of significant increases in gamma amplitude coupling with theta phase in auditory and precuneus cortices, phase synchronization was calculated within the theta-band (5-7Hz). Connectivity was assessed for all attend and ignore trials during the entire length of the trial. To compute PLV, source resolved cortical activity was band-pass filtered (5 – 7Hz) and a Hilbert transform was used to obtain instantaneous phase data. The PLV between two regions i and j was calculated:

$$PLV_{ij} = \frac{1}{T} \left| \sum_{t=1}^{T} e^{-i(\varphi i(t) - \varphi j(t))} \right|$$

In the above equation, *T* is the number of data points in the time series and $\varphi(t)$ represents the phase of each signal at timepoint *t*.

4.3.2.2 Precuneus Clustering Approach

The HCP-MMP defines the precuneus into 12 bilateral functional subregions (**Figure 14**). Each subregion was used as a seed region, and PLV was calculated between each subregion and the other HCP-MMP parcels. PLV was calculated between each vertex in the seed region and each vertex in each parcel, and then the phase-locking values were averaged for each region. This resulted is a connectivity vector for each precuneus subregion with one averaged phase-locking value for each region of interest. This was done for attend and ignore conditions, and t-values comparing attend vs ignore in healthy controls were calculated for each subregion. To identify clusters within the precuneus, subregions were then clustered together based on their connectivity difference patterns.

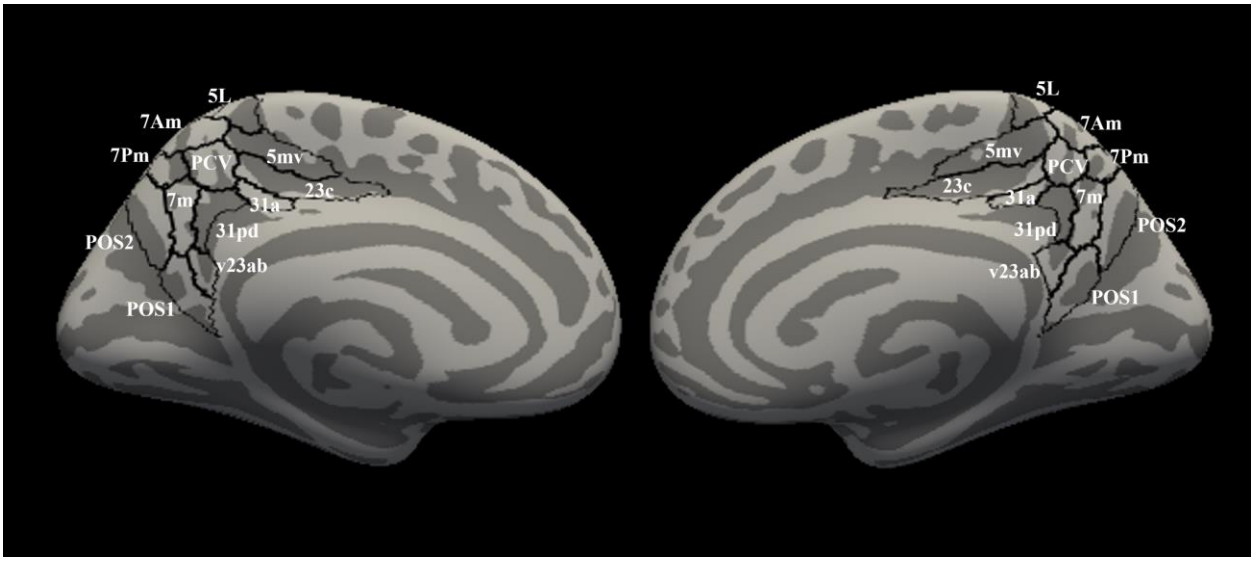

Figure 14. Precuneus Functional Subregions Defined by the HCP-MMP.

The Human Connectome Project's Multimodal Parcellation (HCP-MMP) parcellates the general precuneus area into 12 bilateral functional subregions labeled here.

To accomplish this, t-distributed stochastic neighbor embedding (t-SNE) was implemented in Matlab. T-SNE is a statistical method for high-dimensional data that gives each datapoint (in this case, each precuneus subregion) a location in a two-dimensional map. First, t-SNE calculates the similarity of the high-dimensional connectivity profiles for the precuneus regions and constructs a probability distribution over pairs of regions, in which regions with similar connectivity profiles are assigned a higher probability while dissimilar regions are assigned a lower probability. Then, the precuneus regions are randomly plotted as points on a two-dimensional plot, and t-SNE calculates a similar probability distribution of similarity scores between the points (or regions) on the plot. T-SNE reiterates this second step of plotting the points (or regions) on the two-dimensional plot until it minimizes the distance (using Kullback–Leibler divergence) between the original distribution and the two-dimensional plot distribution, so regions that had similar high-

dimensional connectivity profiles were plotted more closely in the two-dimensional plot than those with more dissimilar connectivity profiles.

Clustering the two-dimensional data was performed with k-Means clustering, which clusters the data into a given number of clusters in a way that minimizes within-cluster variation (Lloyd, 1982). The elbow method was used to determine the optimal number clusters. In this approach, the within-cluster sum of squared errors (WSS) was calculated for a range of cluster values (1-10), and the number of clusters is chosen as when the WSS diminishes and greater than 90% of the variance is explained, visible as an elbow in the plot.

Once the regions were clustered, the parcels were merged within Brainstorm, and the PLV connectivity was calculated again using the entire cluster as a seed region. Then, it was determined which HCP-MMP parcels had significantly greater connectivity with the cluster with attention.

4.3.2.3 Analysis

An FDR of 0.1 was used to control for multiple comparisons of the whole brain connectivity between precuneus clusters and HCP-parcellated regions. The FDR controls for Type I error (false positives), and a cutoff of 0.1, would indicate that in the significant results, there could be at most 10% false positives. An FDR of 0.1 was selected to balance the expected relatively small effect sizes of connectivity differences with attention due to relatively smaller sample sizes (31 HC) and the large number of comparisons (~360). Further the goal was to identify areas with strong changes in connectivity in healthy individuals and examine if FEP are impaired in these regions. The precuneus clusters differ in connectivity patterns, and the goal of this analysis was to identify areas demonstrating most strong changes with attention.

For group difference comparisons, repeated measures ANOVAs were used with one between-subjects factor (Group: Control or FEP) and one within-subject factor (Region).

4.3.3 Results

4.3.3.1 Precuneus Subregion Clustering

The clustering analysis yielded 4 clusters of functional subregions based on their whole brain connectivity in the theta band (**Figure 15 A-B**). Cluster 1 included left hemisphere regions area 23-part c (23c), anterior area 31 (31a), lateral area 5 (5L), medial-ventral area 5 (5mv), anterior-medial area 7 (7am), and precuneus visual area (PCV) (**Figure 15C**). The second cluster included right hemisphere regions 23c, 31a, posterior-dorsal area 31 (31pd), 5L, 5mv, 7am, and PCV (**Figure 15D**). The third cluster included left 31pd, left medial area 7 (7m), left posterior-medial area 7 (7pm), left posterior precuneus 2 (POS2), right 7m, right 7pm, and right POS2 (**Figure 15E**). The fourth cluster included left posterior precuneus 1 (POS1), left ventral 23ab, right POS1, and right ventral 23ab (**Figure 15F**).

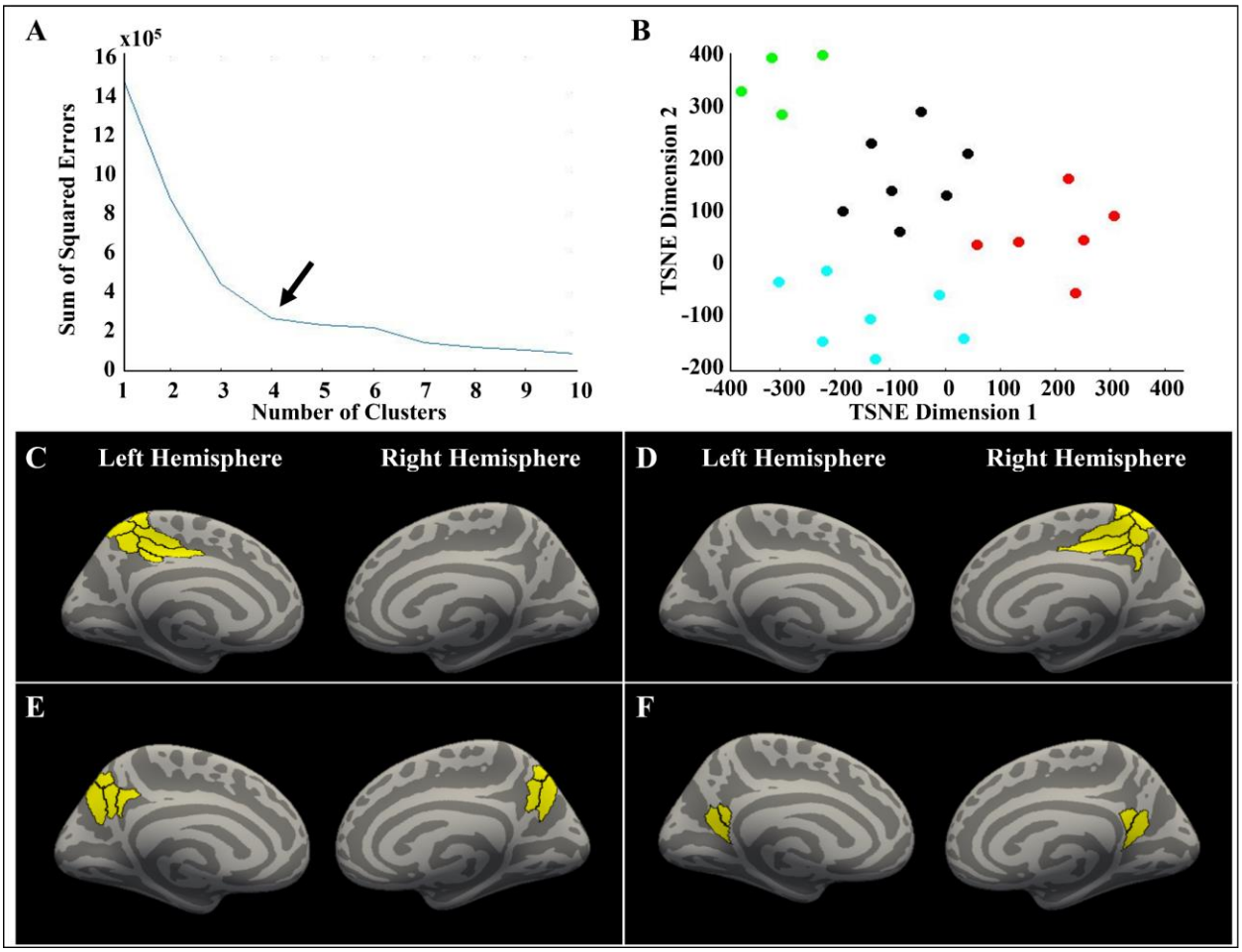

Figure 15. Cluster Analysis.

A. K-means clustering and the elbow-method was used to determine the optimal number of clusters, which was determined to be four clusters, indicated by the arrow. B. The two-dimensional t-SNE plot with each point representing a precuneus subregion. Each region's location on the plot is determined by the region's whole-brain connectivity profile in the theta band. If regions have more similar connectivity profiles, they will be located closer to each other on the t-SNE plot. The clusters are denoted by different colors. The four clusters are shown on the cortical surface. There was a left hemisphere cluster (C), a right hemisphere cluster (D), and two bilateral clusters (E-F).

4.3.3.2 Cluster Connectivity with Attention in Healthy Individuals

In healthy individuals, the left lateralized anterior precuneus cluster showed significantly greater connectivity with attention with left medial belt (MBelt), left dorsal posterior superior temporal sulcus (STSdp), left temporo-parieto-occipital junction 1 and 2 (TPOJ1 & TPOJ2), left visual area 3b (V3B), and posterior frontal pole area 10 (p10p) (FDR<0.1) (**Figure 16A**). In healthy individuals, the right lateralized anterior precuneus cluster showed significantly greater connectivity with attention with right medial superior temporal area (MST), right lateral occipital area 1 (LO1), right visual area 7 (V7), right posterior area 9-ventral area 46 in the dorso-lateral prefrontal cortex (p9-46v) (FDR<0.1) (**Figure 16B**). The other two precuneus clusters did not have connectivity increases with attention that survived FDR correction (FDR>0.1).

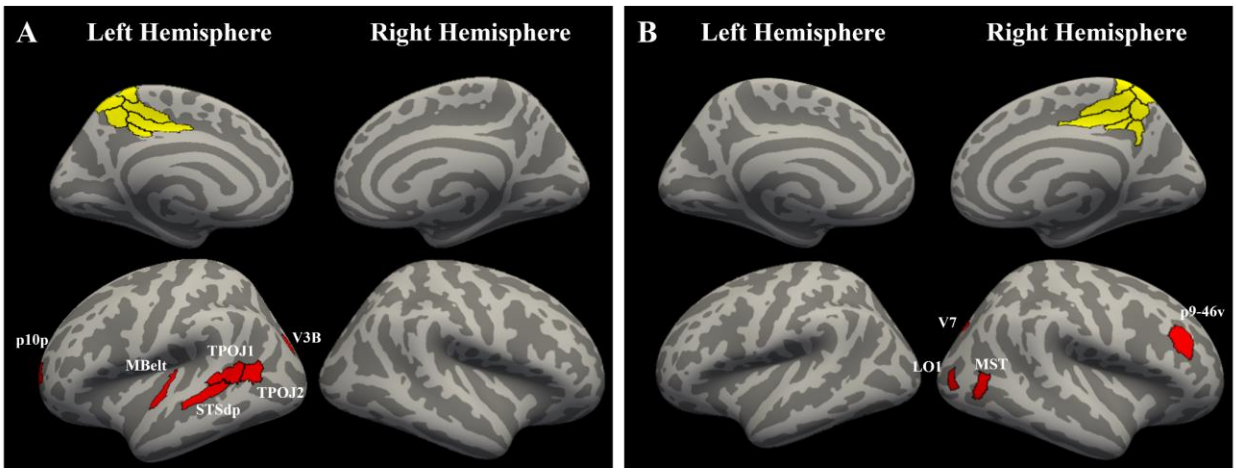

Figure 16. Regions with Signficant Connectivity Increases with Attention.

A. The left hemisphere precuneus cluster had signficant increases in theta phase connectivity with attention with left medial belt (MBelt), left dorsal posterior superior temporal sulcus (STSdp), left temporo-parieto-occipital junction 1 and 2 (TPOJ1 & TPOJ2), left visual area 3b (V3B), and posterior frontal pole area 10 (p10p) (FDR<0.1). B. The right hemisphere precuneus cluster had signficant increases in theta phase connectivity with attention with right medial superior temporal area (MST), right lateral occipital area 1 (LO1), right visual area 7 (V7), right posterior area 9-ventral area 46 in the dorso-lateral prefrontal cortex (p9-46v)(FDR<0.1).

4.3.3.3 Cluster Connectivity Differences between Groups

In the left hemisphere network, FEP were significantly impaired in the ability to enhance connectivity with attention ($F_{1,56}$=8.58, p<0.01) (**Figure 17**). There was no significant interaction with region (p>0.1). Similarly, in the right hemisphere, FEP were significantly impaired in the ability to enhance connectivity with attention ($F_{1,56}$=7.67, p<0.01) (**Figure 18**). There was no significant interaction with region (p>0.1). Values for the change with attention for each region are reported in **Table 10**.

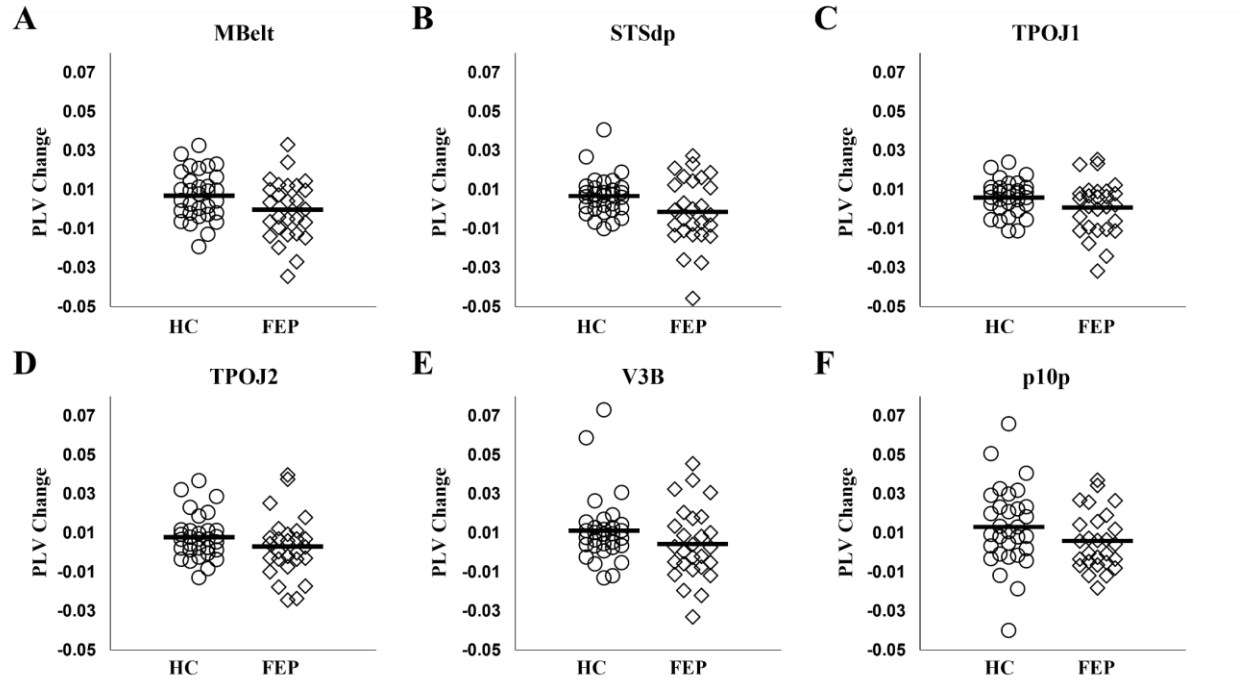

Figure 17. Left Hemisphere Network Connectivity Changes in HC and FEP.

There was a signficinat reduction in the modulation of theta band connectivity with attention (measured with change in phase-locking value) across regions in the left hemisphere network in FEP (A-F).

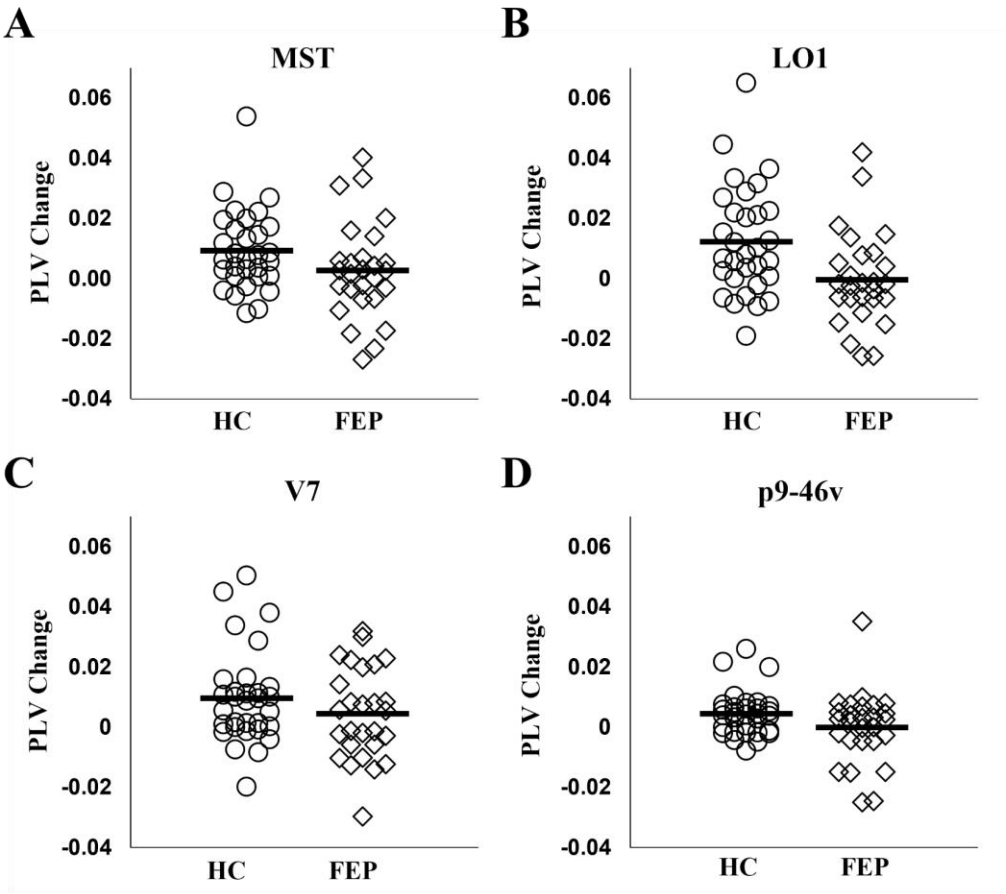

Figure 18. Right Hemisphere Network Connectivity Changes in HC and FEP.

Similar to the left hemisphere network, there was a signficinat reduction in the modulation of theta band connectivity with attention (measured with change in phase-locking value) across regions in the right hemisphere network in FEP (A-D).

Table 10. Connectivity Changes with Attention.

Changes in theta band phase-locking value with the precuneus cluster with attention (Attend-Ignore) in healthy controls (HC) and individuals at the first episode of psychosis (FEP).

	Mean±SD			
	HC (n=31)	FEP (n=27)	*t*	*p*
Left Hemisphere				
MBelt	0.0079 ± 0.012	-0.0013 ± 0.016	2.53	0.01
STSdp	0.0067 ± 0.010	-0.0014 ± 0.017	2.21	0.03
TPOJ1	0.0059 ± 0.008	0.0007 ± 0.014	1.72	0.09
TPOJ2	0.0078 ± 0.011	0.0030 ± 0.016	1.36	0.18
V3B	0.0112 ± 0.017	0.0044 ± 0.018	1.45	0.15
p10p	0.0131 ± 0.021	0.0059 ± 0.015	1.51	0.18
Right Hemisphere				
MST	0.0092 ± 0.013	0.0026 ± 0.016	1.72	0.09
LO1	0.0123 ± 0.018	-0.0004 ± 0.016	2.82	0.01
V7	0.0096 ± 0.016	0.0044 ± 0.015	1.27	0.21
p9-46v	0.0045 ± 0.007	-0.0001 ± 0.011	1.78	0.08

Abbreviations: MBelt, Medial belt; STSdp, dorsal posterior superior temporal sulcus; TPOJ1, temporo-parieto-occipital junction 1; TPOJ2, temporo-parieto-occipital junction 2; V3B, visual area 3b; p10p, posterior frontal pole area 10; MST, medial superior temporal area; LO1, lateral occipital area 1; V7, visual area 7; p9-46v, posterior area 9-ventral area 46

4.3.4 Discussion

This study demonstrated two networks of cortical regions that increased connectivity with attention in healthy individuals, but FEP were impaired in the ability to enhance connectivity with attention in these networks. Following the finding of the role of the precuneus in the modulation of the M100 with attention, it was hypothesized that the precuneus, being a hub for cognitive control, would also increase functional connectivity with other cortical regions for attentional control. Using the quasi-functional HCP-MMP, the precuneus was parcellated into functional subregions and these subregions were clustered based on the connectivity profile. The precuneus was grouped into four functional clusters with distinctly different connectivity patterns with the

rest of the brain. Two of these clusters, one in the left hemisphere and one in the right hemisphere, had significantly greater theta connectivity with several other cortical regions with attention. The left precuneus network included left auditory cortex, temporo-parieto-occipital junction, superior occipital, and posterior frontal pole. The right precuneus network included right prefrontal cortex and lateral occipital cortex. FEP were significantly impaired in the ability to enhance theta connectivity between these regions in the service of attention.

These findings agree with literature that the phase synchrony of the cognitive control of auditory attention occurs in the theta frequency range (Cavanagh & Frank, 2014; Doesburg et al., 2012; Keller et al., 2017). Theta oscillations are at least in part generated by the interactions of somatostatin and multipolar bursting GABA interneurons with pyramidal cells (Blatow et al., 2003; Womelsdorf et al., 2014). It has previously been proposed that impaired interneuron interaction with pyramidal cells may be impaired in schizophrenia (Javitt & Sweet, 2015). Thus, the inability to increase theta connectivity with attention in FEP could be related to this interneuron-pyramidal interaction. Here, with the use of the functionally specific HCP-MMP, specific network regions have been identified as regions for future translational study to directly investigate if these specific interneuron groups are particularly impaired within these regions in psychosis.

These networks shared some general correspondence but also had some divergence with canonical fMRI-defined auditory attention networks. The role of the precuneus has previously been described as a core component of the default mode network and is important for changing connectivity during cognitive processing, such as auditory attention (Degerman et al., 2006; Petersen & Posner, 2012; Utevsky et al., 2014). In the context of auditory attention, early auditory cortex, such as MBelt, is modulated by attention (Kong et al., 2014; Tobyne et al., 2017). The right

dorsolateral prefrontal cortex has been implicated as a canonical region for top-down cognitive control (Dosenbach et al., 2008). While not always included in canonical attention networks, the higher order auditory cortices, such as the superior temporal sulcus and temporo-parietal junction, have been implicated in attention to human voice stimuli (Alho et al., 2006). Functional MRI has demonstrated visual area 3 deactivates during auditory attention tasks, and thus it could be postulated that the phase connectivity increase with attention could be transferring a signal to visual cortices to reduce visual cortex activity (Kong et al., 2014). The frontal pole is involved in multitasking and lesions to this region in the primate result in impaired cognitive control adjustments (Burgess, Veitch, de Lacy Costello, & Shallice, 2000; Dreher, Koechlin, Tierney, & Grafman, 2008; Mansouri, Buckley, Mahboubi, & Tanaka, 2015). While right lateral occipital areas are not typically discussed in the context of auditory attention, it has been suggested that lateral occipital regions have changes in connectivity with default mode regions (such as the precuneus) with changes in visual attention (Karten, Pantazatos, Khalil, Zhang, & Hirsch, 2013). Since this task involves visual stimuli in both conditions, it is possible the connectivity changes identified in this study are related to these changes in visual attention in the service of paying attention to versus ignoring the sounds. Finally, fMRI has implicated visual area 7 in the role of visual spatial attention (Baker, Burks, Briggs, Stafford, et al., 2018; Tootell et al., 1998). The inclusion of several occipital lobe regions that are implicated in visual attention by fMRI suggests that the functional connectivity increases in the attend condition in the task of the current study may be related to the cross-modal nature of the task. The precuneus may increase connectivity with these regions while attending to auditory stimuli to downmodulate local neuronal activity within these regions. Future studies can investigate this more directly.

These novel findings indicate a distributed attention modulation circuit with functional deficits in very early psychosis. This circuitopathy provides a systems-level target for novel interventions, such as non-invasive brain stimulation. Improvement of attention modulation deficits in FEP, should improve real-world functioning, and might improve functional outcome if targeted early in the disorder.

5.0 Gray Matter Correlates of the Auditory Attention Measures

5.1 Introduction

Psychosis is associated with underlying structural changes detected with high-resolution brain imaging. In chronic schizophrenia (Sz), there is a widespread decrease in cortical and subcortical gray matter. Cortical volume loss is seen in prefrontal, parietal, temporal, and parahippocampal cortices. Subcortical volume loss is experienced in the hippocampus, amygdala, and thalamus (Birur et al., 2017; Cropley et al., 2017; Goldman et al., 2009; Haijma et al., 2013; Rimol et al., 2010; Shenton et al., 2001; T. G. van Erp et al., 2016). Schizophrenia is also associated with cortical thinning across the cortex, with the greatest occurring in the frontal temporal cortices (Rimol et al., 2010; Rimol et al., 2012; T. G. M. van Erp et al., 2018; van Haren et al., 2011). There is a progressive decline in gray matter during the early course of schizophrenia and specific regional gray matter differences can be detected at first episode of psychosis with the greatest differences restricted to frontal, temporal, and parahippocampal cortices (Curtis, Coffman, & Salisbury, 2021a; DeLisi et al., 1997; Ellison-Wright et al., 2008; Gur et al., 1998; Hirayasu et al., 1998; Kasai, Shenton, Salisbury, Hirayasu, Onitsuka, et al., 2003; Keshavan et al., 1998; Vita et al., 2006). Gray matter is impacted in the disorder even before the full onset of psychotic symptoms, as gray matter differences are reported as early as the prodrome for psychosis. Individuals at clinical high-risk for psychosis (CHR) who later convert to psychosis have less gray matter volume in lateral and medial temporal, frontal, cingulate, and bilateral insula cortices (Mechelli et al., 2011; Pantelis et al., 2003; Takahashi, Wood, Yung, Phillips, et al., 2009). Thus,

gray matter deficits are present even before the first episode of psychosis and there is a widespread progressive decline in volume and thickness experienced throughout the disorder.

Gray matter is related to several aspects of cognitive functioning in psychosis. Cognitive deficits are a core feature of psychotic disorders that are also present before the onset of psychosis and endure throughout the disorder (Green & Nuechterlein, 1999; McCleery et al., 2015; Seidman et al., 2010). Gray matter in temporal and frontal lobes are related to cognitive functioning in chronic schizophrenia, but these relationships are not often reported in early psychosis (Baare et al., 1999; Crespo-Facorro et al., 2011; Hirayasu, McCarley, et al., 2000; Hirayasu et al., 2001; C. U. Lee et al., 2002; Nestor et al., 1993; Radua et al., 2012; Shenton et al., 2001). Gray matter is also associated with functioning measured with neurophysiology, such as the mismatch negativity. As previously introduced, the MMN is a response elicited by changes in stimuli (e.g., changes in tone pitch). Gray matter volumes are related to MMN in chronic schizophrenia (Rasser et al., 2011), and in early psychosis (Curtis et al., 2021b; T. K. Murphy et al., 2020; Salisbury et al., 2007). Thus, there appears to be a relationship between the functional deficits manifested in early psychosis and the underlying structural changes occurring at the same time.

In the previous work, we have established an operationalized functional deficit in the M100 modulation with attention and an underlying network with functional impairments in early psychosis. In addition, we validated the utility of the HCP-MMP in detection of gray matter deficits and structure-function relationships. Because there are progressive structural changes in the early course of psychosis in addition to the functional deficits in early psychosis, we hypothesize that selective attention deficits in FEP are related to underlying subtle structural deficits within the selective attention network. Here, gray matter was calculated within the auditory cortex regions and attention network regions and relationships with functional measures were investigated.

5.2 Methods

5.2.1 MRI Data Acquisition and Processing.

MRI data acquisition and processing were the same as previously described. High-resolution MRI data were acquired on a Siemens 3T MAGNETOM Prisma scanner using a 32-channel phase array head coil. Sagittal T1-weighted anatomical MR images were obtained with a 3D MPRAGE sequence [TR/TE/TI = 2400/2.22/1000 ms, flip angle = 7°, field of view (FOV) = 256x240 mm, 0.8 mm isotropic voxel size, 208 slices, GRAPPA acceleration factor = 2]. T2-weighted T2-SPACE images were obtained [TR=3200 ms TE=563 ms, FOV = 256x240, 0.8 mm isotropic voxel size, 208 slices]. A standard fieldmap [TR=731ms, TE= 4.92/7.38, FOV=208x180, 2.0mm voxel size, 72 slices] was collected for correcting readout distortion in the T1w and T2w images. Ten minutes of eyes-open (passive crosshair viewing) resting state BOLD fMRI data were acquired using a multiband pulse sequence [TR =800 ms, TE =37 ms, multiband factor=8, flip angle = 52°, FOV=208x208mm, voxel size = 2.0 mm3, 72 slices]. A single-band reference image with no slice acceleration was acquired at the beginning of each run to improve registrations. Finally, two spin echo EPI images (TR=8000ms, TE=66ms, flip angle=90, FOV=208x208mm, 2.0mm voxel size, 72 slices) with reversed phase encoding directions were acquired. For quality assurance, the MRI scans were visually inspected for scanner artifacts, motion, and gross neuroanatomical abnormalities

The publicly available HCP-pipelines (https://github.com/Washington-University/HCPpipelines) were used for MRI processing (detailed in Glasser et al., 2013). The structural images were corrected for gradient nonlinearity, readout, and bias field, followed by AC-PC alignment. Myelin maps were created by dividing the T1w image by the T2w image.

Native space images were used to generate white and pial surfaces with Freesurfer software, which were then refined using T2w data (Dale et al., 1999; Fischl & Dale, 2000; Fischl et al., 1999). Then, the individual's native-mesh surfaces were registered with a multimodal surface matching (MSM) algorithm with MSMsulc to the Conte69 folding-based template (Robinson et al., 2014; Van Essen et al., 2012).

The functional resting-state data were first corrected for gradient-nonlinearity and registered to the single-band reference image. The single band reference image was registered to the T1w image with FreeSurfer's BBRegister (Greve & Fischl, 2009). All the transforms and distortion correction were applied in a single resampling step. The data were intensity normalized to a 4D whole brain mean of 10,000. Then, a voxel to surface mapping was performed to sample the volumetric fMRI data to the individual's native surfaces, which were subsequently resampled to a standard 32k fs_LR surface. The ICA+FIX pipeline was used to remove artifactual noise (Griffanti et al., 2014; Salimi-Khorshidi et al., 2014). Finally, individual subjects were registered to a group average atlas surface using the multimodal surface matching (MSM) algorithm (Robinson et al., 2014). The group average HCP-MMP was applied to individuals' MRI data and mapped to individuals' native space where thicknesses and volumes were computed.

5.2.2 Analysis

The first analysis consisted of investigating gray matter volume and thickness group differences in the auditory cortex regions of interest used in Chapter 3 (bilateral A1, LBelt, and PBelt). The next analysis examined gray matter volume and thickness group differences in the regions with significant increases in functional connectivity enhancement with the left precuneus cluster from Chapter 4 (Left MBelt, STSdp, TPOJ1, TPOJ2, V3B, & p10p). The final group

difference analysis was with the regions with significant increases in functional connectivity enhancement with the right precuneus cluster from Chapter 4 (Right MST, LO1, V7, & p9-46v). Gray matter volume group comparisons were made with analysis of covariance (ANCOVA) on the relative volumes (absolute volume/intracranial content (ICC)) with gender and age as covariates. The statistical conclusions reported remained the same when using ANCOVA on absolute volumes with intracranial content (ICC), gender, and age as covariates. Gray matter thickness group comparisons were made with analysis of covariance (ANCOVA) with gender, and age as covariates. The statistical conclusions reported remained the same when we used ANOVA without the use of gender and age as covariates.

Correlations with gray matter volumes and thicknesses were also investigated. In the first analysis, in HC and FEP, gray matter volume and thicknesses were correlated with the source activity of the M100 modulation in auditory cortex regions from Chapter 3 (bilateral A1, LBelt, and PBelt). In HC and FEP, gray matter volume and thicknesses were also correlated with phase-amplitude coupling modulation with attention in left A1 from Chapter 4. In HC and FEP, gray matter volume and thicknesses were correlated with theta connectivity modulation in the areas with significant connectivity from Chapter 4 (Left hemisphere regions: MBelt, STSdp, TPOJ1, TPOJ2, V3B, & p10p; right hemisphere regions: MST, LO1, V7, & p9-46v). Absolute volumes and thickness within regions were used for correlations, and correlations were assessed with Spearman's rho.

5.3 Results

5.3.1 Gray Matter Group Differences

There were no group differences in gray matter volume or thickness in the auditory cortex regions of interest (bilateral A1, LBelt, PBelt) (*p*'s>0.1).

There was a significant group difference in gray matter thickness in the left hemisphere precuneus network, where FEP had thinner gray matter within the regions connected to the left precuneus (left MBelt, STSdp, TPOJ1, TPOJ2, V3B, & p10p) ($F_{1,54}$=5.14, *p*=0.02) (**Figure 19**). There was no interaction between region and group. There were no differences in gray matter volume (*p*>0.1).

There were no group differences in gray matter volume or thickness within the right hemisphere precuneus network (*p*'s>0.1). Gray matter thickness values are reported in **Table 11** and volumes are reported in **Table 12**.

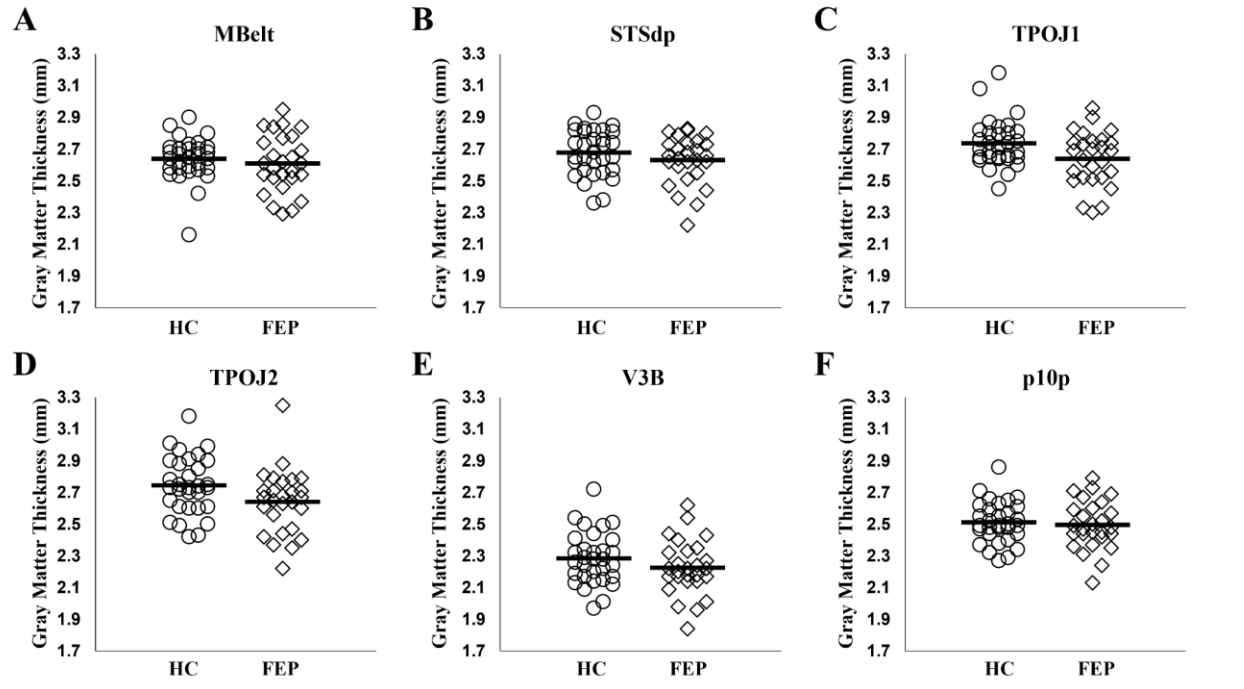

Figure 19. Gray Matter Thickness in the Left Hemisphere Attention Network.

Compared to healthy controls, individuals with first-episode of psychosis (FEP) showed signficant reductions in gray matter thickness across the regions in the left hemisphere precuneus attention network (p<0.05)(A-F).

Table 11. Gray Matter Thickness.

Gray matter thickness in mm (mean±SD) differences between healthy controls (HC) and individuals at the first-episode pscyhosis (FEP) from the ROIs in the left and right hemisphere attention networks.

	Mean±SD			
	HC (n=31)	FEP (n=27)	*t*	*p*
Left Hemisphere				
MBelt	2.64 ± 0.14	2.61 ± 0.18	0.78	0.44
STSdp	2.68 ± 0.14	2.63 ± 0.15	1.18	0.24
TPOJ1	2.74 ± 0.15	2.64 ± 0.17	2.38	0.02
TPOJ2	2.75 ± 0.18	2.64 ± 0.20	2.09	0.04
V3B	2.28 ± 0.17	2.22 ± 0.17	1.32	0.19
p10p	2.51 ± 0.13	2.50 ± 0.15	0.40	0.69
Right Hemisphere				
MST	2.52 ± 0.18	2.49 ± 0.18	0.72	0.47
LO1	2.42 ± 0.20	2.45 ± 0.16	-0.80	0.43
V7	2.33 ± 0.20	2.25 ± 0.22	1.52	0.14
p9-46v	2.67 ± 0.15	2.72 ± 0.19	-1.12	0.27

Abbreviations: MBelt, Medial belt; STSdp, dorsal posterior superior temporal sulcus; TPOJ1, temporo-parieto-occipital junction 1; TPOJ2, temporo-parieto-occipital junction 2; V3B, visual area 3b; p10p, posterior frontal pole area 10; MST, medial superior temporal area; LO1, lateral occipital area 1; V7, visual area 7; p9-46v, posterior area 9-ventral area 46

Table 12. Gray Matter Volume.

Differences in gray matter volume corrected for intracranial content in mm^3 (volume/ICC) (mean±SD) between healthy controls (HC) and individuals at the first-episode pscyhosis (FEP) from the ROIs in the left and right hemisphere attention networks.

	Mean±SD			
	HC (n=31)	FEP (n=27)	*t*	*p*
Intracranial Content	$1.20 \times 10^6 \pm 0.15 \times 10^6$	$1.17 \times 10^6 \pm 0.13 \times 10^6$	0.74	0.46
Left Hemisphere				
MBelt	0.065 ± 0.010	0.068 ± 0.011	-1.18	0.24
STSdp	0.103 ± 0.016	0.104 ± 0.014	-0.09	0.93
TPOJ1	0.103 ± 0.018	0.100 ± 0.020	0.55	0.59
TPOJ2	0.100 ± 0.030	0.101 ± 0.033	-0.11	0.91
V3B	0.039 ± 0.008	0.037 ± 0.010	0.65	0.52
p10p	0.110 ± 0.020	0.109 ± 0.190	0.10	0.92
Right Hemisphere				
MST	0.050 ± 0.013	0.053 ± 0.014	-0.54	0.59
LO1	0.050 ± 0.012	0.050 ± 0.012	-0.04	0.97
V7	0.049 ± 0.013	0.047 ± 0.009	0.84	0.41
p9-46v	0.185 ± 0.053	0.190 ± 0.039	-0.41	0.68

Abbreviations: MBelt, Medial belt; STSdp, dorsal posterior superior temporal sulcus; TPOJ1, temporo-parieto-occipital junction 1; TPOJ2, temporo-parieto-occipital junction 2; V3B, visual area 3b; p10p, posterior frontal pole area 10; MST, medial superior temporal area; LO1, lateral occipital area 1; V7, visual area 7; p9-46v, posterior area 9-ventral area 46

5.3.2 Gray Matter Correlations with M100 Modulation, PAC, and PLV

In both HC and FEP, there were no significant correlations between the amount of source-resolved M100 modulation and gray matter volume or thickness within bilateral A1, LBelt, and PBelt (*p*'s>0.1). In HC and FEP, there were no significant correlations between PAC and gray matter in left A1 (*p*'s>0.1). In HC and FEP, there were no significant correlations between PLV and gray matter in any of the precuneus network regions previously identified (*p*'s>0.1).

5.4 Discussion

In this study, the investigation focused on gray matter deficits in FEP and whether gray matter was related to the functional auditory attention measures previously extracted. While FEP did not differ in auditory cortex gray matter, they had significantly thinner cortices within the left hemisphere attention network regions. This identifies a network important for attention modulation with both functional and structural deficits in FEP. Gray matter loss in schizophrenia is due to a reduction in cortical neuropil (Selemon & Goldman-Rakic, 1999), and in auditory cortex specifically, there is a reduction in layer III pyramidal soma size and a decreased number and density of dendritic spines (Lewis & Sweet, 2009; Parker & Sweet, 2017; Sweet et al., 2004; Sweet et al., 2009). It is hypothesized that the consequence of these reductions is reduced synaptic connectivity (Lewis & Sweet, 2009; Salisbury et al., 2007; Todd et al., 2013). Thus, it is postulated that neuropil reductions within this left attention network reduces synaptic connectivity with interneuron groups controlling theta rhythms. There were no direct correlations between gray matter and the theta phase-locking value measures, which may suggest either a mediator between the two measures or a nonlinear relationship between the measures in which gray matter thins to a certain extent or threshold that results in functional deficits, but further thinning doesn't necessarily indicate further functional deficits as they may reach a floor effect on the ability to modulate connectivity with attention. Future investigation can investigate this more directly.

While functional network PLV deficits were found in both left and right hemispheres, gray matter deficits were only found in the left hemisphere. There is evidence of left hemisphere bias of gray matter deficits in early psychosis. Left temporal lobe gray matter deficits are prevalent early in the disorder and in individuals at high risk for psychosis who later develop psychosis exhibit progressive gray matter reduction in the left temporal lobe (Job, Whalley, Johnstone, &

Lawrie, 2005; Pantelis et al., 2003; Takahashi, Wood, Yung, Soulsby, et al., 2009). Reduced gray matter within these left hemisphere regions correlate with positive symptoms such as hallucinations and thought disorder and neurophysiological measures such as the mismatch negativity (Barta et al., 1990; Curtis et al., 2021b; Salisbury et al., 2007; Salisbury et al., 2020; Shenton et al., 1992; Takahashi et al., 2006). With auditory hallucinations and thought disorder being prominent features for psychosis, and these symptoms linked to primarily left hemisphere language circuitry, it has been suggested that left hemisphere frontal and temporal abnormalities are particularly impacted early in the disorder (Salisbury et al., 2007; Takahashi, Wood, Yung, Soulsby, et al., 2009). However, it should be noted that left hemisphere specific deficits in those who transition to psychosis are not always reported (Cannon et al., 2015; Fortea et al., 2021). Thus, it remains inconclusive, but there could be certain subgroups of patients that experience left hemisphere specific gray matter deficits that relate to positive symptoms and functional deficits.

This study identified gray matter deficits in FEP within the previously identified left hemisphere network involved in attention modulation and is functionally impaired in FEP. As gray matter loss in psychosis is associated with a loss in neuropil, this suggests that in early psychosis a loss of neuropil within these regions may underly the functional attention deficits seen within this network. The identification of this network that has both structural and functional impairments can improve treatment specificity with either non-invasive brain stimulation or cognitive enhancement therapy, which can be neuroprotective in early psychosis (Eack et al., 2010). Future analyses can investigate these directly.

6.0 Overall Discussion

6.1 Summary and Significance

The goal of the endeavor presented in this dissertation was to identify alterations in the cortical network underlying executive control of auditory attention deficits in early psychosis. Psychosis is a devastating disorder with few treatment options that effectively treat deficits in cognitive functioning, such as attention. The most effective treatments are those implemented early in the disorder, thus underscoring the need for a better understanding of these deficits early in psychosis to improve treatment options.

Selective attention is a core cognitive deficit present in early psychosis. An objective measure of attention is the increase in EEG-measured N100 and MEG-measured M100 amplitude when attending to tones. This ability to modulate the N100 with attention is impaired in early psychosis. However, it was unknown what cortical areas were particularly impaired in this N100 modulation deficit and what executive attention modulation network was involved in this task. Understanding the precise cortical areas underlying this impaired ability to modulate the N100 with selective attention in the early disease course is necessary to gain insight to the underlying mechanisms of the disorder, identify circuit regions for translation to animal models, and identify potential targets for improved therapeutic interventions.

To address these questions, this investigation utilized MEG to gain an improved source solution compared to EEG, while maintaining high temporal resolution not provided by fMRI. In addition, the advanced processing pipelines developed by the Human Connectome Project (HCP) and the HCP multimodal parcellation (HCP-MMP) were used to provide the state-of-the-art

processing methods for the high-resolution MR data acquired and high parcellation specificity of cortical regions not previously available.

These novel methods were implemented and validated in the detection of gray matter deficits and structure-function relationships in early psychosis. In the first experiment, the HCP-MMP was used to automatically and precisely parcellate cortex into 360 regions of interest. A functional subregion of the parahippocampal area was found to have significantly less gray matter in first-episode schizophrenia (FESz). Gray matter within this region was also related to hallucination severity and cognitive performance in FESz. In the second experiment, gray matter in precisely parcellated auditory and inferior frontal cortex regions and scalp-recorded MMN activity were investigated. The results from this second experiment provided new evidence on the relationship between gray matter in these quasi-functional areas and brain function measured by the mismatch negativity in first episode psychosis. These two experiments validated the use of the novel HCP pipelines and HCP-MMP, as it could accurately and automatically detect many cortical areas, leading to novel understandings of structure-function relationships in early psychosis. The HCP-MMP also can provide a crucial link for translational models, particularly in auditory cortex where parcels have clear correspondence between the human A1 (and belt) and animal A1 (and belt) regions (Sweet et al., 2005).

We next used this infrastructure to investigate a model system with functional deficits in early psychosis, the auditory attention network. In the third experiment, it was determined that individuals at the first episode of psychosis (FEP) were impaired in the sensory MEG-measured M100 source response and the modulation of the M100 with attention in auditory cortex regions. This experiment provides crucial insight into the specific auditory cortical areas involved in the sensory and attention deficits in FEP. The novel use of the HCP-MMP revealed the precise

auditory areas underlying attention modulation impairments in FEP, providing an understanding critical for translational study and for potential early interventions.

With the knowledge that attention modulation of the M100 likely involves an executive attention network, the focus shifted to identifying the regions involved in this network. First, a whole-brain analysis of attention modulation during the time-window of the M100 was performed. This analysis identified several cortical regions in the prefrontal, posterior parietal, and auditory cortices with significant increases in activity with attention, as was hypothesized. In particular, the precuneus demonstrated large increases in activity with attention, identifying it as a potential hub for coordinating attention modulation.

The following experiments set out to further examine the network by investigating functional connectivity in the spectral domain. To investigate the network dynamics, first, we performed a time-frequency analysis in primary auditory cortex and examined coupling between low frequency phase and local high frequency gamma amplitude in auditory areas. This experiment identified significant increases with attention in theta power and coupling between theta phase and gamma amplitude in left primary auditory cortex. Interestingly, FEP did not appear to have deficits in either theta power or phase-amplitude coupling, suggesting the mechanisms supporting these processes are intact in early psychosis. Nonetheless, this experiment identified theta as the carrier frequency coming from cortical executive areas.

In the next experiment, theta-band connectivity changes with attention were investigated, using the precuneus functional subregions as seed regions for detecting an executive auditory attention network through theta connectivity. This experiment identified a left hemisphere and a right hemisphere network associated with increases in connectivity with attention in healthy individuals. FEP had impairments in both networks in that they were unable to increase

connectivity with attention. These novel findings identified a distributed attention modulation circuit with functional deficits in very early psychosis.

Finally, gray matter deficits and correlates were investigated to explore structure-function relationships with respect to these measures of auditory attention impairment in FEP. The regions in the left hemisphere attention network were significantly thinner in FEP, suggesting underlying neuropil reduction that may be contributing to this functional deficit of executive control of attention in FEP. This circuitopathy provides a systems-level target for novel interventions, such as non-invasive brain stimulation. Improvement of attention modulation deficits in FEP should improve real-world functioning and might improve functional outcome if targeted early in the disorder.

6.2 Limitations

This study was not without limitations. The sample size is relatively small compared to larger multisite studies; thus, this study would garner strength with replication of these findings in larger samples. Further a limitation of the HCP-MMP is its restriction to cortex. Many deficits in psychosis, particularly gray matter deficits, include subcortical regions, which we were unable to identify here. Future studies can use traditional volumetric approaches to examine subcortical contributions to this attention circuit and potential deficits in FEP. In addition, it is unclear if these deficits are specific to certain psychotic disorders such as schizophrenia-spectrum or if it is common to other disorders of psychosis. There were no significant differences between schizophrenia-spectrum and affective psychosis in the M100 modulation deficits, but the sample sizes are too small to rule out potential differences. Future studies with much larger samples can

more directly investigate this. In addition, it is unknown if the networks identified in this study are generalizable to other forms of auditory attention or specific to this relatively simple cross-modal task. Some of the regions identified as part of the networks appear to suggest specificity to the cross-modal aspect (e.g., visual regions), and it can be possible these regions would be less involved in a unimodal task, in which individuals select between different auditory streams. While the HCP multimodal parcellation offers significant improvement from other parcellations, the underlying assumption that correspondence between structural anatomy and functional topography is stable across individuals, which is not necessarily the case. Future work can investigate ways to account for individual differences and improve individual parcellations. Finally, it is unclear if these deficits are related to the transition to psychosis. This study was a cross-sectional design, and future studies investigating clinical high-risk patients can investigate the longitudinal trajectories of these deficits.

6.3 Further Considerations and Future Directions

6.3.1 Effective Connectivity

While networks were identified as being functionally connected and increased connectivity with attention with theta phase coherence, the direction of communication is unclear. The next analyses can directly investigate this directionality with methods such as Granger causality or phase-transfer entropy, which identify if the activity from one region can predict activity in another. The first analysis would be to disentangle the very fast temporal dynamics of communication likely occurring between A1, LBelt, and PBelt during the time-window of the

M100. With the M100 being relatively late in the processing stream of tones, it is likely there is both bottom-up and top-down communication occurring between these hierarchical auditory areas. Understanding the direction of communication during the M100 time window, how communication changes with attention modulation, and where specific impairments within this communication in FEP would be crucial information to understanding the local auditory deficits of the M100 in FEP. Understanding the local neurodynamics would also allow for pharmacologic interventions to target molecular aspects of the high-frequency communication.

Effective connectivity analyses would also identify the generators and direction of information flow of the theta oscillations in the larger networks. Within the identified networks, it is uncertain which area is responsible for generating the attention modulation signal. It could be speculated that frontal or prefrontal regions enhance communication to the precuneus with attention, which relays signals in the theta band to the network regions to modulate with attention. Alternatively, the precuneus itself could generate the signal changes with attention to send to other cortical regions. Identification of the effective connectivity path of the signal would aid in identification of areas to target with potential future treatments.

6.3.2 Treatments Impacting Cortical Oscillations

Future studies can also directly investigate treatments for improving attention deficits in early psychosis. Non-invasive brain stimulation techniques may be uniquely helpful for the oscillatory deficits identified in this study. Transcranial magnetic stimulation (TMS) and its repetitive form (rhythmic TMS) generate magnetic fields to induce electric currents in the cortex, which changes transmembrane potentials and can lead to the generation of action potentials. Transcranial direct current stimulation (tDCS) changes the resting potentials of cortical

populations, making it easier (or harder) for neurons to fire when engaged in a task of interest (Stagg & Nitsche, 2011). Several studies have identified the efficiency of these techniques for improving theta oscillatory activity and improving performance on cognitive tasks such as working memory and visual selective attention (Albouy, Weiss, Baillet, & Zatorre, 2017; Jones, Johnson, & Berryhill, 2020; McDermott et al., 2019).

Several considerations need to be taken when speculating about the optimal stimulation paradigm in this case. The first is the area to stimulate. The precuneus is a potential fruitful candidate, with its role in attention during the M100 time-window and its role as a hub for connectivity within the attention networks identified. It also may be an ideal target region because it contained a cluster of functional subregions identified with the HCP-MMP. Modern stimulation paradigms, while improving, produce diffuse effects that may impact cortex surrounding the target. Targeting the central precuneus region of the identified clusters in the left and right hemispheres may produce effects that effectively impact the entirety of the cluster. However, another consideration is that stimulation paradigms are typically most effective for regions near the surface of the scalp, with deeper brain regions difficult to effectively reach. The precuneus is located on the medial part of cortex and some parts are deeper within cortex, thus potentially limiting the impact of non-invasive stimulation. Prefrontal regions such as the dorsolateral prefrontal cortex are often areas of target with non-invasive brain stimulation, particularly in treatment of depression (Cash et al., 2021). The right dorsolateral prefrontal cortex may be a candidate target to engage the right hemisphere attention network. The left frontal pole may be a potential target for stimulation in the left hemisphere network, though caution would need to be taken in case it may stimulate facial muscles and be uncomfortable for individuals. Auditory areas may be considered for targets of stimulation; however, it can be speculated that the auditory areas are more downstream regions

of the activity directed from the precuneus and frontal regions, thus, potentially missing the opportunity to address the problem at the upstream targets of interest.

An additional consideration is the potential issue of undesired off-target effects. The precuneus has many functional roles in the brain, as it is part of the default mode network and several cognitive functions. TMS paradigms typically can either activate or inhibit (dependent on the stimulation paradigm) neuronal activity within a region to which it is applied. Transcranial direct current stimulation in contrast can increase the probability of neurons firing, they will likely only fire if actively engaged in a task (Thair, Holloway, Newport, & Smith, 2017). Thus, if the precuneus is the target of interest, it is likely that tDCS during an attention task may be the more efficacious route, as it would more selectively engage the attention modulation circuit, including the precuneus, and the tDCS treatment would make it easier for the precuneus neuronal populations to fire and thus improve oscillatory connectivity with other attention network regions.

Thus, it can be speculated that the optimal non-invasive stimulation paradigm would be tDCS of the precuneus during an auditory attention task. Previous paradigms have been successful in targeting the precuneus (Hebscher, Meltzer, & Gilboa, 2019; Mancini et al., 2017). However, if the precuneus is too challenging to effectively target, other network regions, such as frontal regions, may be potential targets. Future analysis can use the regions identified here as a guide for potential regions to stimulate and improve theta oscillatory activity with attention and ultimately improve attention performance.

6.3.3 White Matter Connectivity

In addition to gray matter deficits in psychosis, white matter abnormalities are also present in the disorder. In schizophrenia, there are whole brain deficits in fractional anisotropy (FA), a

measure of white matter integrity (Kanaan, Picchioni, McDonald, Shergill, & McGuire, 2017). The most frequent findings in chronic schizophrenia include decreased FA within PFC and temporal lobes and in fibers connecting them (uncinate fasciculus, arcuate fasciculus, and cingulum bundle). While white matter deficits appear to be more pronounced later in the disorder, some specific deficits are reported in early psychosis. In first episode psychosis, there are specific abnormalities in frontal, parietal, and temporal regions and in the fornix, transcollosal tracts, superior longitudinal fasciculus, and uncinate fasciculus (Fitzsimmons et al., 2014; Kubicki et al., 2007; Lei et al., 2015; Salisbury, Wang, Yeh, & Coffman, 2021; Sun et al., 2015; Whitford et al., 2007). Deficits in white matter tracts are associated with cognitive deficits, so future studies can investigate white matter structural integrity deficits and the relationship with attention modulation functional measures (Kochunov et al., 2017). Therefore, future studies can investigate white matter tract integrity between the cortical regions identified here as part of the auditory attention network.

6.3.4 Relevance for a Biomarker for Psychosis

In schizophrenia, there is a progressive gray matter loss associated with the course of the disorder, with temporal and frontal lobes particularly impacted early in the disorder (Cropley et al., 2017). This progressive decline begins in the prodrome, even before the onset of severe psychotic symptoms (Mechelli et al., 2011; Pantelis et al., 2003). The individuals in this study were within 2 months of their first clinical contact for psychosis, very early in the disorder. Thus, it can be speculated that the M100 modulation deficit with attention could be investigated in future studies as a potential biomarker for psychosis. In populations at clinical high risk for psychosis, only approximately thirty percent eventually experience a worsening of symptoms that develop into psychotic disorders (Seidman et al., 2010). Among those individuals, and even among

individuals with known psychosis, there is no biological test for the disorder. With a specific, objective measure of attention modulation (M100 modulation with attention) with functional deficiencies in psychosis, underlying oscillatory attention networks with functional deficits, and left hemisphere specific gray matter deficits, it is possible these particular measures could be uniquely sensitive to identifying individuals in the prodrome that may convert to psychosis. Early identification of individuals who will convert to psychosis would lead to earlier interventions that could blunt or perhaps even prevent severe psychotic symptoms. Future longitudinal analyses in individuals at high risk for psychosis can directly investigate these measures for use as a biomarker.

6.3.5 Mechanistic and Animal Model Relevance

The underlying mechanism of these deficits in early psychosis are unknown. Human postmortem analyses suggest reductions, not in the number of neurons, but in the somal size and number of dendritic spines (Selemon & Goldman-Rakic, 1999; Sweet et al., 2009). Interneuron groups also likely contribute to these deficits. An interneuron group expressing parvalbumin (PV) protein called PV basket cells are altered in schizophrenia and contribute to gamma oscillation dysfunction in schizophrenia. PV basket cells interact with pyramidal cells to produce gamma-band synchrony, as they allow rapid depolarization of pyramidal cells for faster firing rates. Dysfunction within these interneuron groups leads to a disruption of gamma signal (Lewis, Curley, Glausier, & Volk, 2012). In the current study, M100 modulation and theta rhythm connectivity within specific networks were impaired in psychosis. Theta rhythms are most related to interneurons expressing somatostatin (SST) and multipolar bursting-type interneurons (MB). Thus, perhaps these particular interneuron groups are dysfunctional in early psychosis. This work provides specific functional regions in auditory cortex and higher-order areas that can more readily

be translated to animal models for targeted study of the hypothesis that SST and MB interneurons within these specific auditory and network regions contribute to the M100 modulation and theta-connectivity changes with attention and are dysfunctional in early psychosis.

Animal models can also help elucidate where within the local circuit deficits arise. Since functions such as local phase-amplitude coupling appear to be intact in early psychosis, it can be speculated that the dysfunction could be from the incoming signal to the auditory cortical regions. Local mechanisms could allow for healthy phase-amplitude coupling, but the disrupted signal could lead to other local dysfunction in healthy sensory processing and modulation with attention., such as gamma power changes. With the specificity of the deficits provided by the use of the HCP-MMP, future collaborations could help investigate these specific cortical regions in animal models to elucidate these potential microcircuit dysfunctions.

6.4 Conclusion

Using state-of-the-art processing techniques and the novel HCP multimodal atlas, this work provides a novel understanding of the structural-functional relationships present in the early course of psychotic disorders. Specifically, it provides a novel understanding of the functional selective attention deficits in auditory cortex and network-wide circuitopathy in early psychosis. Specific auditory attention deficits in auditory cortex and in underlying attention networks that coincided with left hemisphere gray matter deficits in early psychosis were identified. The identification of these auditory cortex and network level deficits can guide future therapeutics that can be implemented early in the disorder and improve selective attention functioning for individuals with psychotic disorders.

Bibliography

Ahveninen, J., Jaaskelainen, I. P., Raij, T., Bonmassar, G., Devore, S., Hamalainen, M., . . . Belliveau, J. W. (2006). Task-modulated "what" and "where" pathways in human auditory cortex. Proc Natl Acad Sci U S A, 103(39), 14608-14613. doi:10.1073/pnas.0510480103

Albouy, P., Weiss, A., Baillet, S., & Zatorre, R. J. (2017). Selective Entrainment of Theta Oscillations in the Dorsal Stream Causally Enhances Auditory Working Memory Performance. Neuron, 94(1), 193-206 e195. doi:10.1016/j.neuron.2017.03.015

Alho, K. (1995). Cerebral generators of mismatch negativity (MMN) and its magnetic counterpart (MMNm) elicited by sound changes. Ear Hear, 16(1), 38-51. doi:10.1097/00003446-199502000-00004

Alho, K., Vorobyev, V. A., Medvedev, S. V., Pakhomov, S. V., Roudas, M. S., Tervaniemi, M., . . . Naatanen, R. (2003). Hemispheric lateralization of cerebral blood-flow changes during selective listening to dichotically presented continuous speech. Brain Res Cogn Brain Res, 17(2), 201-211. doi:10.1016/s0926-6410(03)00091-0

Alho, K., Vorobyev, V. A., Medvedev, S. V., Pakhomov, S. V., Starchenko, M. G., Tervaniemi, M., & Naatanen, R. (2006). Selective attention to human voice enhances brain activity bilaterally in the superior temporal sulcus. Brain Res, 1075(1), 142-150. doi:10.1016/j.brainres.2005.11.103

American Psychiatric, A., & American Psychiatric Association, D. S. M. T. F. (2013). Diagnostic and statistical manual of mental disorders : DSM-5 (5th ed.). Washington, D.C.: American Psychiatric Association.

Aminoff, E. M., Kveraga, K., & Bar, M. (2013). The role of the parahippocampal cortex in cognition. Trends Cogn Sci, 17(8), 379-390. doi:10.1016/j.tics.2013.06.009

Antoniades, M., Schoeler, T., Radua, J., Valli, I., Allen, P., Kempton, M. J., & McGuire, P. (2018). Verbal learning and hippocampal dysfunction in schizophrenia: A meta-analysis. Neurosci Biobehav Rev, 86, 166-175. doi:10.1016/j.neubiorev.2017.12.001

Arciniegas, D. B. (2015). Psychosis. Continuum (Minneap Minn), 21(3 Behavioral Neurology and Neuropsychiatry), 715-736. doi:10.1212/01.CON.0000466662.89908.e7

Ardila, A., Bernal, B., & Rosselli, M. (2016). How Localized are Language Brain Areas? A Review of Brodmann Areas Involvement in Oral Language. Arch Clin Neuropsychol, 31(1), 112-122. doi:10.1093/arclin/acv081

Asami, T., Bouix, S., Whitford, T. J., Shenton, M. E., Salisbury, D. F., & McCarley, R. W. (2012). Longitudinal loss of gray matter volume in patients with first-episode schizophrenia:

DARTEL automated analysis and ROI validation. Neuroimage, 59(2), 986-996. doi:10.1016/j.neuroimage.2011.08.066

Ashok, A. H., Baugh, J., & Yeragani, V. K. (2012). Paul Eugen Bleuler and the origin of the term schizophrenia (SCHIZOPRENIEGRUPPE). Indian J Psychiatry, 54(1), 95-96. doi:10.4103/0019-5545.94660

Baare, W. F., Hulshoff Pol, H. E., Hijman, R., Mali, W. P., Viergever, M. A., & Kahn, R. S. (1999). Volumetric analysis of frontal lobe regions in schizophrenia: relation to cognitive function and symptomatology. Biol Psychiatry, 45(12), 1597-1605. doi:10.1016/s0006-3223(98)00266-2

Bahramisharif, A., van Gerven, M. A., Aarnoutse, E. J., Mercier, M. R., Schwartz, T. H., Foxe, J. J., . . . Jensen, O. (2013). Propagating neocortical gamma bursts are coordinated by traveling alpha waves. J Neurosci, 33(48), 18849-18854. doi:10.1523/JNEUROSCI.2455-13.2013

Baker, C. M., Burks, J. D., Briggs, R. G., Conner, A. K., Glenn, C. A., Morgan, J. P., . . . Sughrue, M. E. (2018). A Connectomic Atlas of the Human Cerebrum-Chapter 2: The Lateral Frontal Lobe. Oper Neurosurg (Hagerstown), 15(suppl_1), S10-S74. doi:10.1093/ons/opy254

Baker, C. M., Burks, J. D., Briggs, R. G., Conner, A. K., Glenn, C. A., Robbins, J. M., . . . Sughrue, M. E. (2018). A Connectomic Atlas of the Human Cerebrum-Chapter 5: The Insula and Opercular Cortex. Oper Neurosurg (Hagerstown), 15(suppl_1), S175-S244. doi:10.1093/ons/opy259

Baker, C. M., Burks, J. D., Briggs, R. G., Milton, C. K., Conner, A. K., Glenn, C. A., . . . Sughrue, M. E. (2018). A Connectomic Atlas of the Human Cerebrum-Chapter 6: The Temporal Lobe. Oper Neurosurg (Hagerstown), 15(suppl_1), S245-S294. doi:10.1093/ons/opy260

Baker, C. M., Burks, J. D., Briggs, R. G., Stafford, J., Conner, A. K., Glenn, C. A., . . . Sughrue, M. E. (2018). A Connectomic Atlas of the Human Cerebrum-Chapter 9: The Occipital Lobe. Oper Neurosurg (Hagerstown), 15(suppl_1), S372-S406. doi:10.1093/ons/opy263

Barta, P. E., Pearlson, G. D., Powers, R. E., Richards, S. S., & Tune, L. E. (1990). Auditory hallucinations and smaller superior temporal gyral volume in schizophrenia. Am J Psychiatry, 147(11), 1457-1462. doi:10.1176/ajp.147.11.1457

Birur, B., Kraguljac, N. V., Shelton, R. C., & Lahti, A. C. (2017). Brain structure, function, and neurochemistry in schizophrenia and bipolar disorder-a systematic review of the magnetic resonance neuroimaging literature. NPJ Schizophr, 3, 15. doi:10.1038/s41537-017-0013-9

Blatow, M., Rozov, A., Katona, I., Hormuzdi, S. G., Meyer, A. H., Whittington, M. A., . . . Monyer, H. (2003). A novel network of multipolar bursting interneurons generates theta frequency oscillations in neocortex. Neuron, 38(5), 805-817. doi:10.1016/s0896-6273(03)00300-3

Bleuler, E. (1950). Dementia praecox; or, The group of schizophrenias. New York: International Universities Press.

Borgwardt, S. J., Riecher-Rossler, A., Dazzan, P., Chitnis, X., Aston, J., Drewe, M., . . . McGuire, P. K. (2007). Regional gray matter volume abnormalities in the at risk mental state. Biol Psychiatry, 61(10), 1148-1156. doi:10.1016/j.biopsych.2006.08.009

Brookes, M. J., Woolrich, M., Luckhoo, H., Price, D., Hale, J. R., Stephenson, M. C., . . . Morris, P. G. (2011). Investigating the electrophysiological basis of resting state networks using magnetoencephalography. Proc Natl Acad Sci U S A, 108(40), 16783-16788. doi:10.1073/pnas.1112685108

Buffalo, E. A., Fries, P., Landman, R., Buschman, T. J., & Desimone, R. (2011). Laminar differences in gamma and alpha coherence in the ventral stream. Proc Natl Acad Sci U S A, 108(27), 11262-11267. doi:10.1073/pnas.1011284108

Burgess, P. W., Veitch, E., de Lacy Costello, A., & Shallice, T. (2000). The cognitive and neuroanatomical correlates of multitasking. Neuropsychologia, 38(6), 848-863. doi:10.1016/s0028-3932(99)00134-7

Burton, H., Firszt, J. B., Holden, T., Agato, A., & Uchanski, R. M. (2012). Activation lateralization in human core, belt, and parabelt auditory fields with unilateral deafness compared to normal hearing. Brain Res, 1454, 33-47. doi:10.1016/j.brainres.2012.02.066

Cahn, W., Hulshoff Pol, H. E., Bongers, M., Schnack, H. G., Mandl, R. C., Van Haren, N. E., . . . Kahn, R. S. (2002). Brain morphology in antipsychotic-naive schizophrenia: a study of multiple brain structures. Br J Psychiatry Suppl, 43, s66-72. doi:10.1192/bjp.181.43.s66

Cannon, T. D., Chung, Y., He, G., Sun, D., Jacobson, A., van Erp, T. G., . . . Consortium, N. A. P. L. S. (2015). Progressive reduction in cortical thickness as psychosis develops: a multisite longitudinal neuroimaging study of youth at elevated clinical risk. Biol Psychiatry, 77(2), 147-157. doi:10.1016/j.biopsych.2014.05.023

Cash, R. F. H., Cocchi, L., Lv, J., Wu, Y., Fitzgerald, P. B., & Zalesky, A. (2021). Personalized connectivity-guided DLPFC-TMS for depression: Advancing computational feasibility, precision and reproducibility. Hum Brain Mapp, 42(13), 4155-4172. doi:10.1002/hbm.25330

Caspi, A., Reichenberg, A., Weiser, M., Rabinowitz, J., Kaplan, Z., Knobler, H., . . . Davidson, M. (2003). Cognitive performance in schizophrenia patients assessed before and following the first psychotic episode. Schizophr Res, 65(2-3), 87-94.

Cavanagh, J. F., & Frank, M. J. (2014). Frontal theta as a mechanism for cognitive control. Trends Cogn Sci, 18(8), 414-421. doi:10.1016/j.tics.2014.04.012

Cho, R. Y., Konecky, R. O., & Carter, C. S. (2006). Impairments in frontal cortical gamma synchrony and cognitive control in schizophrenia. Proc Natl Acad Sci U S A, 103(52), 19878-19883. doi:10.1073/pnas.0609440103

Cho, R. Y., Walker, C. P., Polizzotto, N. R., Wozny, T. A., Fissell, C., Chen, C. M., & Lewis, D. A. (2015). Development of sensory gamma oscillations and cross-frequency coupling from childhood to early adulthood. Cereb Cortex, 25(6), 1509-1518. doi:10.1093/cercor/bht341

Chung, Y., Allswede, D., Addington, J., Bearden, C. E., Cadenhead, K., Cornblatt, B., . . . Consortium, N. A. P. L. S. (2019). Cortical abnormalities in youth at clinical high-risk for psychosis: Findings from the NAPLS2 cohort. Neuroimage Clin, 23, 101862. doi:10.1016/j.nicl.2019.101862

Cloutier, M., Aigbogun, M. S., Guerin, A., Nitulescu, R., Ramanakumar, A. V., Kamat, S. A., . . . Wu, E. (2016). The Economic Burden of Schizophrenia in the United States in 2013. J Clin Psychiatry, 77(6), 764-771. doi:10.4088/JCP.15m10278

Coffman, B., & Salisbury, D. (2020). MEG Methods: A Primer of Basic MEG Analysis. In D. F. S. Brian A. Coffman (Ed.), Neuroimaging in Schizophrenia.

Cornblatt, B., Obuchowski, M., Roberts, S., Pollack, S., & Erlenmeyer-Kimling, L. (1999). Cognitive and behavioral precursors of schizophrenia. Dev Psychopathol, 11(3), 487-508.

Cornblatt, B. A., Lencz, T., Smith, C. W., Correll, C. U., Auther, A. M., & Nakayama, E. (2003). The schizophrenia prodrome revisited: a neurodevelopmental perspective. Schizophr Bull, 29(4), 633-651.

Crespo-Facorro, B., Roiz-Santianez, R., Perez-Iglesias, R., Rodriguez-Sanchez, J. M., Mata, I., Tordesillas-Gutierrez, D., . . . Vazquez-Barquero, J. L. (2011). Global and regional cortical thinning in first-episode psychosis patients: relationships with clinical and cognitive features. Psychol Med, 41(7), 1449-1460. doi:10.1017/S003329171000200X

Cropley, V. L., Klauser, P., Lenroot, R. K., Bruggemann, J., Sundram, S., Bousman, C., . . . Zalesky, A. (2017). Accelerated Gray and White Matter Deterioration With Age in Schizophrenia. Am J Psychiatry, 174(3), 286-295. doi:10.1176/appi.ajp.2016.16050610

Csepe, V. (1995). On the origin and development of the mismatch negativity. Ear Hear, 16(1), 91-104. doi:10.1097/00003446-199502000-00007

Ćurčić-Blake, B., Ford, J. M., Hubl, D., Orlov, N. D., Sommer, I. E., Waters, F., . . . Aleman, A. (2017). Interaction of language, auditory and memory brain networks in auditory verbal hallucinations. Prog Neurobiol, 148, 1-20. doi:10.1016/j.pneurobio.2016.11.002

Curtis, M. T., Coffman, B. A., & Salisbury, D. F. (2021a). Parahippocampal area three gray matter is reduced in first-episode schizophrenia spectrum: Discovery and replication samples. Hum Brain Mapp, 42(3), 724-736. doi:10.1002/hbm.25256

Curtis, M. T., Coffman, B. A., & Salisbury, D. F. (2021b). Pitch and Duration Mismatch Negativity are Associated With Distinct Auditory Cortex and Inferior Frontal Cortex Volumes in the First-Episode Schizophrenia Spectrum. Schizophr Bull Open, 2(1), sgab005. doi:10.1093/schizbullopen/sgab005

Dale, A. M., Fischl, B., & Sereno, M. I. (1999). Cortical surface-based analysis. I. Segmentation and surface reconstruction. Neuroimage, 9(2), 179-194. doi:10.1006/nimg.1998.0395

de Pasquale, F., Della Penna, S., Snyder, A. Z., Lewis, C., Mantini, D., Marzetti, L., . . . Corbetta, M. (2010). Temporal dynamics of spontaneous MEG activity in brain networks. Proc Natl Acad Sci U S A, 107(13), 6040-6045. doi:10.1073/pnas.0913863107

Degerman, A., Rinne, T., Salmi, J., Salonen, O., & Alho, K. (2006). Selective attention to sound location or pitch studied with fMRI. Brain Res, 1077(1), 123-134. doi:10.1016/j.brainres.2006.01.025

DeLisi, L. E., Sakuma, M., Tew, W., Kushner, M., Hoff, A. L., & Grimson, R. (1997). Schizophrenia as a chronic active brain process: a study of progressive brain structural change subsequent to the onset of schizophrenia. Psychiatry Res, 74(3), 129-140.

Delorme, A., & Makeig, S. (2004). EEGLAB: an open source toolbox for analysis of single-trial EEG dynamics including independent component analysis. J Neurosci Methods, 134(1), 9-21. doi:10.1016/j.jneumeth.2003.10.009

Diederen, K. M., Neggers, S. F., Daalman, K., Blom, J. D., Goekoop, R., Kahn, R. S., & Sommer, I. E. (2010). Deactivation of the parahippocampal gyrus preceding auditory hallucinations in schizophrenia. Am J Psychiatry, 167(4), 427-435. doi:10.1176/appi.ajp.2009.09040456

Dierks, T., Linden, D. E., Jandl, M., Formisano, E., Goebel, R., Lanfermann, H., & Singer, W. (1999). Activation of Heschl's gyrus during auditory hallucinations. Neuron, 22(3), 615-621.

Doesburg, S. M., Green, J. J., McDonald, J. J., & Ward, L. M. (2009). From local inhibition to long-range integration: a functional dissociation of alpha-band synchronization across cortical scales in visuospatial attention. Brain Res, 1303, 97-110. doi:10.1016/j.brainres.2009.09.069

Doesburg, S. M., Green, J. J., McDonald, J. J., & Ward, L. M. (2012). Theta modulation of inter-regional gamma synchronization during auditory attention control. Brain Res, 1431, 77-85. doi:10.1016/j.brainres.2011.11.005

Donde, C., Martinez, A., Kantrowitz, J. T., Silipo, G., Dias, E. C., Patel, G. H., . . . Javitt, D. C. (2019). Bimodal distribution of tone-matching deficits indicates discrete pathophysiological entities within the syndrome of schizophrenia. Transl Psychiatry, 9(1), 221. doi:10.1038/s41398-019-0557-8

Dosenbach, N. U., Fair, D. A., Cohen, A. L., Schlaggar, B. L., & Petersen, S. E. (2008). A dual-networks architecture of top-down control. Trends Cogn Sci, 12(3), 99-105. doi:10.1016/j.tics.2008.01.001

Dreher, J. C., Koechlin, E., Tierney, M., & Grafman, J. (2008). Damage to the fronto-polar cortex is associated with impaired multitasking. PLoS One, 3(9), e3227. doi:10.1371/journal.pone.0003227

Eack, S. M., Hogarty, G. E., Cho, R. Y., Prasad, K. M., Greenwald, D. P., Hogarty, S. S., & Keshavan, M. S. (2010). Neuroprotective effects of cognitive enhancement therapy against gray matter loss in early schizophrenia: results from a 2-year randomized controlled trial. Arch Gen Psychiatry, 67(7), 674-682. doi:10.1001/archgenpsychiatry.2010.63

Ehrlich, S., Brauns, S., Yendiki, A., Ho, B. C., Calhoun, V., Schulz, S. C., . . . Sponheim, S. R. (2012). Associations of cortical thickness and cognition in patients with schizophrenia and healthy controls. Schizophr Bull, 38(5), 1050-1062. doi:10.1093/schbul/sbr018

Elgueda, D., Duque, D., Radtke-Schuller, S., Yin, P., David, S. V., Shamma, S. A., & Fritz, J. B. (2019). State-dependent encoding of sound and behavioral meaning in a tertiary region of the ferret auditory cortex. Nat Neurosci, 22(3), 447-459. doi:10.1038/s41593-018-0317-8

Ellison-Wright, I., Glahn, D. C., Laird, A. R., Thelen, S. M., & Bullmore, E. (2008). The anatomy of first-episode and chronic schizophrenia: an anatomical likelihood estimation meta-analysis. Am J Psychiatry, 165(8), 1015-1023. doi:10.1176/appi.ajp.2008.07101562

Epstein, J., Stern, E., & Silbersweig, D. (1999). Mesolimbic activity associated with psychosis in schizophrenia. Symptom-specific PET studies. Ann N Y Acad Sci, 877, 562-574. doi:10.1111/j.1749-6632.1999.tb09289.x

Erickson, M. A., Ruffle, A., & Gold, J. M. (2016). A Meta-Analysis of Mismatch Negativity in Schizophrenia: From Clinical Risk to Disease Specificity and Progression. Biol Psychiatry, 79(12), 980-987. doi:10.1016/j.biopsych.2015.08.025

Escartí, M. J., de la Iglesia-Vayá, M., Martí-Bonmatí, L., Robles, M., Carbonell, J., Lull, J. J., . . . Sanjuán, J. (2010). Increased amygdala and parahippocampal gyrus activation in schizophrenic patients with auditory hallucinations: an fMRI study using independent component analysis. Schizophr Res, 117(1), 31-41. doi:10.1016/j.schres.2009.12.028

Fett, A. K., Viechtbauer, W., Dominguez, M. D., Penn, D. L., van Os, J., & Krabbendam, L. (2011). The relationship between neurocognition and social cognition with functional outcomes in schizophrenia: a meta-analysis. Neurosci Biobehav Rev, 35(3), 573-588. doi:10.1016/j.neubiorev.2010.07.001

Fiebelkorn, I. C., & Kastner, S. (2020). Functional Specialization in the Attention Network. Annu Rev Psychol, 71, 221-249. doi:10.1146/annurev-psych-010418-103429

First, M. B., Spitzer, R. L., Gibbon, M., & Williams, J. (1997). Structured Clinical Interview for DSM-IV Axis I Disorders. Biometrics Research Department.

Fischl, B., & Dale, A. M. (2000). Measuring the thickness of the human cerebral cortex from magnetic resonance images. Proc Natl Acad Sci U S A, 97(20), 11050-11055. doi:10.1073/pnas.200033797

Fischl, B., Sereno, M. I., & Dale, A. M. (1999). Cortical surface-based analysis. II: Inflation, flattening, and a surface-based coordinate system. Neuroimage, 9(2), 195-207. doi:10.1006/nimg.1998.0396

Fitzsimmons, J., Hamoda, H. M., Swisher, T., Terry, D., Rosenberger, G., Seidman, L. J., . . . Kubicki, M. (2014). Diffusion tensor imaging study of the fornix in first episode schizophrenia and in healthy controls. Schizophr Res, 156(2-3), 157-160. doi:10.1016/j.schres.2014.04.022

Fortea, A., Batalla, A., Radua, J., van Eijndhoven, P., Baeza, I., Albajes-Eizagirre, A., . . . Sugranyes, G. (2021). Cortical gray matter reduction precedes transition to psychosis in individuals at clinical high-risk for psychosis: A voxel-based meta-analysis. Schizophr Res, 232, 98-106. doi:10.1016/j.schres.2021.05.008

Foxe, J. J., Simpson, G. V., & Ahlfors, S. P. (1998). Parieto-occipital approximately 10 Hz activity reflects anticipatory state of visual attention mechanisms. Neuroreport, 9(17), 3929-3933. doi:10.1097/00001756-199812010-00030

Foxe, J. J., & Snyder, A. C. (2011). The Role of Alpha-Band Brain Oscillations as a Sensory Suppression Mechanism during Selective Attention. Front Psychol, 2, 154. doi:10.3389/fpsyg.2011.00154

Foxe, J. J., Yeap, S., Snyder, A. C., Kelly, S. P., Thakore, J. H., & Molholm, S. (2011). The N1 auditory evoked potential component as an endophenotype for schizophrenia: high-density electrical mapping in clinically unaffected first-degree relatives, first-episode, and chronic schizophrenia patients. Eur Arch Psychiatry Clin Neurosci, 261(5), 331-339. doi:10.1007/s00406-010-0176-0

Fries, P. (2005). A mechanism for cognitive dynamics: neuronal communication through neuronal coherence. Trends Cogn Sci, 9(10), 474-480. doi:10.1016/j.tics.2005.08.011

Frith, C. D., Friston, K. J., Liddle, P. F., & Frackowiak, R. S. (1991). A PET study of word finding. Neuropsychologia, 29(12), 1137-1148.

Fritz, J., Shamma, S., Elhilali, M., & Klein, D. (2003). Rapid task-related plasticity of spectrotemporal receptive fields in primary auditory cortex. Nat Neurosci, 6(11), 1216-1223. doi:10.1038/nn1141

Frodl-Bauch, T., Kathmann, N., Moller, H. J., & Hegerl, U. (1997). Dipole localization and test-retest reliability of frequency and duration mismatch negativity generator processes. Brain Topogr, 10(1), 3-8. doi:10.1023/a:1022214905452

Fu, K. M., Foxe, J. J., Murray, M. M., Higgins, B. A., Javitt, D. C., & Schroeder, C. E. (2001). Attention-dependent suppression of distracter visual input can be cross-modally cued as indexed by anticipatory parieto-occipital alpha-band oscillations. Brain Res Cogn Brain Res, 12(1), 145-152. doi:10.1016/s0926-6410(01)00034-9

Gaebler, A. J., Zweerings, J., Koten, J. W., Konig, A. A., Turetsky, B. I., Zvyagintsev, M., & Mathiak, K. (2020). Impaired Subcortical Detection of Auditory Changes in Schizophrenia but Not in Major Depression. Schizophr Bull, 46(1), 193-201. doi:10.1093/schbul/sbz027

Garrido, M. I., Friston, K. J., Kiebel, S. J., Stephan, K. E., Baldeweg, T., & Kilner, J. M. (2008). The functional anatomy of the MMN: a DCM study of the roving paradigm. Neuroimage, 42(2), 936-944. doi:10.1016/j.neuroimage.2008.05.018

Garrido, M. I., Kilner, J. M., Kiebel, S. J., & Friston, K. J. (2009). Dynamic causal modeling of the response to frequency deviants. J Neurophysiol, 101(5), 2620-2631. doi:10.1152/jn.90291.2008

Giard, M. H., Lavikahen, J., Reinikainen, K., Perrin, F., Bertrand, O., Pernier, J., & Naatanen, R. (1995). Separate representation of stimulus frequency, intensity, and duration in auditory sensory memory: an event-related potential and dipole-model analysis. J Cogn Neurosci, 7(2), 133-143. doi:10.1162/jocn.1995.7.2.133

Giard, M. H., Perrin, F., Pernier, J., & Bouchet, P. (1990). Brain generators implicated in the processing of auditory stimulus deviance: a topographic event-related potential study. Psychophysiology, 27(6), 627-640. doi:10.1111/j.1469-8986.1990.tb03184.x

Glasser, M. F., Coalson, T. S., Robinson, E. C., Hacker, C. D., Harwell, J., Yacoub, E., . . . Van Essen, D. C. (2016). A multi-modal parcellation of human cerebral cortex. Nature, 536(7615), 171-178. doi:10.1038/nature18933

Glasser, M. F., Goyal, M. S., Preuss, T. M., Raichle, M. E., & Van Essen, D. C. (2014). Trends and properties of human cerebral cortex: correlations with cortical myelin content. Neuroimage, 93 Pt 2, 165-175. doi:10.1016/j.neuroimage.2013.03.060

Glasser, M. F., Sotiropoulos, S. N., Wilson, J. A., Coalson, T. S., Fischl, B., Andersson, J. L., . . . Consortium, W. U. M. H. C. P. (2013). The minimal preprocessing pipelines for the Human Connectome Project. Neuroimage, 80, 105-124. doi:10.1016/j.neuroimage.2013.04.127

Goldman, A. L., Pezawas, L., Mattay, V. S., Fischl, B., Verchinski, B. A., Chen, Q., . . . Meyer-Lindenberg, A. (2009). Widespread reductions of cortical thickness in schizophrenia and spectrum disorders and evidence of heritability. Arch Gen Psychiatry, 66(5), 467-477. doi:10.1001/archgenpsychiatry.2009.24

Gomez-Ramirez, M., Kelly, S. P., Molholm, S., Sehatpour, P., Schwartz, T. H., & Foxe, J. J. (2011). Oscillatory sensory selection mechanisms during intersensory attention to rhythmic auditory and visual inputs: a human electrocorticographic investigation. J Neurosci, 31(50), 18556-18567. doi:10.1523/JNEUROSCI.2164-11.2011

Gonzalez-Burgos, G., Cho, R. Y., & Lewis, D. A. (2015). Alterations in cortical network oscillations and parvalbumin neurons in schizophrenia. Biol Psychiatry, 77(12), 1031-1040. doi:10.1016/j.biopsych.2015.03.010

Gooch, C. M., Wiener, M., Hamilton, A. C., & Coslett, H. B. (2011). Temporal discrimination of sub- and suprasecond time intervals: a voxel-based lesion mapping analysis. Front Integr Neurosci, 5, 59. doi:10.3389/fnint.2011.00059

Grady, C. L., Van Meter, J. W., Maisog, J. M., Pietrini, P., Krasuski, J., & Rauschecker, J. P. (1997). Attention-related modulation of activity in primary and secondary auditory cortex. Neuroreport, 8(11), 2511-2516. doi:10.1097/00001756-199707280-00019

Green, M. F., & Nuechterlein, K. H. (1999). Should schizophrenia be treated as a neurocognitive disorder? Schizophr Bull, 25(2), 309-319. doi:10.1093/oxfordjournals.schbul.a033380

Gregoriou, G. G., Gotts, S. J., & Desimone, R. (2012). Cell-type-specific synchronization of neural activity in FEF with V4 during attention. Neuron, 73(3), 581-594. doi:10.1016/j.neuron.2011.12.019

Gregoriou, G. G., Gotts, S. J., Zhou, H., & Desimone, R. (2009). High-frequency, long-range coupling between prefrontal and visual cortex during attention. Science, 324(5931), 1207-1210. doi:10.1126/science.1171402

Greve, D. N., & Fischl, B. (2009). Accurate and robust brain image alignment using boundary-based registration. Neuroimage, 48(1), 63-72. doi:10.1016/j.neuroimage.2009.06.060

Griffanti, L., Salimi-Khorshidi, G., Beckmann, C. F., Auerbach, E. J., Douaud, G., Sexton, C. E., . . . Smith, S. M. (2014). ICA-based artefact removal and accelerated fMRI acquisition for improved resting state network imaging. Neuroimage, 95, 232-247. doi:10.1016/j.neuroimage.2014.03.034

Gruber, T., Muller, M. M., Keil, A., & Elbert, T. (1999). Selective visual-spatial attention alters induced gamma band responses in the human EEG. Clin Neurophysiol, 110(12), 2074-2085. doi:10.1016/s1388-2457(99)00176-5

Guimond, S., Chakravarty, M. M., Bergeron-Gagnon, L., Patel, R., & Lepage, M. (2016). Verbal memory impairments in schizophrenia associated with cortical thinning. Neuroimage Clin, 11, 20-29. doi:10.1016/j.nicl.2015.12.010

Gupta, T., Kelley, N. J., Pelletier-Baldelli, A., & Mittal, V. A. (2018). Transcranial Direct Current Stimulation, Symptomatology, and Cognition in Psychosis: A Qualitative Review. Front Behav Neurosci, 12, 94. doi:10.3389/fnbeh.2018.00094

Gur, R. E., Maany, V., Mozley, P. D., Swanson, C., Bilker, W., & Gur, R. C. (1998). Subcortical MRI volumes in neuroleptic-naive and treated patients with schizophrenia. Am J Psychiatry, 155(12), 1711-1717. doi:10.1176/ajp.155.12.1711

Haigh, S. M., Coffman, B. A., & Salisbury, D. F. (2017). Mismatch Negativity in First-Episode Schizophrenia: A Meta-Analysis. Clin EEG Neurosci, 48(1), 3-10. doi:10.1177/1550059416645980

Haijma, S. V., Van Haren, N., Cahn, W., Koolschijn, P. C., Hulshoff Pol, H. E., & Kahn, R. S. (2013). Brain volumes in schizophrenia: a meta-analysis in over 18 000 subjects. Schizophr Bull, 39(5), 1129-1138. doi:10.1093/schbul/sbs118

Hari, R., Hamalainen, M., Ilmoniemi, R., Kaukoranta, E., Reinikainen, K., Salminen, J., . . . Sams, M. (1984). Responses of the primary auditory cortex to pitch changes in a sequence of tone pips: neuromagnetic recordings in man. Neurosci Lett, 50(1-3), 127-132. doi:10.1016/0304-3940(84)90474-9

Hari, R., Rif, J., Tiihonen, J., & Sams, M. (1992). Neuromagnetic mismatch fields to single and paired tones. Electroencephalogr Clin Neurophysiol, 82(2), 152-154. doi:10.1016/0013-4694(92)90159-f

Harrington, D. L., Haaland, K. Y., & Knight, R. T. (1998). Cortical networks underlying mechanisms of time perception. J Neurosci, 18(3), 1085-1095.

Hartwigsen, G., Neef, N. E., Camilleri, J. A., Margulies, D. S., & Eickhoff, S. B. (2019). Functional Segregation of the Right Inferior Frontal Gyrus: Evidence From Coactivation-Based Parcellation. Cereb Cortex, 29(4), 1532-1546. doi:10.1093/cercor/bhy049

Hebscher, M., Meltzer, J. A., & Gilboa, A. (2019). A causal role for the precuneus in network-wide theta and gamma oscillatory activity during complex memory retrieval. Elife, 8. doi:10.7554/eLife.43114

Hirano, S., Nakhnikian, A., Hirano, Y., Oribe, N., Kanba, S., Onitsuka, T., . . . Spencer, K. M. (2018). Phase-Amplitude Coupling of the Electroencephalogram in the Auditory Cortex in Schizophrenia. Biol Psychiatry Cogn Neurosci Neuroimaging, 3(1), 69-76. doi:10.1016/j.bpsc.2017.09.001

Hirayasu, Y., McCarley, R. W., Salisbury, D. F., Tanaka, S., Kwon, J. S., Frumin, M., . . . Shenton, M. E. (2000). Planum temporale and Heschl gyrus volume reduction in schizophrenia: a magnetic resonance imaging study of first-episode patients. Arch Gen Psychiatry, 57(7), 692-699.

Hirayasu, Y., Shenton, M. E., Salisbury, D. F., Dickey, C. C., Fischer, I. A., Mazzoni, P., . . . McCarley, R. W. (1998). Lower left temporal lobe MRI volumes in patients with first-episode schizophrenia compared with psychotic patients with first-episode affective disorder and normal subjects. Am J Psychiatry, 155(10), 1384-1391. doi:10.1176/ajp.155.10.1384

Hirayasu, Y., Shenton, M. E., Salisbury, D. F., & McCarley, R. W. (2000). Hippocampal and superior temporal gyrus volume in first-episode schizophrenia. Arch Gen Psychiatry, 57(6), 618-619. doi:10.1001/archpsyc.57.6.618

Hirayasu, Y., Tanaka, S., Shenton, M. E., Salisbury, D. F., DeSantis, M. A., Levitt, J. J., . . . McCarley, R. W. (2001). Prefrontal gray matter volume reduction in first episode schizophrenia. Cereb Cortex, 11(4), 374-381. doi:10.1093/cercor/11.4.374

Hjorthoj, C., Sturup, A. E., McGrath, J. J., & Nordentoft, M. (2017). Years of potential life lost and life expectancy in schizophrenia: a systematic review and meta-analysis. Lancet Psychiatry, 4(4), 295-301. doi:10.1016/S2215-0366(17)30078-0

Hocherman, S., Benson, D. A., Goldstein, M. H., Jr., Heffner, H. E., & Hienz, R. D. (1976). Evoked unit activity in auditory cortex of monkeys performing a selective attention task. Brain Res, 117(1), 51-68. doi:10.1016/0006-8993(76)90555-2

Hoff, A. L., Sakuma, M., Wieneke, M., Horon, R., Kushner, M., & DeLisi, L. E. (1999). Longitudinal neuropsychological follow-up study of patients with first-episode schizophrenia. Am J Psychiatry, 156(9), 1336-1341. doi:10.1176/ajp.156.9.1336

Hoffman, R. E. (1986). Verbal hallucinations and language production processes in schizophrenia. Behavioral and Brain Sciences, 9(3), 503-517. doi:10.1017/S0140525X00046781

Hopfinger, J. B., Buonocore, M. H., & Mangun, G. R. (2000). The neural mechanisms of top-down attentional control. Nat Neurosci, 3(3), 284-291. doi:10.1038/72999

Hurlemann, R., Jessen, F., Wagner, M., Frommann, I., Ruhrmann, S., Brockhaus, A., . . . Maier, W. (2008). Interrelated neuropsychological and anatomical evidence of hippocampal pathology in the at-risk mental state. Psychol Med, 38(6), 843-851. doi:10.1017/S0033291708003279

Jancke, L., Mirzazade, S., & Shah, N. J. (1999). Attention modulates activity in the primary and the secondary auditory cortex: a functional magnetic resonance imaging study in human subjects. Neurosci Lett, 266(2), 125-128. doi:10.1016/s0304-3940(99)00288-8

Jardri, R., Pouchet, A., Pins, D., & Thomas, P. (2011). Cortical activations during auditory verbal hallucinations in schizophrenia: a coordinate-based meta-analysis. Am J Psychiatry, 168(1), 73-81. doi:10.1176/appi.ajp.2010.09101522

Javitt, D. C., Steinschneider, M., Schroeder, C. E., Vaughan, H. G., Jr., & Arezzo, J. C. (1994). Detection of stimulus deviance within primate primary auditory cortex: intracortical mechanisms of mismatch negativity (MMN) generation. Brain Res, 667(2), 192-200. doi:10.1016/0006-8993(94)91496-6

Javitt, D. C., & Sweet, R. A. (2015). Auditory dysfunction in schizophrenia: integrating clinical and basic features. Nat Rev Neurosci, 16(9), 535-550. doi:10.1038/nrn4002

Jervis, B. W., Nichols, M. J., Johnson, T. E., Allen, E., & Hudson, N. R. (1983). A fundamental investigation of the composition of auditory evoked potentials. IEEE Trans Biomed Eng, 30(1), 43-50. doi:10.1109/tbme.1983.325165

Job, D. E., Whalley, H. C., Johnstone, E. C., & Lawrie, S. M. (2005). Grey matter changes over time in high risk subjects developing schizophrenia. Neuroimage, 25(4), 1023-1030. doi:10.1016/j.neuroimage.2005.01.006

Jones, K. T., Johnson, E. L., & Berryhill, M. E. (2020). Frontoparietal theta-gamma interactions track working memory enhancement with training and tDCS. Neuroimage, 211, 116615. doi:10.1016/j.neuroimage.2020.116615

Jung, W. H., Kim, J. S., Jang, J. H., Choi, J. S., Jung, M. H., Park, J. Y., . . . Kwon, J. S. (2011). Cortical thickness reduction in individuals at ultra-high-risk for psychosis. Schizophr Bull, 37(4), 839-849. doi:10.1093/schbul/sbp151

Kanaan, R. A., Picchioni, M. M., McDonald, C., Shergill, S. S., & McGuire, P. K. (2017). White matter deficits in schizophrenia are global and don't progress with age. Aust N Z J Psychiatry, 51(10), 1020-1031. doi:10.1177/0004867417700729

Kane, J. M. (2012). Addressing nonresponse in schizophrenia. J Clin Psychiatry, 73(2), e07. doi:10.4088/JCP.11076tx2c

Kane, J. M., Robinson, D. G., Schooler, N. R., Mueser, K. T., Penn, D. L., Rosenheck, R. A., . . . Heinssen, R. K. (2016). Comprehensive Versus Usual Community Care for First-Episode Psychosis: 2-Year Outcomes From the NIMH RAISE Early Treatment Program. Am J Psychiatry, 173(4), 362-372. doi:10.1176/appi.ajp.2015.15050632

Karten, A., Pantazatos, S. P., Khalil, D., Zhang, X., & Hirsch, J. (2013). Dynamic coupling between the lateral occipital-cortex, default-mode, and frontoparietal networks during bistable perception. Brain Connect, 3(3), 286-293. doi:10.1089/brain.2012.0119

Kasai, K., Nakagome, K., Itoh, K., Koshida, I., Hata, A., Iwanami, A., . . . Kato, N. (1999). Multiple generators in the auditory automatic discrimination process in humans. Neuroreport, 10(11), 2267-2271. doi:10.1097/00001756-199908020-00008

Kasai, K., Shenton, M. E., Salisbury, D. F., Hirayasu, Y., Lee, C. U., Ciszewski, A. A., . . . McCarley, R. W. (2003). Progressive decrease of left superior temporal gyrus gray matter volume in patients with first-episode schizophrenia. Am J Psychiatry, 160(1), 156-164. doi:10.1176/appi.ajp.160.1.156

Kasai, K., Shenton, M. E., Salisbury, D. F., Hirayasu, Y., Onitsuka, T., Spencer, M. H., . . . McCarley, R. W. (2003). Progressive decrease of left Heschl gyrus and planum temporale gray matter volume in first-episode schizophrenia: a longitudinal magnetic resonance imaging study. Arch Gen Psychiatry, 60(8), 766-775. doi:10.1001/archpsyc.60.8.766

Kastner, S., Pinsk, M. A., De Weerd, P., Desimone, R., & Ungerleider, L. G. (1999). Increased activity in human visual cortex during directed attention in the absence of visual stimulation. Neuron, 22(4), 751-761. doi:10.1016/s0896-6273(00)80734-5

Kay, S. R., Fiszbein, A., & Opler, L. A. (1987). The positive and negative syndrome scale (PANSS) for schizophrenia. Schizophr Bull, 13(2), 261-276. doi:10.1093/schbul/13.2.261

Keller, A. S., Payne, L., & Sekuler, R. (2017). Characterizing the roles of alpha and theta oscillations in multisensory attention. Neuropsychologia, 99, 48-63. doi:10.1016/j.neuropsychologia.2017.02.021

Kennedy, N. I., Lee, W. H., & Frangou, S. (2018). Efficacy of non-invasive brain stimulation on the symptom dimensions of schizophrenia: A meta-analysis of randomized controlled trials. Eur Psychiatry, 49, 69-77. doi:10.1016/j.eurpsy.2017.12.025

Keshavan, M. S., Haas, G. L., Kahn, C. E., Aguilar, E., Dick, E. L., Schooler, N. R., . . . Pettegrew, J. W. (1998). Superior temporal gyrus and the course of early schizophrenia: progressive, static, or reversible? J Psychiatr Res, 32(3-4), 161-167.

Kirihara, K., Rissling, A. J., Swerdlow, N. R., Braff, D. L., & Light, G. A. (2012). Hierarchical organization of gamma and theta oscillatory dynamics in schizophrenia. Biol Psychiatry, 71(10), 873-880. doi:10.1016/j.biopsych.2012.01.016

Klausberger, T., & Somogyi, P. (2008). Neuronal diversity and temporal dynamics: the unity of hippocampal circuit operations. Science, 321(5885), 53-57. doi:10.1126/science.1149381

Klimesch, W., Sauseng, P., & Hanslmayr, S. (2007). EEG alpha oscillations: the inhibition-timing hypothesis. Brain Res Rev, 53(1), 63-88. doi:10.1016/j.brainresrev.2006.06.003

Kochunov, P., Coyle, T. R., Rowland, L. M., Jahanshad, N., Thompson, P. M., Kelly, S., . . . Hong, L. E. (2017). Association of White Matter With Core Cognitive Deficits in Patients With Schizophrenia. JAMA Psychiatry, 74(9), 958-966. doi:10.1001/jamapsychiatry.2017.2228

Koh, Y., Shin, K. S., Kim, J. S., Choi, J. S., Kang, D. H., Jang, J. H., . . . Kwon, J. S. (2011). An MEG study of alpha modulation in patients with schizophrenia and in subjects at high risk of developing psychosis. Schizophr Res, 126(1-3), 36-42. doi:10.1016/j.schres.2010.10.001

Kong, L., Michalka, S. W., Rosen, M. L., Sheremata, S. L., Swisher, J. D., Shinn-Cunningham, B. G., & Somers, D. C. (2014). Auditory spatial attention representations in the human cerebral cortex. Cereb Cortex, 24(3), 773-784. doi:10.1093/cercor/bhs359

Kraepelin, E. (1889). Psychiatrie: ein lehrbuch für studirende und aerzte (3rd ed): Leipzig, Abel.

Kropotov, J. D., Naatnen, R., Sevostianov, A. V., Alho, K., Reinikainen, K., & Kropotova, O. V. (1995). Mismatch negativity to auditory stimulus change recorded directly from the human temporal cortex. Psychophysiology, 32(4), 418-422. doi:10.1111/j.1469-8986.1995.tb01226.x

Krumbholz, K., Nobis, E. A., Weatheritt, R. J., & Fink, G. R. (2009). Executive control of spatial attention shifts in the auditory compared to the visual modality. Hum Brain Mapp, 30(5), 1457-1469. doi:10.1002/hbm.20615

Kubicki, M., McCarley, R., Westin, C. F., Park, H. J., Maier, S., Kikinis, R., . . . Shenton, M. E. (2007). A review of diffusion tensor imaging studies in schizophrenia. J Psychiatr Res, 41(1-2), 15-30. doi:10.1016/j.jpsychires.2005.05.005

Kusmierek, P., & Rauschecker, J. P. (2009). Functional specialization of medial auditory belt cortex in the alert rhesus monkey. J Neurophysiol, 102(3), 1606-1622. doi:10.1152/jn.00167.2009

Lachaux, J. P., Rodriguez, E., Martinerie, J., & Varela, F. J. (1999). Measuring phase synchrony in brain signals. Hum Brain Mapp, 8(4), 194-208. doi:10.1002/(sici)1097-0193(1999)8:4<194::aid-hbm4>3.0.co;2-c

Lahti, A. C., Weiler, M. A., Holcomb, H. H., Tamminga, C. A., Carpenter, W. T., & McMahon, R. (2006). Correlations between rCBF and symptoms in two independent cohorts of drug-free patients with schizophrenia. Neuropsychopharmacology, 31(1), 221-230. doi:10.1038/sj.npp.1300837

Lai, V. T., van Dam, W., Conant, L. L., Binder, J. R., & Desai, R. H. (2015). Familiarity differentially affects right hemisphere contributions to processing metaphors and literals. Front Hum Neurosci, 9, 44. doi:10.3389/fnhum.2015.00044

Lakatos, P., Schroeder, C. E., Leitman, D. I., & Javitt, D. C. (2013). Predictive suppression of cortical excitability and its deficit in schizophrenia. J Neurosci, 33(28), 11692-11702. doi:10.1523/JNEUROSCI.0010-13.2013

Lakatos, P., Shah, A. S., Knuth, K. H., Ulbert, I., Karmos, G., & Schroeder, C. E. (2005). An oscillatory hierarchy controlling neuronal excitability and stimulus processing in the auditory cortex. J Neurophysiol, 94(3), 1904-1911. doi:10.1152/jn.00263.2005

Lee, C. U., Shenton, M. E., Salisbury, D. F., Kasai, K., Onitsuka, T., Dickey, C. C., . . . McCarley, R. W. (2002). Fusiform gyrus volume reduction in first-episode schizophrenia: a magnetic resonance imaging study. Arch Gen Psychiatry, 59(9), 775-781.

Lee, K., & Choo, H. (2013). A critical review of selective attention: an interdisciplinary perspective. Artificial Intelligence Review, 40(1), 27-50. doi:10.1007/s10462-011-9278-y

Lee, M., Sehatpour, P., Hoptman, M. J., Lakatos, P., Dias, E. C., Kantrowitz, J. T., . . . Javitt, D. C. (2017). Neural mechanisms of mismatch negativity dysfunction in schizophrenia. Mol Psychiatry, 22(11), 1585-1593. doi:10.1038/mp.2017.3

Lei, W., Li, N., Deng, W., Li, M., Huang, C., Ma, X., . . . Li, T. (2015). White matter alterations in first episode treatment-naïve patients with deficit schizophrenia: a combined VBM and DTI study. Sci Rep, 5, 12994. doi:10.1038/srep12994

Levanen, S., Ahonen, A., Hari, R., McEvoy, L., & Sams, M. (1996). Deviant auditory stimuli activate human left and right auditory cortex differently. Cereb Cortex, 6(2), 288-296. doi:10.1093/cercor/6.2.288

Lewis, D. A., Curley, A. A., Glausier, J. R., & Volk, D. W. (2012). Cortical parvalbumin interneurons and cognitive dysfunction in schizophrenia. Trends Neurosci, 35(1), 57-67. doi:10.1016/j.tins.2011.10.004

Lewis, D. A., & Sweet, R. A. (2009). Schizophrenia from a neural circuitry perspective: advancing toward rational pharmacological therapies. J Clin Invest, 119(4), 706-716. doi:10.1172/JCI37335

Lieder, F., Stephan, K. E., Daunizeau, J., Garrido, M. I., & Friston, K. J. (2013). A neurocomputational model of the mismatch negativity. PLoS Comput Biol, 9(11), e1003288. doi:10.1371/journal.pcbi.1003288

Light, G. A., & Naatanen, R. (2013). Mismatch negativity is a breakthrough biomarker for understanding and treating psychotic disorders. Proc Natl Acad Sci U S A, 110(38), 15175-15176. doi:10.1073/pnas.1313287110

Lipska, B. K., Jaskiw, G. E., & Weinberger, D. R. (1993). Postpubertal emergence of hyperresponsiveness to stress and to amphetamine after neonatal excitotoxic hippocampal damage: a potential animal model of schizophrenia. Neuropsychopharmacology, 9(1), 67-75. doi:10.1038/npp.1993.44

Lipska, B. K., & Weinberger, D. R. (2002). A neurodevelopmental model of schizophrenia: neonatal disconnection of the hippocampus. Neurotox Res, 4(5-6), 469-475. doi:10.1080/1029842021000022089

Lizarazu, M., Lallier, M., & Molinaro, N. (2019). Phase-amplitude coupling between theta and gamma oscillations adapts to speech rate. Ann N Y Acad Sci, 1453(1), 140-152. doi:10.1111/nyas.14099

Lloyd, S. (1982). Least squares quantization in PCM. IEEE Transactions on Information Theory, 28(2), 129-137. doi:10.1109/TIT.1982.1056489

Lobier, M., Palva, J. M., & Palva, S. (2018). High-alpha band synchronization across frontal, parietal and visual cortex mediates behavioral and neuronal effects of visuospatial attention. Neuroimage, 165, 222-237. doi:10.1016/j.neuroimage.2017.10.044

Luck, S. J., Chelazzi, L., Hillyard, S. A., & Desimone, R. (1997). Neural mechanisms of spatial selective attention in areas V1, V2, and V4 of macaque visual cortex. J Neurophysiol, 77(1), 24-42. doi:10.1152/jn.1997.77.1.24

Mancini, M., Mastropasqua, C., Bonni, S., Ponzo, V., Cercignani, M., Conforto, S., . . . Bozzali, M. (2017). Theta Burst Stimulation of the Precuneus Modulates Resting State Connectivity in the Left Temporal Pole. Brain Topogr, 30(3), 312-319. doi:10.1007/s10548-017-0559-x

Mansouri, F. A., Buckley, M. J., Mahboubi, M., & Tanaka, K. (2015). Behavioral consequences of selective damage to frontal pole and posterior cingulate cortices. Proc Natl Acad Sci U S A, 112(29), E3940-3949. doi:10.1073/pnas.1422629112

Marshall, M., Lewis, S., Lockwood, A., Drake, R., Jones, P., & Croudace, T. (2005). Association between duration of untreated psychosis and outcome in cohorts of first-episode patients: a systematic review. Arch Gen Psychiatry, 62(9), 975-983. doi:10.1001/archpsyc.62.9.975

Marzetti, L., Basti, A., Chella, F., D'Andrea, A., Syrjala, J., & Pizzella, V. (2019). Brain Functional Connectivity Through Phase Coupling of Neuronal Oscillations: A Perspective From Magnetoencephalography. Front Neurosci, 13, 964. doi:10.3389/fnins.2019.00964

McAdams, C. J., & Reid, R. C. (2005). Attention modulates the responses of simple cells in monkey primary visual cortex. J Neurosci, 25(47), 11023-11033. doi:10.1523/JNEUROSCI.2904-05.2005

McCleery, A., Lee, J., Joshi, A., Wynn, J. K., Hellemann, G. S., & Green, M. F. (2015). Meta-analysis of face processing event-related potentials in schizophrenia. Biol Psychiatry, 77(2), 116-126. doi:10.1016/j.biopsych.2014.04.015

McDermott, T. J., Wiesman, A. I., Mills, M. S., Spooner, R. K., Coolidge, N. M., Proskovec, A. L., . . . Wilson, T. W. (2019). tDCS modulates behavioral performance and the neural oscillatory dynamics serving visual selective attention. Hum Brain Mapp, 40(3), 729-740. doi:10.1002/hbm.24405

McGlashan, T. H. (1999). Duration of untreated psychosis in first-episode schizophrenia: marker or determinant of course? Biol Psychiatry, 46(7), 899-907. doi:10.1016/s0006-3223(99)00084-0

McGorry, P. D., Nelson, B., Phillips, L. J., Yuen, H. P., Francey, S. M., Thampi, A., . . . Yung, A. R. (2013). Randomized controlled trial of interventions for young people at ultra-high risk of psychosis: twelve-month outcome. J Clin Psychiatry, 74(4), 349-356. doi:10.4088/JCP.12m07785

Mechelli, A., Riecher-Rossler, A., Meisenzahl, E. M., Tognin, S., Wood, S. J., Borgwardt, S. J., . . . McGuire, P. (2011). Neuroanatomical abnormalities that predate the onset of psychosis: a multicenter study. Arch Gen Psychiatry, 68(5), 489-495. doi:10.1001/archgenpsychiatry.2011.42

Meisenzahl, E. M., Koutsouleris, N., Gaser, C., Bottlender, R., Schmitt, G. J., McGuire, P., . . . Moller, H. J. (2008). Structural brain alterations in subjects at high-risk of psychosis: a voxel-based morphometric study. Schizophr Res, 102(1-3), 150-162. doi:10.1016/j.schres.2008.02.023

Merchant, H., Harrington, D. L., & Meck, W. H. (2013). Neural basis of the perception and estimation of time. Annu Rev Neurosci, 36, 313-336. doi:10.1146/annurev-neuro-062012-170349

Michalka, S. W., Kong, L., Rosen, M. L., Shinn-Cunningham, B. G., & Somers, D. C. (2015). Short-Term Memory for Space and Time Flexibly Recruit Complementary Sensory-Biased Frontal Lobe Attention Networks. Neuron, 87(4), 882-892. doi:10.1016/j.neuron.2015.07.028

Michie, P. T. (2001). What has MMN revealed about the auditory system in schizophrenia? Int J Psychophysiol, 42(2), 177-194. doi:10.1016/s0167-8760(01)00166-0

Michie, P. T., Innes-Brown, H., Todd, J., & Jablensky, A. V. (2002). Duration mismatch negativity in biological relatives of patients with schizophrenia spectrum disorders. Biol Psychiatry, 52(7), 749-758. doi:10.1016/s0006-3223(02)01379-3

Millan, M. J., Andrieux, A., Bartzokis, G., Cadenhead, K., Dazzan, P., Fusar-Poli, P., . . . Weinberger, D. (2016). Altering the course of schizophrenia: progress and perspectives. Nat Rev Drug Discov, 15(7), 485-515. doi:10.1038/nrd.2016.28

Molholm, S., Martinez, A., Ritter, W., Javitt, D. C., & Foxe, J. J. (2005). The neural circuitry of pre-attentive auditory change-detection: an fMRI study of pitch and duration mismatch negativity generators. Cereb Cortex, 15(5), 545-551. doi:10.1093/cercor/bhh155

Molina, V., Sanz, J., Sarramea, F., Benito, C., & Palomo, T. (2004). Lower prefrontal gray matter volume in schizophrenia in chronic but not in first episode schizophrenia patients. Psychiatry Res, 131(1), 45-56. doi:10.1016/j.pscychresns.2004.01.005

Moreno-Kustner, B., Martin, C., & Pastor, L. (2018). Prevalence of psychotic disorders and its association with methodological issues. A systematic review and meta-analyses. PLoS One, 13(4), e0195687. doi:10.1371/journal.pone.0195687

Mormann, F., Lehnertz, K., David, P., & E. Elger, C. (2000). Mean phase coherence as a measure for phase synchronization and its application to the EEG of epilepsy patients. Physica D: Nonlinear Phenomena, 144(3), 358-369. doi:https://doi.org/10.1016/S0167-2789(00)00087-7

Morris, S. E., & Cuthbert, B. N. (2012). Research Domain Criteria: cognitive systems, neural circuits, and dimensions of behavior. Dialogues Clin Neurosci, 14(1), 29-37.

Murphy, N., Ramakrishnan, N., Walker, C. P., Polizzotto, N. R., & Cho, R. Y. (2020). Intact Auditory Cortical Cross-Frequency Coupling in Early and Chronic Schizophrenia. Front Psychiatry, 11, 507. doi:10.3389/fpsyt.2020.00507

Murphy, T. K., Haigh, S. M., Coffman, B. A., & Salisbury, D. F. (2020). Mismatch Negativity and Impaired Social Functioning in Long-Term and in First Episode Schizophrenia Spectrum Psychosis. Front Psychiatry, 11, 544. doi:10.3389/fpsyt.2020.00544

Naatanen, R., & Alho, K. (1995). Generators of electrical and magnetic mismatch responses in humans. Brain Topogr, 7(4), 315-320. doi:10.1007/bf01195257

Naatanen, R., & Kahkonen, S. (2009). Central auditory dysfunction in schizophrenia as revealed by the mismatch negativity (MMN) and its magnetic equivalent MMNm: a review. Int J Neuropsychopharmacol, 12(1), 125-135. doi:10.1017/S1461145708009322

Narr, K. L., Bilder, R. M., Toga, A. W., Woods, R. P., Rex, D. E., Szeszko, P. R., . . . Thompson, P. M. (2005). Mapping cortical thickness and gray matter concentration in first episode schizophrenia. Cereb Cortex, 15(6), 708-719. doi:10.1093/cercor/bhh172

Neef, N. E., Butfering, C., Anwander, A., Friederici, A. D., Paulus, W., & Sommer, M. (2016). Left posterior-dorsal area 44 couples with parietal areas to promote speech fluency, while right area 44 activity promotes the stopping of motor responses. Neuroimage, 142, 628-644. doi:10.1016/j.neuroimage.2016.08.030

Neelon, M. F., Williams, J., & Garell, P. C. (2006). The effects of auditory attention measured from human electrocorticograms. Clin Neurophysiol, 117(3), 504-521. doi:10.1016/j.clinph.2005.11.009

Nestor, P. G., Shenton, M. E., McCarley, R. W., Haimson, J., Smith, R. S., O'Donnell, B., . . . Jolesz, F. A. (1993). Neuropsychological correlates of MRI temporal lobe abnormalities in schizophrenia. Am J Psychiatry, 150(12), 1849-1855. doi:10.1176/ajp.150.12.1849

NIMH. Schizophrenia. Retrieved from https://www.nimh.nih.gov/health/statistics/schizophrenia

Nuechterlein, K. H., Green, M. F., Kern, R. S., Baade, L. E., Barch, D. M., Cohen, J. D., . . . Marder, S. R. (2008). The MATRICS Consensus Cognitive Battery, part 1: test selection, reliability, and validity. Am J Psychiatry, 165(2), 203-213. doi:10.1176/appi.ajp.2007.07010042

O'Donnell, B. F., Hokama, H., McCarley, R. W., Smith, R. S., Salisbury, D. F., Mondrow, E., . . . Shenton, M. E. (1994). Auditory ERPs to non-target stimuli in schizophrenia: relationship to probability, task-demands, and target ERPs. Int J Psychophysiol, 17(3), 219-231.

Paavilainen, P., Alho, K., Reinikainen, K., Sams, M., & Naatanen, R. (1991). Right hemisphere dominance of different mismatch negativities. Electroencephalogr Clin Neurophysiol, 78(6), 466-479. doi:10.1016/0013-4694(91)90064-b

Palva, S., & Palva, J. M. (2007). New vistas for alpha-frequency band oscillations. Trends Neurosci, 30(4), 150-158. doi:10.1016/j.tins.2007.02.001

Palva, S., & Palva, J. M. (2011). Functional roles of alpha-band phase synchronization in local and large-scale cortical networks. Front Psychol, 2, 204. doi:10.3389/fpsyg.2011.00204

Pantelis, C., Velakoulis, D., McGorry, P. D., Wood, S. J., Suckling, J., Phillips, L. J., . . . McGuire, P. K. (2003). Neuroanatomical abnormalities before and after onset of psychosis: a cross-sectional and longitudinal MRI comparison. Lancet, 361(9354), 281-288. doi:10.1016/S0140-6736(03)12323-9

Parasuraman, R. (1985). Event-Related Brain Potentials and Intermodal Divided Attention. Proceedings of the Human Factors and Ergonomics Society Annual Meeting, 29, 971-975.

Park, H. J., Kwon, J. S., Youn, T., Pae, J. S., Kim, J. J., Kim, M. S., & Ha, K. S. (2002). Statistical parametric mapping of LORETA using high density EEG and individual MRI: application to mismatch negativities in schizophrenia. Hum Brain Mapp, 17(3), 168-178. doi:10.1002/hbm.10059

Parker, E. M., & Sweet, R. A. (2017). Stereological Assessments of Neuronal Pathology in Auditory Cortex in Schizophrenia. Front Neuroanat, 11, 131. doi:10.3389/fnana.2017.00131

Persson, J., & Soderlund, H. (2015). Hippocampal hemispheric and long-axis differentiation of stimulus content during episodic memory encoding and retrieval: An activation likelihood estimation meta-analysis. Hippocampus, 25(12), 1614-1631. doi:10.1002/hipo.22482

Petersen, S. E., & Posner, M. I. (2012). The attention system of the human brain: 20 years after. Annu Rev Neurosci, 35, 73-89. doi:10.1146/annurev-neuro-062111-150525

Petkov, C. I., Kang, X., Alho, K., Bertrand, O., Yund, E. W., & Woods, D. L. (2004). Attentional modulation of human auditory cortex. Nat Neurosci, 7(6), 658-663. doi:10.1038/nn1256

Prasad, K. M., Rohm, B. R., & Keshavan, M. S. (2004). Parahippocampal gyrus in first episode psychotic disorders: a structural magnetic resonance imaging study. Prog Neuropsychopharmacol Biol Psychiatry, 28(4), 651-658. doi:10.1016/j.pnpbp.2004.01.017

Radua, J., Borgwardt, S., Crescini, A., Mataix-Cols, D., Meyer-Lindenberg, A., McGuire, P. K., & Fusar-Poli, P. (2012). Multimodal meta-analysis of structural and functional brain changes in first episode psychosis and the effects of antipsychotic medication. Neurosci Biobehav Rev, 36(10), 2325-2333. doi:10.1016/j.neubiorev.2012.07.012

Raij, T. T., Valkonen-Korhonen, M., Holi, M., Therman, S., Lehtonen, J., & Hari, R. (2009). Reality of auditory verbal hallucinations. Brain, 132(Pt 11), 2994-3001. doi:10.1093/brain/awp186

Rao, S. M., Harrington, D. L., Haaland, K. Y., Bobholz, J. A., Cox, R. W., & Binder, J. R. (1997). Distributed neural systems underlying the timing of movements. J Neurosci, 17(14), 5528-5535.

Rasser, P. E., Schall, U., Todd, J., Michie, P. T., Ward, P. B., Johnston, P., . . . Thompson, P. M. (2011). Gray matter deficits, mismatch negativity, and outcomes in schizophrenia. Schizophr Bull, 37(1), 131-140. doi:10.1093/schbul/sbp060

Ren, X., Fribance, S. N., Coffman, B. A., & Salisbury, D. F. (2021). Deficits in attentional modulation of auditory N100 in first-episode schizophrenia. Eur J Neurosci. doi:10.1111/ejn.15128

Reynolds, J. H., & Heeger, D. J. (2009). The normalization model of attention. Neuron, 61(2), 168-185. doi:10.1016/j.neuron.2009.01.002

Rimol, L. M., Hartberg, C. B., Nesvåg, R., Fennema-Notestine, C., Hagler, D. J., Pung, C. J., . . . Agartz, I. (2010). Cortical thickness and subcortical volumes in schizophrenia and bipolar disorder. Biol Psychiatry, 68(1), 41-50. doi:10.1016/j.biopsych.2010.03.036

Rimol, L. M., Nesvåg, R., Hagler, D. J., Bergmann, O., Fennema-Notestine, C., Hartberg, C. B., . . . Dale, A. M. (2012). Cortical volume, surface area, and thickness in schizophrenia and bipolar disorder. Biol Psychiatry, 71(6), 552-560. doi:10.1016/j.biopsych.2011.11.026

Rinne, T., Alho, K., Ilmoniemi, R. J., Virtanen, J., & Naatanen, R. (2000). Separate time behaviors of the temporal and frontal mismatch negativity sources. Neuroimage, 12(1), 14-19. doi:10.1006/nimg.2000.0591

Rinne, T., Stecker, G. C., Kang, X., Yund, E. W., Herron, T. J., & Woods, D. L. (2007). Attention modulates sound processing in human auditory cortex but not the inferior colliculus. Neuroreport, 18(13), 1311-1314. doi:10.1097/WNR.0b013e32826fb3bb

Robinson, E. C., Jbabdi, S., Glasser, M. F., Andersson, J., Burgess, G. C., Harms, M. P., . . . Jenkinson, M. (2014). MSM: a new flexible framework for Multimodal Surface Matching. Neuroimage, 100, 414-426. doi:10.1016/j.neuroimage.2014.05.069

Rosburg, T. (2003). Left hemispheric dipole locations of the neuromagnetic mismatch negativity to frequency, intensity and duration deviants. Brain Res Cogn Brain Res, 16(1), 83-90. doi:10.1016/s0926-6410(02)00222-7

Rosburg, T., Boutros, N. N., & Ford, J. M. (2008). Reduced auditory evoked potential component N100 in schizophrenia--a critical review. Psychiatry Res, 161(3), 259-274. doi:10.1016/j.psychres.2008.03.017

Rosburg, T., Trautner, P., Dietl, T., Korzyukov, O. A., Boutros, N. N., Schaller, C., . . . Kurthen, M. (2005). Subdural recordings of the mismatch negativity (MMN) in patients with focal epilepsy. Brain, 128(Pt 4), 819-828. doi:10.1093/brain/awh442

Saalmann, Y. B., Pigarev, I. N., & Vidyasagar, T. R. (2007). Neural mechanisms of visual attention: how top-down feedback highlights relevant locations. Science, 316(5831), 1612-1615. doi:10.1126/science.1139140

Saha, S., Chant, D., Welham, J., & McGrath, J. (2005). A systematic review of the prevalence of schizophrenia. PLoS Med, 2(5), e141. doi:10.1371/journal.pmed.0020141

Salimi-Khorshidi, G., Douaud, G., Beckmann, C. F., Glasser, M. F., Griffanti, L., & Smith, S. M. (2014). Automatic denoising of functional MRI data: combining independent component analysis and hierarchical fusion of classifiers. Neuroimage, 90, 449-468. doi:10.1016/j.neuroimage.2013.11.046

Salisbury, D. F., Collins, K. C., & McCarley, R. W. (2010). Reductions in the N1 and P2 auditory event-related potentials in first-hospitalized and chronic schizophrenia. Schizophr Bull, 36(5), 991-1000. doi:10.1093/schbul/sbp003

Salisbury, D. F., Kohler, J., Shenton, M. E., & McCarley, R. W. (2019). Deficit Effect Sizes and Correlations of Auditory Event-Related Potentials at First Hospitalization in the Schizophrenia Spectrum. Clin EEG Neurosci, 1550059419868115. doi:10.1177/1550059419868115

Salisbury, D. F., Kuroki, N., Kasai, K., Shenton, M. E., & McCarley, R. W. (2007). Progressive and interrelated functional and structural evidence of post-onset brain reduction in schizophrenia. Arch Gen Psychiatry, 64(5), 521-529. doi:10.1001/archpsyc.64.5.521

Salisbury, D. F., Polizzotto, N. R., Nestor, P. G., Haigh, S. M., Koehler, J., & McCarley, R. W. (2017). Pitch and Duration Mismatch Negativity and Premorbid Intellect in the First Hospitalized Schizophrenia Spectrum. Schizophr Bull, 43(2), 407-416. doi:10.1093/schbul/sbw074

Salisbury, D. F., Shafer, A. R., Murphy, T. K., Haigh, S. M., & Coffman, B. A. (2020). Pitch and Duration Mismatch Negativity and Heschl's Gyrus Volume in First-Episode Schizophrenia-Spectrum Individuals. Clin EEG Neurosci, 1550059420914214. doi:10.1177/1550059420914214

Salisbury, D. F., Shenton, M. E., Griggs, C. B., Bonner-Jackson, A., & McCarley, R. W. (2002). Mismatch negativity in chronic schizophrenia and first-episode schizophrenia. Arch Gen Psychiatry, 59(8), 686-694. doi:10.1001/archpsyc.59.8.686

Salisbury, D. F., Wang, Y., Yeh, F. C., & Coffman, B. A. (2021). White Matter Microstructural Abnormalities in the Broca's-Wernicke's-Putamen "Hoffman Hallucination Circuit" and Auditory Transcallosal Fibers in First-Episode Psychosis With Auditory Hallucinations. Schizophr Bull, 47(1), 149-159. doi:10.1093/schbul/sbaa105

Schneider, F., Dheerendra, P., Balezeau, F., Ortiz-Rios, M., Kikuchi, Y., Petkov, C. I., . . . Griffiths, T. D. (2018). Auditory figure-ground analysis in rostral belt and parabelt of the macaque monkey. Sci Rep, 8(1), 17948. doi:10.1038/s41598-018-36903-1

Schultz, C. C., Koch, K., Wagner, G., Roebel, M., Schachtzabel, C., Gaser, C., . . . Schlösser, R. G. (2010). Reduced cortical thickness in first episode schizophrenia. Schizophr Res, 116(2-3), 204-209. doi:10.1016/j.schres.2009.11.001

Seidman, L. J., Giuliano, A. J., Meyer, E. C., Addington, J., Cadenhead, K. S., Cannon, T. D., . . . Group, N. A. P. L. S. (2010). Neuropsychology of the prodrome to psychosis in the NAPLS consortium: relationship to family history and conversion to psychosis. Arch Gen Psychiatry, 67(6), 578-588. doi:10.1001/archgenpsychiatry.2010.66

Selemon, L. D., & Goldman-Rakic, P. S. (1999). The reduced neuropil hypothesis: a circuit based model of schizophrenia. Biol Psychiatry, 45(1), 17-25.

Shenton, M. E., Dickey, C. C., Frumin, M., & McCarley, R. W. (2001). A review of MRI findings in schizophrenia. Schizophr Res, 49(1-2), 1-52.

Shenton, M. E., Kikinis, R., Jolesz, F. A., Pollak, S. D., LeMay, M., Wible, C. G., . . . et al. (1992). Abnormalities of the left temporal lobe and thought disorder in schizophrenia. A quantitative magnetic resonance imaging study. N Engl J Med, 327(9), 604-612. doi:10.1056/NEJM199208273270905

Shibata, T., Shimoyama, I., Ito, T., Abla, D., Iwasa, H., Koseki, K., . . . Nakajima, Y. (1999). Attention changes the peak latency of the visual gamma-band oscillation of the EEG. Neuroreport, 10(6), 1167-1170. doi:10.1097/00001756-199904260-00002

Singer, W., & Gray, C. M. (1995). Visual feature integration and the temporal correlation hypothesis. Annu Rev Neurosci, 18, 555-586. doi:10.1146/annurev.ne.18.030195.003011

Spaak, E., Bonnefond, M., Maier, A., Leopold, D. A., & Jensen, O. (2012). Layer-specific entrainment of γ-band neural activity by the α rhythm in monkey visual cortex. Curr Biol, 22(24), 2313-2318. doi:10.1016/j.cub.2012.10.020

Spitzer, H., Desimone, R., & Moran, J. (1988). Increased attention enhances both behavioral and neuronal performance. Science, 240(4850), 338-340.

Sprooten, E., Papmeyer, M., Smyth, A. M., Vincenz, D., Honold, S., Conlon, G. A., . . . Lawrie, S. M. (2013). Cortical thickness in first-episode schizophrenia patients and individuals at high familial risk: a cross-sectional comparison. Schizophr Res, 151(1-3), 259-264. doi:10.1016/j.schres.2013.09.024

Squire, L. R., Stark, C. E., & Clark, R. E. (2004). The medial temporal lobe. Annu Rev Neurosci, 27, 279-306. doi:10.1146/annurev.neuro.27.070203.144130

Srihari, V. H., Shah, J., & Keshavan, M. S. (2012). Is early intervention for psychosis feasible and effective? Psychiatr Clin North Am, 35(3), 613-631. doi:10.1016/j.psc.2012.06.004

Stagg, C. J., & Nitsche, M. A. (2011). Physiological basis of transcranial direct current stimulation. Neuroscientist, 17(1), 37-53. doi:10.1177/1073858410386614

Sun, H., Lui, S., Yao, L., Deng, W., Xiao, Y., Zhang, W., . . . Gong, Q. (2015). Two Patterns of White Matter Abnormalities in Medication-Naive Patients With First-Episode Schizophrenia Revealed by Diffusion Tensor Imaging and Cluster Analysis. JAMA Psychiatry, 72(7), 678-686. doi:10.1001/jamapsychiatry.2015.0505

Sweet, R. A., Bergen, S. E., Sun, Z., Sampson, A. R., Pierri, J. N., & Lewis, D. A. (2004). Pyramidal cell size reduction in schizophrenia: evidence for involvement of auditory feedforward circuits. Biol Psychiatry, 55(12), 1128-1137. doi:10.1016/j.biopsych.2004.03.002

Sweet, R. A., Dorph-Petersen, K. A., & Lewis, D. A. (2005). Mapping auditory core, lateral belt, and parabelt cortices in the human superior temporal gyrus. J Comp Neurol, 491(3), 270-289. doi:10.1002/cne.20702

Sweet, R. A., Henteleff, R. A., Zhang, W., Sampson, A. R., & Lewis, D. A. (2009). Reduced dendritic spine density in auditory cortex of subjects with schizophrenia. Neuropsychopharmacology, 34(2), 374-389. doi:10.1038/npp.2008.67

Tadel, F., Baillet, S., Mosher, J. C., Pantazis, D., & Leahy, R. M. (2011). Brainstorm: a user-friendly application for MEG/EEG analysis. Comput Intell Neurosci, 2011, 879716. doi:10.1155/2011/879716

Takahashi, T., Suzuki, M., Zhou, S. Y., Tanino, R., Hagino, H., Niu, L., . . . Kurachi, M. (2006). Temporal lobe gray matter in schizophrenia spectrum: a volumetric MRI study of the

fusiform gyrus, parahippocampal gyrus, and middle and inferior temporal gyri. Schizophr Res, 87(1-3), 116-126. doi:10.1016/j.schres.2006.04.023

Takahashi, T., Wood, S. J., Yung, A. R., Phillips, L. J., Soulsby, B., McGorry, P. D., . . . Pantelis, C. (2009). Insular cortex gray matter changes in individuals at ultra-high-risk of developing psychosis. Schizophr Res, 111(1-3), 94-102. doi:10.1016/j.schres.2009.03.024

Takahashi, T., Wood, S. J., Yung, A. R., Soulsby, B., McGorry, P. D., Suzuki, M., . . . Pantelis, C. (2009). Progressive gray matter reduction of the superior temporal gyrus during transition to psychosis. Arch Gen Psychiatry, 66(4), 366-376. doi:10.1001/archgenpsychiatry.2009.12

Tallon-Baudry, C., Bertrand, O., Delpuech, C., & Permier, J. (1997). Oscillatory gamma-band (30-70 Hz) activity induced by a visual search task in humans. J Neurosci, 17(2), 722-734.

Tallon-Baudry, C., Bertrand, O., Henaff, M. A., Isnard, J., & Fischer, C. (2005). Attention modulates gamma-band oscillations differently in the human lateral occipital cortex and fusiform gyrus. Cereb Cortex, 15(5), 654-662. doi:10.1093/cercor/bhh167

Thair, H., Holloway, A. L., Newport, R., & Smith, A. D. (2017). Transcranial Direct Current Stimulation (tDCS): A Beginner's Guide for Design and Implementation. Front Neurosci, 11, 641. doi:10.3389/fnins.2017.00641

Tobyne, S. M., Osher, D. E., Michalka, S. W., & Somers, D. C. (2017). Sensory-biased attention networks in human lateral frontal cortex revealed by intrinsic functional connectivity. Neuroimage, 162, 362-372. doi:10.1016/j.neuroimage.2017.08.020

Todd, J., Harms, L., Schall, U., & Michie, P. T. (2013). Mismatch negativity: translating the potential. Front Psychiatry, 4, 171. doi:10.3389/fpsyt.2013.00171

Tognin, S., Riecher-Rössler, A., Meisenzahl, E. M., Wood, S. J., Hutton, C., Borgwardt, S. J., . . . Mechelli, A. (2014). Reduced parahippocampal cortical thickness in subjects at ultra-high risk for psychosis. Psychol Med, 44(3), 489-498. doi:10.1017/S0033291713000998

Tootell, R. B., Hadjikhani, N., Hall, E. K., Marrett, S., Vanduffel, W., Vaughan, J. T., & Dale, A. M. (1998). The retinotopy of visual spatial attention. Neuron, 21(6), 1409-1422. doi:10.1016/s0896-6273(00)80659-5

Tseng, Y. L., Liu, H. H., Liou, M., Tsai, A. C., Chien, V. S. C., Shyu, S. T., & Yang, Z. S. (2019). Lingering Sound: Event-Related Phase-Amplitude Coupling and Phase-Locking in Fronto-Temporo-Parietal Functional Networks During Memory Retrieval of Music Melodies. Front Hum Neurosci, 13, 150. doi:10.3389/fnhum.2019.00150

Tukker, J. J., Fuentealba, P., Hartwich, K., Somogyi, P., & Klausberger, T. (2007). Cell type-specific tuning of hippocampal interneuron firing during gamma oscillations in vivo. J Neurosci, 27(31), 8184-8189. doi:10.1523/JNEUROSCI.1685-07.2007

Umbricht, D., & Krljes, S. (2005). Mismatch negativity in schizophrenia: a meta-analysis. Schizophr Res, 76(1), 1-23. doi:10.1016/j.schres.2004.12.002

Utevsky, A. V., Smith, D. V., & Huettel, S. A. (2014). Precuneus is a functional core of the default-mode network. J Neurosci, 34(3), 932-940. doi:10.1523/JNEUROSCI.4227-13.2014

Uusitalo, M. A., & Ilmoniemi, R. J. (1997). Signal-space projection method for separating MEG or EEG into components. Med Biol Eng Comput, 35(2), 135-140. doi:10.1007/BF02534144

van der Gaag, M., Nieman, D. H., Rietdijk, J., Dragt, S., Ising, H. K., Klaassen, R. M., . . . Linszen, D. H. (2012). Cognitive behavioral therapy for subjects at ultrahigh risk for developing psychosis: a randomized controlled clinical trial. Schizophr Bull, 38(6), 1180-1188. doi:10.1093/schbul/sbs105

van Erp, T. G., Hibar, D. P., Rasmussen, J. M., Glahn, D. C., Pearlson, G. D., Andreassen, O. A., . . . Turner, J. A. (2016). Subcortical brain volume abnormalities in 2028 individuals with schizophrenia and 2540 healthy controls via the ENIGMA consortium. Mol Psychiatry, 21(4), 585. doi:10.1038/mp.2015.118

van Erp, T. G. M., Walton, E., Hibar, D. P., Schmaal, L., Jiang, W., Glahn, D. C., . . . Turner, J. A. (2018). Cortical Brain Abnormalities in 4474 Individuals With Schizophrenia and 5098 Control Subjects via the Enhancing Neuro Imaging Genetics Through Meta Analysis (ENIGMA) Consortium. Biol Psychiatry, 84(9), 644-654. doi:10.1016/j.biopsych.2018.04.023

Van Essen, D. C., Glasser, M. F., Dierker, D. L., Harwell, J., & Coalson, T. (2012). Parcellations and hemispheric asymmetries of human cerebral cortex analyzed on surface-based atlases. Cereb Cortex, 22(10), 2241-2262. doi:10.1093/cercor/bhr291

van Haren, N. E., Schnack, H. G., Cahn, W., van den Heuvel, M. P., Lepage, C., Collins, L., . . . Kahn, R. S. (2011). Changes in cortical thickness during the course of illness in schizophrenia. Arch Gen Psychiatry, 68(9), 871-880. doi:10.1001/archgenpsychiatry.2011.88

van Lutterveld, R., van den Heuvel, M. P., Diederen, K. M., de Weijer, A. D., Begemann, M. J., Brouwer, R. M., . . . Sommer, I. E. (2014). Cortical thickness in individuals with non-clinical and clinical psychotic symptoms. Brain, 137(Pt 10), 2664-2669. doi:10.1093/brain/awu167

Vita, A., De Peri, L., Silenzi, C., & Dieci, M. (2006). Brain morphology in first-episode schizophrenia: a meta-analysis of quantitative magnetic resonance imaging studies. Schizophr Res, 82(1), 75-88. doi:10.1016/j.schres.2005.11.004

Vohs, J. L., Chambers, R. A., Krishnan, G. P., O'Donnell, B. F., Berg, S., & Morzorati, S. L. (2010). GABAergic modulation of the 40 Hz auditory steady-state response in a rat model of schizophrenia. Int J Neuropsychopharmacol, 13(4), 487-497. doi:10.1017/S1461145709990307

Vohs, J. L., Chambers, R. A., Krishnan, G. P., O'Donnell, B. F., Hetrick, W. P., Kaiser, S. T., . . . Morzorati, S. L. (2009). Auditory sensory gating in the neonatal ventral hippocampal lesion model of schizophrenia. Neuropsychobiology, 60(1), 12-22. doi:10.1159/000234813

von Stein, A., Chiang, C., & Konig, P. (2000). Top-down processing mediated by interareal synchronization. Proc Natl Acad Sci U S A, 97(26), 14748-14753. doi:10.1073/pnas.97.26.14748

Vossel, S., Geng, J. J., & Fink, G. R. (2014). Dorsal and ventral attention systems: distinct neural circuits but collaborative roles. Neuroscientist, 20(2), 150-159. doi:10.1177/1073858413494269

Voytek, B., Canolty, R. T., Shestyuk, A., Crone, N. E., Parvizi, J., & Knight, R. T. (2010). Shifts in gamma phase-amplitude coupling frequency from theta to alpha over posterior cortex during visual tasks. Front Hum Neurosci, 4, 191. doi:10.3389/fnhum.2010.00191

Walsh, B. J., Buonocore, M. H., Carter, C. S., & Mangun, G. R. (2011). Integrating conflict detection and attentional control mechanisms. J Cogn Neurosci, 23(9), 2211-2221. doi:10.1162/jocn.2010.21595

Whitford, T. J., Grieve, S. M., Farrow, T. F., Gomes, L., Brennan, J., Harris, A. W., . . . Williams, L. M. (2007). Volumetric white matter abnormalities in first-episode schizophrenia: a longitudinal, tensor-based morphometry study. Am J Psychiatry, 164(7), 1082-1089. doi:10.1176/ajp.2007.164.7.1082

Woldorff, M. G., Gallen, C. C., Hampson, S. A., Hillyard, S. A., Pantev, C., Sobel, D., & Bloom, F. E. (1993). Modulation of early sensory processing in human auditory cortex during auditory selective attention. Proc Natl Acad Sci U S A, 90(18), 8722-8726.

Womelsdorf, T., & Fries, P. (2007). The role of neuronal synchronization in selective attention. Curr Opin Neurobiol, 17(2), 154-160. doi:10.1016/j.conb.2007.02.002

Womelsdorf, T., Valiante, T. A., Sahin, N. T., Miller, K. J., & Tiesinga, P. (2014). Dynamic circuit motifs underlying rhythmic gain control, gating and integration. Nat Neurosci, 17(8), 1031-1039. doi:10.1038/nn.3764

Wood, S. J., Pantelis, C., Velakoulis, D., Yucel, M., Fornito, A., & McGorry, P. D. (2008). Progressive changes in the development toward schizophrenia: studies in subjects at increased symptomatic risk. Schizophr Bull, 34(2), 322-329. doi:10.1093/schbul/sbm149

Worden, M. S., Foxe, J. J., Wang, N., & Simpson, G. V. (2000). Anticipatory biasing of visuospatial attention indexed by retinotopically specific alpha-band electroencephalography increases over occipital cortex. J Neurosci, 20(6), RC63.

Zatorre, R. J., Mondor, T. A., & Evans, A. C. (1999). Auditory attention to space and frequency activates similar cerebral systems. Neuroimage, 10(5), 544-554. doi:10.1006/nimg.1999.0491